TECHNISCHE UNIVERSITÄT WIEN

VIENNA UNIVERSITY OF TECHNOLOGY

Diplomarbeit

2,3,5,6-tetrakis(benzimidazol-2´-yl)pyrazine – a Novel Ligand for Potential Spin Crossover Complexes

ausgeführt am
Institut für Angewandte Synthesechemie E163
der Technischen Universität Wien

unter Anleitung von

Ao.Univ.Prof. Dipl.Ing. Dr. Wolfgang Linert
und
Univ.Ass. Dipl.Ing. Dr. Peter Weinberger
als verantwortlich mitwirkenden Universitätsassistenten

durch
Eleni Siakkou
Matr.Nr. 0225027
Sooßerstraße 30
2540 Bad Vöslau

Wien, im November 2007

Kurzfassung

Im Rahmen dieser Arbeit wurde ein neuer mehrzähniger Ligand, 2,3,5,6-tetrakis(benzimidazol-2´-yl)-pyrazin, kurz [$(bi)_4pz$] genannt, der zwei dreizähnige Koordinationsstellen für Metallionen aufweist, synthetisiert und mit Hilfe von NMR, IR, UV-VIS-NIR, Elementaranalyse, sowie XRD und TGA charakterisiert.

Aufgrund bisheriger Arbeitern in der Forschungsgruppe an der Stoffklasse der Bis(benzimidazol-2´-yl)pyridine war es das Ziel, einen mehrzähnigen Brückenliganden für Eisen(II)-Koordinationspolymere herzustellen, der ähnliche Spin Crossover-Eigenschaften zeigt, wie die Serie der bereits bekannten mononuklearen [$Fe(bzimpy)_2$]-Verbindungen. In der Hoffnung, einen polynuklearen Komplex ähnlicher oder besserer Spin Crossover-Eigenschaften herzustellen, wurden durch Umsetzung des neuartigen Liganden mit Eisen(II)-Salzen die entsprechenden Eisen(II) Komplexe synthetisiert und charakterisiert. Die magnetischen und optischen Eigenschaften der Komplexe wurden mittels SQUID-Magnetometrie zwischen 4.2 K und 300 K, sowie mit temperaturabhängiger UV-VIS-NIR Spektroskopie im Bereich von 123 K bis 373 K untersucht.

Abstract

The novel multidentate ligand 2,3,5,6-tetrakis(benzimidazole-2´-yl)pyrazine is synthesized from pyrazine-2,3,5,6-tetracarboxylic acid and characterized with means of NMR, IR, UV-Vis-NIR, TGA, elementary analysis and XRPD. The tridentate ligand with two coordination sites forms deeply coloured low-spin complexes with $Fe(ClO_4)_2$ and $Fe(BF_4)_2$, respectively.

Based on former work within the research group with the substance class of bis(benzimidazol-2´-yl)pyridines the major aim of this work is the synthesis of a bridging ligand to form polynuclear iron(II) compounds of a similar spin transition behaviour as it has been observed in the series of the mononuclear $[Fe(4\text{-}X\text{-}bzimpy)_3]$ compounds. The complexes, which have been synthesized for the first time witin the scope of this work, are of equimolar composition, *i.e.* the ratio of iron(II) to ligand is 1:1, and it is assumed that a one-dimensional network is formed in which units consisting of one ligand-molecule and one coordinated iron are linked to each other. For characterization of the novel complex compounds IR, TGA and XRPD measurements have been conducted. XRPD powder patterns show that predominantly amorphous powders have formed. Investigation of the powders with temperature dependent UV-Vis-NIR spectroscopy and SQUID magnetometry shows no spin crossover behaviour in a range within 123 K and 373 K and within 4.2 K and 300 K, respectively.

Acknowledgments

First of all, I want to thank my supervisor Dr. Wolfgang Linert for making my participation in this project possible, for his support and for allowing me great latitude during my work. Furthermore, I have to express my gratitude to the FWF for the financial support.

Over and above I want to thank Dr. Peter Weinberger, who rendered the maximum possible assistance allowed by his jam-packed schedule in order to guide and assist me in this project.

Many thanks go to Dipl.-Ing. Wolfhardt Freinbichler for the HPLC measurements and the diverting discussions during our coffee breaks. In this regard I would also like to mention my colleagues Dr. Franz Werner, whom I have to thank for the XRD measurements as well as for the interpretation of the powder patterns, Dipl.-Ing. Claudia Feldgitscher and Stefan Krivec, who have conducted the TGA measurements, and Prof. Gerfried Hilscher, who has taken care of the SQID-magnetometry. Furthermore, I yield Dr. Christian Hametner thanks for taking up the challenge of obtaining viable ^{13}C-NMR spectra of something that is as insoluble as a stone and for supplying me with ideas and knowhow concerning organic synthesis. Many thanks also belong to Dr. Matthias Bartel and Dr. Alina Absmeier, who have constantly helped and encouraged me during my research work and authoring of the diploma thesis.

Last but not least I want to say thank you to my dear family and friends for unfailingly and caringly supporting me, cheering me up and everlastingly providing litres of coffee and tons of chocolate chunk cookies during my years of studies.

Inhaltsverzeichnis/Table of Contents

1. Introduction

1.1. Complex Compounds and the Ligand Field Theory [1]

Complex compounds consist of transition metals, which are surrounded by organic ligands. Due to repulsive forces between the d-electrons of the metal and the electrons of the ligands, the transition metal´s d-orbitals (see Fig. 1-1) split into different states of energy. This splitting strongly depends on the geometry of the complex and is described by the so called crystal- or ligand-field theory, where only the d-orbitals of the central atom – the transition metal – are held into account. The surrounding ligands then cause an interference field which lifts the degeneracy of the metal´s d-orbitals.

Within complex compounds where the ligands surround the transition metal in an octahedral geometry two different energy levels are observed: The energy of the d_{z^2} and $d_{x^2-y^2}$ orbitals is increased to form the e_g level, whereas the energy of the d_{xy}, d_{xz} and d_{yz} orbitals is decreased to form the t_{2g} level. This effect may be illustrated and explained by means of a thought experiment (see Fig. 1-2): According to the crystal-field theory the ligands are represented by point charges and the metal centre is considered as a free transition metal ion with five degenerated d-orbitals. The negative charges of the ligand are then distributed isotropically on the surface of a globe which holds the metal ion in its centre. As a result, the electrostatic repulsion between the d-orbitals and the isotropic negative charge distribution increases the energy of the five orbitals without lifting their degeneracy. In a second step an octahedron which determines the coordinate system of the d-orbitals is enrolled into the globe. When the charges on its surface are then condensed into the six corners of the octahedron the splitting of the d-orbitals into the t_{2g} and e_g sets takes place: The d_{z^2} and $d_{x^2-y^2}$ orbitals are orientated towards the point charges of the ligands and thus the e_g orbital is of higher energy than the t_{2g} orbitals, where the orbital lobes are situated between the axis.

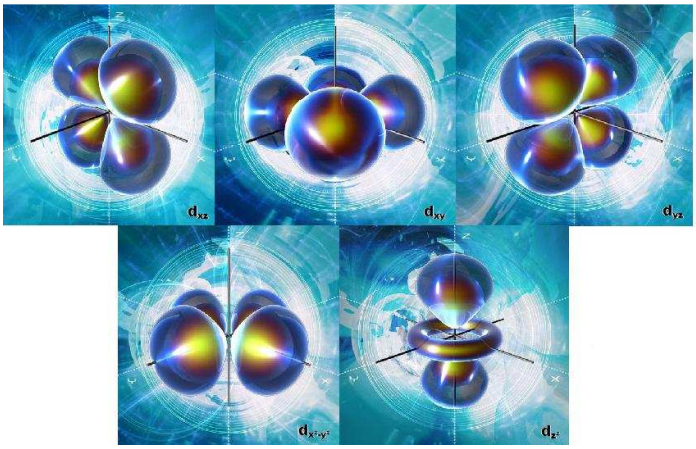

Fig. 1-1: Schematic illustration of the d-orbitals d_{xz}, d_{xy}, d_{yz}, $d_{x^2-y^2}$ and d_{z^2}.

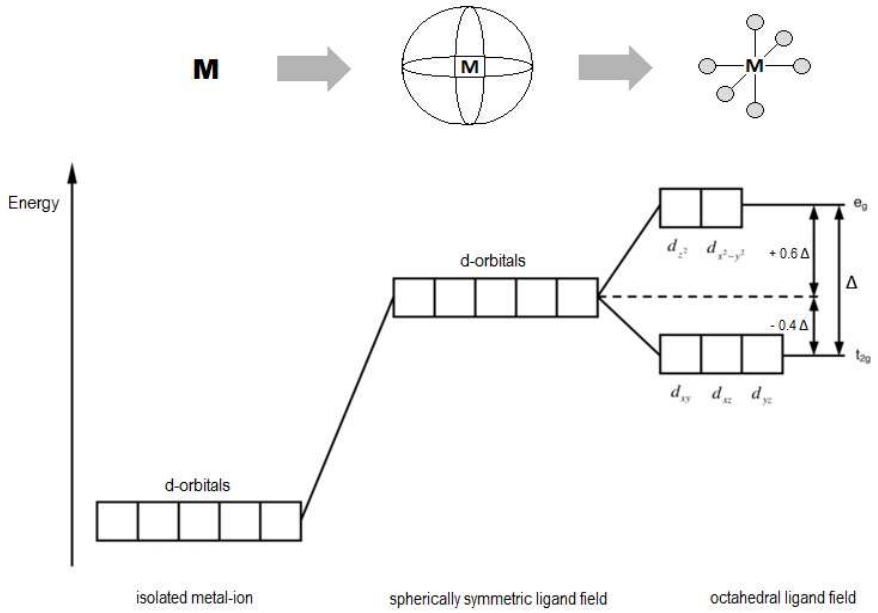

Fig. 1-2: Thought experiment to illustrate the splitting of d-orbitals in an octahedral ligand field.

For transition metal ions with the configuration of d^4 to d^7 the existence of the two different energy levels now leads to two different possibilities to populate the orbitals with electrons (see Fig. 1-3). In which of these two states the transition metal is existent depends strongly on the nature of the surrounding ligands and the ligand field they create. The high-spin (HS) state where the spin multiplicity is at a maximum is the ground state for the metals in weak ligand fields. On the other hand, when the metal is embedded in a strong ligand field, the low-spin (LS) ground state is stabilized and the spin multiplicity is at a minimum. To explain this behaviour the energies of the splitting of the ligand field Δ and the spin pairing P have to be compared. In the case of a weak ligand field, Δ is much smaller than P and Hund´s Rule has to be obeyed which leads to a HS ground state. By contrast a strong ligand field causes a Δ that is much bigger than P and thus the LS state is favoured because of the gain of energy obtained by the spin pairing.

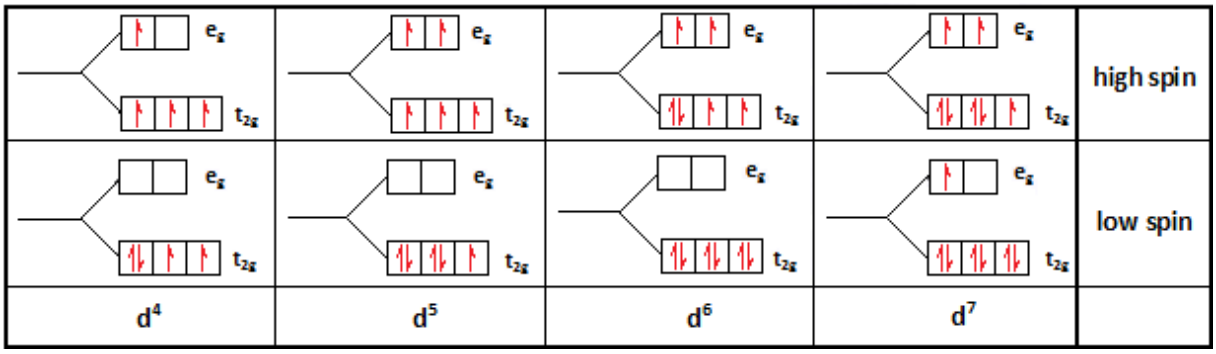

Fig. 1-3: HS and LS states of d^4 to d^7 transition metals in octahedral complexes.

1.2. The Spin Crossover Phenomenon [2]

The splitting of the transition metals´ d-orbitals into the t_{2g} and e_g sets within octahedral complex compounds, as well as the consequential existence of HS and LS states for the 3d elements with an electron configuration of d^4 to d^7 provide a basis for the Spin Crossover Phenomenon. A further condition for a Spin Crossover (SC) is $\Delta E^0_{HL} \approx k_B T$, which means that the energy necessary for the spin transition has to be in the range of thermal energy. From this follows that a SC is a mostly thermally induced change of the central atom´s spin state within a complex compound from HS to LS or vice versa, which may occur in solids as well as in solution. The ligands surrounding the central atom have a strong influence on the behaviour of the spin-transition and thus a change of the ligand sphere may be used to tune it deliberately towards a wanted direction, e.g. to increase the temperature where the SC takes place (see Boča [3] *et al.*).

1.2.1. Historical Background

The first records of the Spin Crossover Phenomenon have been made in the 1930´s when Cambi [4] - [7] *et al.* discovered an unexpected temperature-dependent change in the magnetic behaviour of iron(III)-tris(dithiocarbamate) when cooling the compound down to 194 K. The occurrence of this effect has been at first mistakenly interpreted as the existence of two different isomers of the compound. In the 1960´s Baker [8] *et al.* have synthesized and analyzed the first iron(II)-complex with a temperature-dependent SC, [Fe(phen)2-(NCS)2] (phen = 1,10-Phenanthroline). It has been proved that the change in the magnetic properties of the compound has been due to the spin-transition. An intensive research of the Spin Crossover Phenomenon has followed and it has been shown that it commonly occurred within complex compounds which embody Fe(II), Fe(III) or Co(II) as central atoms. When König [9] has indicated that the distance between the central atom and the ligands within a LS-complex is shorter than within the HS-complex, it has occurred that the SC could also be induced by pressure [10] - [13]. The feasibility of this idea has been experimentally proved by Gütlich [11] and Meissner [12] *et al.* Other methods to induce SC include the trapping of an excited spin-state *via* light, the so called LIESST-effect (**L**ight **I**nduced **S**pin-**S**tate **T**rapping, Decurtins [14], [15], [16] *et al.*) and the production of the excited spin-state *via* nuclear decay (NIESST-effect: **N**uclear Decay **I**nduced **S**pin-**S**tate **T**rapping, Gütlich [11]) or strong magnetic fields (Richter [17] *et al.*).

1.2.2. Possibilities to Induce Spin Transition

1.2.2.1. Spin Transition Induced by Temperature and the Different Types of Temperature Dependent Spin Crossover

In the previous chapter it has been pointed out that the first spin transitions within complex compounds have been observed during low temperature experiments. Thus thermal induction of a spin transition is historically the most commonly used method [(7), (8), (18) - (48)] and all other methods to achieve SC are established on this one.

The progress of a SC is described via the ratio of molecules of a SC-compound (mostly iron(II)-complexes) in the HS state as a function of the temperature and is denoted by the Greek letter $\gamma_{HS}(T)$.

Spin Crossover in Solid State

In solid state curves of $\gamma_{HS}(T)$ may progress quite differently, depending on the cooperative interactions within the solid (see Fig. 1-4).

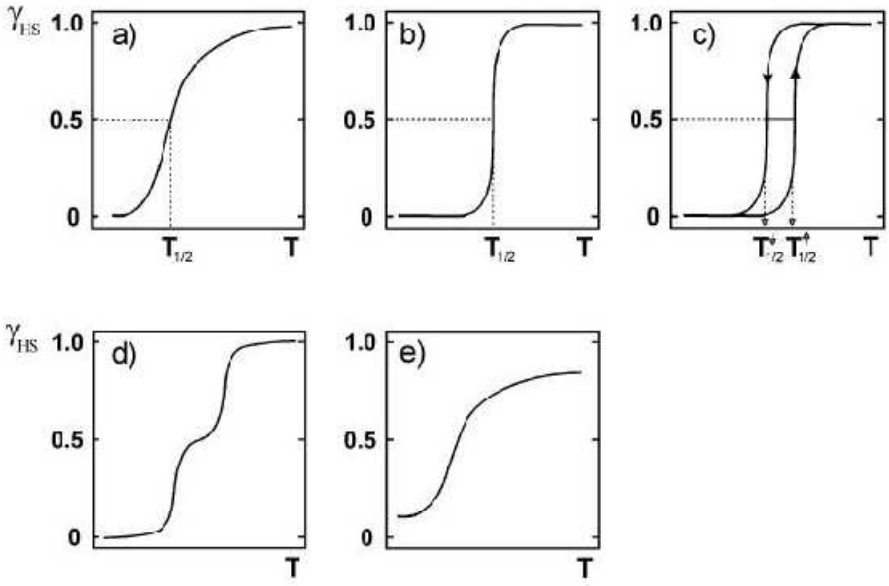

Fig. 1-4: different types of SC behaviour. a) gradual, b) abrupt, c) abrupt with hysteresis, d) two-step, e) incomplete

Continuous SCs

- Gradual SC: The spin transition proceeds gradually and it may take up to more than 100 K to achieve a complete SC.
- Abrupt SC: A complete SC takes place within a narrow temperature range (≤ 10 K).
- Two-step SC: The SC consists of two steps, which may progress gradually or abruptly.

Discontinuous SCs

SC with hysteresis: The cooling and the heating modes produce different SC transition curves.

Incomplete SC

At low temperatures a part of the molecules remains in the HS state and thus $\gamma_{HS}(T)$ ends in a plateau.

As a general rule it can be said, that solids with continuous spin transitions don´t experience a change in their crystal structure during the transition, whereas those of discontinuous SC behaviour mostly change their crystallographic setting [49] . Many examples in literature [50], [49] affirm this general rule, but also several exceptions [51], [52] exist.

An abrupt SC may be very well described via the so called "elastic interactions" between the centres of the molecules [53].- [56]: When the metal centre of a complex changes from LS to HS the bond-lengths between the metal and the ligands perform a significant increase of about 10 rel.%. Consequently the volume of the complex increases and in this process the information about the spin transition is forwarded to the neighbouring complexes, which "sense" the change of geometry. This rather phenomenological explanation of the SC-behaviour demands a well defined crystal lattice, i.e. a far-range ordering.
The occurrence of a hysteresis may be, as in the case of mononuclear iron(II)-complexes, caused by strong intermolecular interactions such as hydrogen-bonds [57] - [59] or π-π interactions [59] - [62]. In the past several SC-compounds [49], [50], [63], [64] that show a hysteresis during the spin transition have been examined in connection with the theorem of Everett et al. [65] - [67], in which is indicated that the mechanism of the discontinuous transition is mainly influenced by the formation of domains with molecules of the same spin-state.
The model of the elastic interactions may also be used to describe the two-step SC, indicating that this behaviour is generated by two crystallographically different iron(II)-centres [68], [69]. However, in the case that the crystallographically different iron(II)-centres are lacking, this model is not apt to describe the two-step SC and other theories have to be consulted. In this connection the thermodynamic theory of A. B. Kudryavtsev [70] may be mentioned. Kudryavtsev postulates a meta-stable transition state which is stable within a temperature range of several K and contains an alternating alignment of HS and LS iron(II)-centres.
The incomplete SC may be caused by two crystallographically different iron(II)-centres where just one centre is changing its spin-state, or by defects and imperfections within the crystal lattice. This SC type is more often observed during continuous spin transitions than during discontinuous ones.

Most of the mathematical approaches for the different types of SC reproduce the experimental data gained e.g. by magnetic measurements quite well.

Spin Crossover in Solution

In contrast to the SC in solid state, the temperature dependent SC in solution always proceeds gradually for the elastic interactions between the centres of the molecules are lacking. Thus Boltzmann´s Law may be used to characterize $\gamma_{HS}(T)$.

1.2.2.2. Spin Transition Induced by Pressure

The fact that the LS state is of smaller molecular volume than the HS state indicates that the LS state is favoured as pressure increases. Therefore the spin transition temperature at high pressure is elevated compared to those at normal pressure. But not only the temperature of the spin transition can be influenced by pressure, also other effects occurring during a SC, like hysteresis loops or the integrity of the transition may be affected [(71)]. This effect is illustrated in Fig. 1-5, which shows temperature-dependent magnetic susceptibility measurements performed at different pressures for a cyanide based SC polymer of the general formula $\{Fe(5\text{-Br-pmd})_z[M(CN)_x]_y\}$ (with M = Ag^I ; 5-Br-pmd = 5-bromopyrimidine; z = 1 or 2, x = 2 or 4, and y = 2 or 1) [(72)].

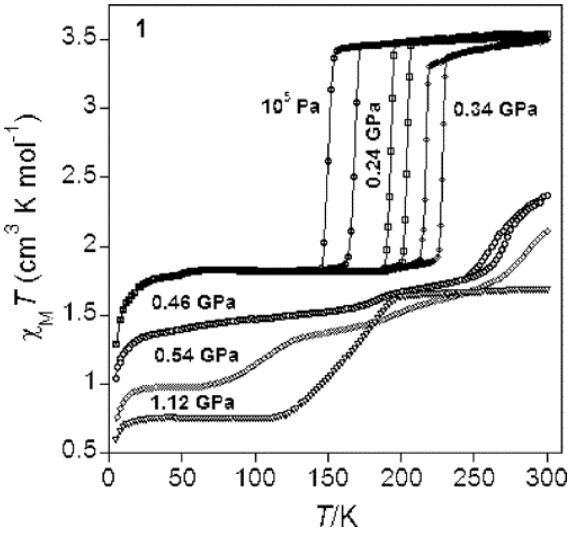

Fig. 1-5: Temperature-dependent magnetic susceptibility measurements performed at 10^5 Pa and 0.24, 0.34, 0.46, 0.54, and 1.12 GPa for the cyanide based SC polymer $\{Fe(5\text{-Br-pmd})_z[Ag(CN)_x]_y\}$ (rate of measurements: 1 K min^{-1}) **[(72)]**.

Recent developments of special hydrostatic pressure cells in combination with magnetic susceptibility measurements as well as optical, Mössbauer, EXAFS and vibrational spectroscopy have paved the way to systematic and detailed studies of the concerted action of temperature and pressure variation of SC compounds [(71), (73)]. In fact, these studies have helped to understand the procedures taking place in SC compounds during a thermal spin transition [(73) - (76)].

Besides the fact that pressure may influence a thermal SC, the application of high pressure also can induce a transition in HS systems for which a thermal spin transition does not occur. Those systems may be complex, such as $[Fe(phen)_2Cl_2]$ [(77)], or simple binary compounds, such as iron(II) oxide or iron(II) sulphide [(78)]. In case of the simple binary systems it can be expected that the pre-decided spin transitions occur in minerals of iron and other first transition series metals in the deep mantle and core of the earth [(71)]

1.2.2.3. Spin Transition Induced by Light – the LIESST Effect

The first evidence of a light-induced spin transition in an iron(II)-SC compound in solution has been reported by McGarvey and Lawthers [79]. Later Decurtins [14], [15] *et al.* have discovered a light induced $^1A_1$ (LS) → $^5T_2$ (HS) conversion at temperatures far below the temperature necessary for a thermally induced spin transition during an optical spectroscopic examination of the complex $[Fe(ptz)_6](BF_4)_2$ in solid state. A mechanism with two steps of intersystem crossing, each with ΔS = 1, from the originally excited $^1T_1$-LS state via the energetically lower $^3T_1$ state to the $^5T_2$ state has been postulated. Due to the significant changes in the bond-lengths at the transition from LS to HS the energy barrier between the two states is big enough to trap the system in the HS state at low temperatures. Therefore the light-induced spin transition is also called Light Induced Excited Spin State Trapping (LIESST). Further investigations of this matter have proved the correctness of the postulated mechanism mentioned above and also a possibility to switch the system back from HS to LS by light, the so called reverse-LIESST effect, have been discovered [80], [81]. Both LIESST and reverse-LIESST are schematically illustrated in Fig. 1-6.

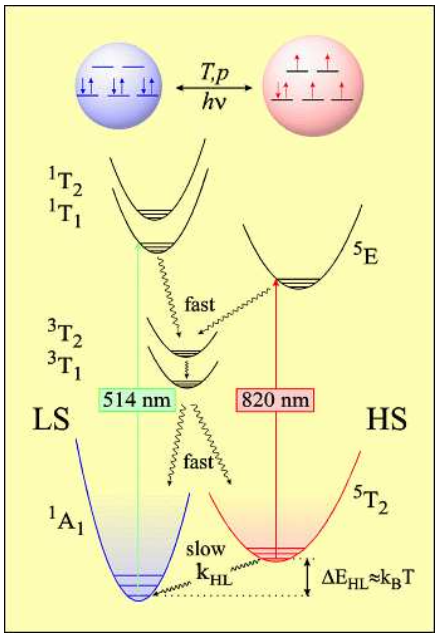

Fig. 1-6: Schematic illustration of LIESST and reverse-LIESST of a SC-complex with a d^6 transition metal centre [82]. Arrows denote the spin allowed d-d transitions and waved lines the radiationless relaxation processes.

The spin allowed excitation $^1A_1$ → $^1T_1$ with typical lifetimes for the $^1T_1$ state in the range of nanoseconds is accomplished by the green light (514 nm) of an Ar^+-laser at temperatures ≤ 50 K. Then a fast relaxation cascading over two successive steps of intersystem crossing ($^1T_1$ → $^3T_1$ → $^5T_2$) populates the metastable $^5T_2$ state. Radiative relaxation to the ground state ($^5T_2$ → $^1A_1$) is forbidden and a decay of the metastable state caused by thermal tunnelling to the ground state is slow at low temperatures. The application of the near infrared light (≈ 820 nm) of a sapphire laser induces the reverse-LIESST effect, where the $^5T_2$ state is excited to the ^5E state. From this state two subsequent intersystem crossing processes lead back to

the LS ground state ($^5E \rightarrow {}^3T_1 \rightarrow {}^1A_1$). Another possibility to achieve a reverse-LIESST effect is via $^5T_2 \rightarrow {}^3T_1 \rightarrow {}^1A_1$ transitions using near infrared light of 980 nm.

Usually the lifetime of the photoinduced HS state is quite long at low temperatures, e.g. weeks for $[Fe(ptz)_6](BF_4)_2$ at 20 K [80], but above 50 K thermal activation accelerates the relaxation *via* tunnelling which leads to the complete decay of the HS state within seconds. The first guideline allowing some estimations and expectations about the lifetime of the photoinduced HS states was introduced by Hauser [83], [84] in the early 1990´s after carefully investigating the dynamics of the LIESST effect in different dilute SC-complexes. The lifetime of the LIESST state extrapolated to $T \rightarrow 0$ (*e.g.* in the tunnelling region [85]), expressed as $\ln k_{HL}(T \rightarrow 0)$, is strongly correlated with the thermal SC temperature. This implies that the lifetime of the metastable LIESST state is inversely proportional to T_{SC}, the temperature at which the first derivative of $\chi \cdot T$ shows a maximum. This relation is also known as the *Inverse-Energy-Gap* Law. Based on this law more than sixty SC-compounds have been investigated by Létard [86], [87] *et al.*, who have summarized the results in the *T(LIESST)*-database to clarify the relation between *T(LIESST)*, which is the maximum temperature at which the *LIESST*-effect is still observable, and T_{SC}.

1.2.2.4. Spin Transition Induced by Nuclear Decay – the NIESST Effect [71]

The Nuclear decay-Induced Excited Spin State Trapping, abbreviated as *NIESST*, has been discovered during studies of the products of nuclear decay of ^{57}Co labelled Fe(II) coordination compounds *via* Mössbauer emission spectroscopy. In the case of Fe(II) complexes possessing a low spin ground state under normal conditions it has been found that metastable high spin states of ^{57}Fe(II) have been produced.

Experiments have shown that the *NIESST* Effect is closely related to the *LIESST* Effect described above, for the relaxation mechanisms are the same in both phenomena and just the means of excitation are different: In *LIESST* experiments external light sources are used to create the long-lived metastable spin states, whereas the *NIESST* Effect takes advantage of nuclear decay as an intrinsic excitation source to trap the generated metastable spin states in the "time window" of Mössbauer spectroscopy.

1.2.2.5. Spin Transition Induced by Strong Magnetic Fields

In 1982 Sasaki and Kambara have been first to demonstrate the possibility to induce a spin transition by applying a magnetic field and they also have proposed a model based on the ligand field theory to predict the effect of large static magnetic fields of 20 – 200 Tesla in ferrous and ferric compounds [88]. Shortly after, the quantification of the effect has been accomplished by Qi *et al.* [89], who have measured a shift of the transition curve of -0.1 K for the SC compound $[Fe(phen)_2(NCS)_2]$ in an applied magnetic field of 5.5 Tesla. In a more

recent work Bousseksou *et al.* [90] have investigated the effect of an intense, pulsed field of 32 Tesla on the spin state of the same compound (see Fig. 1-7). The shift of the transition curve has been reported to be 2.0 K.

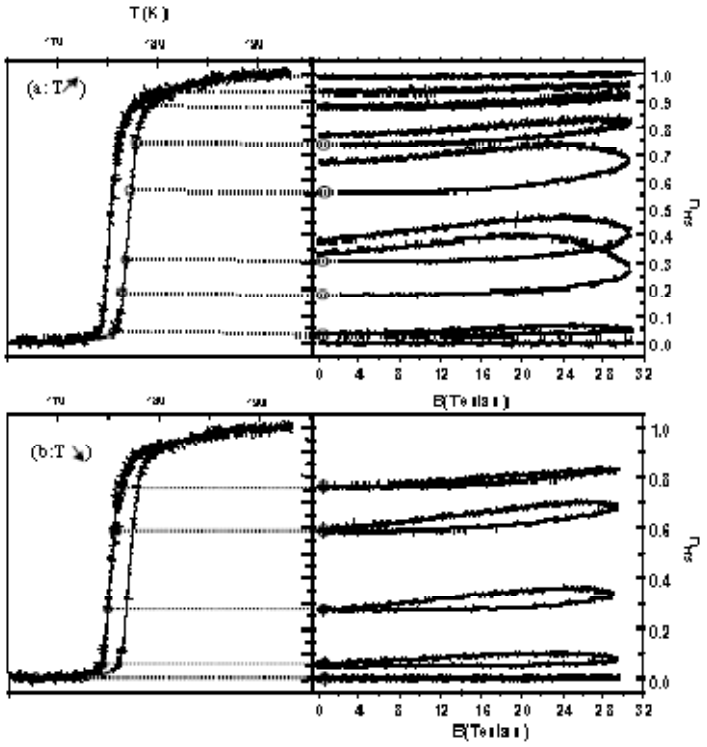

Fig. 1-7: [Fe(phen)2(NCS)], the complete set of pulsed field experiments in the ascending (a) and descending (b) branches of the thermal hysteresis loop [90].

Considering the interest in the designing of molecular switching devices based on SC compounds, the use of pulsed magnetic fields represents a valuable tool for the investigation of the switching dynamics.

1.2.3. Research Methods at a Glance

A spin transition is accompanied by the change of several physical properties of the SC-compound, what from the following research methods (see Tab. 1-1) lend themselves to track the progression of a SC.

Tab. 1-1: General conspectus of measuring methods used to track the SC-behaviour

Method	Measured parameter(s)	Physical condition of the sample
^{57}Fe-Mössbauer-spectroscopy	relative transmission vs. velocity	solid state
Faraday-balance of a Foner- or SQUID-magnetometer	magnetic susceptibility χ(T)	solid state
NMR-Evans-method	magnetic susceptibility χ(T)	in solution
Temperature-dependent FIR and UV-VIS-NIR	vibrational modes ligand-central atom	solid state
X-ray, neutron- or synchrotron-irradiation	diffraction patterns	solid state
Calorimetry	change in enthalpy ΔH or entropy ΔS	solid state
kinetic methods	speed of relaxation after disturbing the state of eqilibrium	solid state or in solution

The temperature-dependent HS to LS transition in solid state is preferentially explored using octahedral iron(II)-complexes, due to their excellent suitability for ^{57}Fe-Mössbauer-spectroscopy which allows to follow the SC as a function of temperature, pressure, time and other parameters.
Another important measurand is the magnetic susceptibility χ(T) of the compound. χ(T), which is mathematically described by the *Van Vleck*-formula [(91)], hinges on the quantity of unpaired electrons and for SC-compounds a high temperature-dependence of the product χ·T can be expected. The magnetic susceptibility is determined by means of magnetic balances, such as the *Faraday*- or *Gouy*-balance, or using a SQUID-magnetometer (SQUID = **S**uperconducting **Qu**antum **I**nterference **D**evice).
Due to the change in bond lengths during a spin transition, an analysis of the crystal structure may also be used to track the SC as well as spectroscopic methods, where different vibrational modes between the ligand and the central atom are observed in the HS or LS state.

1.3. Spin Crossover of Iron(II)-Complexes

A complex containing Fe(II), which is a metal of $3d^6$ configuration, as central atom has the characteristic trait to change its magnetic properties completely during a SC, namely from diamagnetic in the LS state to paramagnetic in the HS state. The LS state is stable at low temperatures and has the electronic configuration t_{2g}^6 where all six electrons are paired so that no magnetic moment may result. During heating the complex undergoes a spin transition to the HS state, whose electronic configuration is $t_{2g}^4 e_g^2$ and a magnetic moment is generated by the four unpaired electrons (see Fig. 1-8).

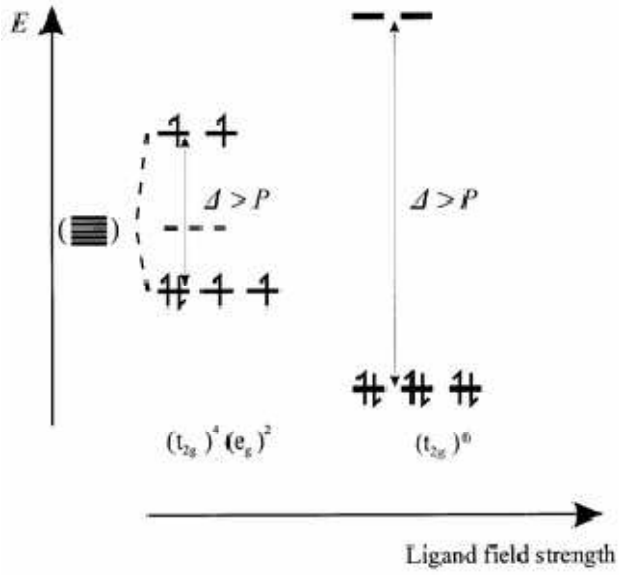

Fig. 1-8: HS and LS configuration of a d^6 transition metal in an octahedral ligand field

The change of the bond length at the spin transition, which has been pointed out by König [9], can be explained by means of the HS state´s configuration: The e_g orbitals, which are occupied in the HS state, are of an anti-bonding nature and thus the electron density between the metal core and the surrounding ligands is decreased. This leads to a weakening of the metal-ligand bond strength and an increase of its length. Due to this difference in the bond length, the potential well of the HS state is situated at higher energies than it is in the LS state (see Fig. 1-9). This difference in energy between the two states can be observed by the means of temperature dependent IR spectroscopy in the FIR-range where the metal-ligand modes change from approximately 250 cm^{-1} for the HS-Fe(II) to approximately 400 cm^{-1} for the LS-Fe(II) [92] - [94].

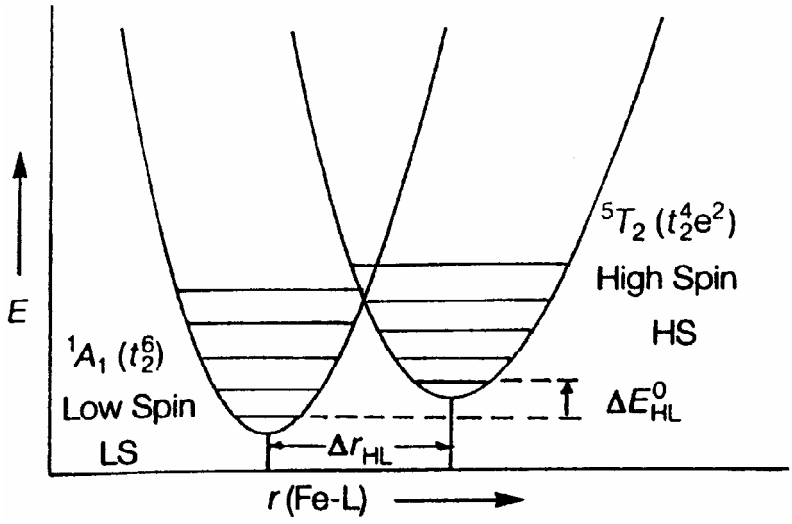

Fig. 1-9: quantum wells of an iron(II)-complex in the HS and the LS state (abscissa: energy, ordinate: bond length metal-ligand)

1.4. Assignment of Tasks

Based on already existing experiences concerning iron(II)-SC compounds with heterocyclic N-coordinating ligands, e.g. (2,6-bis(benzimidazol-2´-yl)pyridine) [3], [95] - [114] and its analogues, new systems of poly-dentate N-coordinating ligands ought to be explored. Particularly tridentate ligands with two separate coordination sites which are apt to form coordination polymers are of interest.

As a further development of the benzimidazole-pyridine system a novel tridentate ligand, namely 2,3,5,6-tetrakis(benzimidazol-2´-yl)pyrazine ((bi)$_4$pz), has to be synthesized and characterized. Subsequently iron(II)-complexes with that ligand are to be prepared, characterized and investigated concerning their SC-behaviour. Assuming that Fe(II) forms octahedral complexes with (bi)$_4$pz, the possibility for the generation of infinite 1D chains with meridionally coordinating ligands and Fe(II) ions alternating one another is provided. Due to the rigidity of the chains a strong cooperative effect and thus an abrupt SC-behaviour is reckoned. The SC behaviour has to be investigated at first with means of temperature dependent UV-Vis-NIR spectroscopy and then, in case of an observed spin transition, other more elaborate measuring methods, such as Mössbauer spectroscopy, may be used for further investigations.

2. Experimental Part

2.1. Chemicals and Standard Physical Characterization

2,3,5,6-tetramethylpyrazine (98%) and o-phenylenediamine (98%) were obtained from Aldrich. All other chemicals were standard reagent grade and used as supplied.

Elementary analysis:
Elementary analysis (C, H and N) was performed by the Mikroanalytisches Laboratiorium, Faculty of Chemistry, Vienna University, Währingerstraße 42, A-1090 Vienna, Austria.

Mid-range FTIR Spectroscopy:
The IR spectra were obtained using a Perkin-Elmer 16PC FTIR spectrometer.
The spectra of the compounds were recorded as KBr-pellets within the range of 400 – 4000 cm^{-1}. The pellets were obtained by mixing a small amount of the compound with KBr and pressing the powdered mixture *in vacuo* using a hydraulic press where a pressure of 10.000 $kgcm^{-2}$ was applied for 5 minutes.

NMR (Nuclear Magnetic Resonance):
For the recording of ^{1}H-NMR and ^{13}C-NMR spectra a Bruker DPX 200 MHz spectrometer was used.
The samples were prepared by dissolving approximately 14 mg of a compound in an appropriate deuterated solvent. The solvents used were D_2O, d_6-DMSO and deuterated trifluoroacetic acid (d-TFA), respectively.

UV-VIS-NIR Spectroscopy:
UV-Vis-NIR spectra were recorded using a Perkin Elmer Lambda 900 UV-VIS-NIR spectrometer within 1500 and 190 nm.
The samples were measured in solid state using the diffuse reflectance technique implemented by a thermostatable sample holder (Praying Mantis™) and controlled by a Harrick temperature controller.

HPLC (High Pressure Liquid Chromatography):
HPLC was performed on a HP 1090 Liquid Chromatograph with a built-in Diode Array Detector and an external HP 1096 Fluorescence Detector, using HPLC-grade methanol as mobile phase and a C_{18} reversed phase (Hypersil ODS) column.
After dissolving the samples in methanol, they were filtered before being injected into the column in order to avoid a plugging of the column with particles.

TGA (Thermo Gravimetric Analysis):
TGA was conducted on a Netzsch TG 209 C with a Netzsch TASC 414/4 controller (temperature range: 20°C – 500°C) and a DuPont 951 Thermogravimetric Analyzer with a DuPont 9900 Computer/Thermal Analyzer (temperature range: 20°C – 1000°C), respectively.

XRPD (X-Ray Powder Diffraction):
X-ray powder patterns were recorded on a Shimadzu XRD-6000 diffractometer, operated at 40 kV/20 mA, in Bragg-Brentano geometry using graphite-monochromatised Cu $K\alpha_{1,2}$ radiation. The 2θ-range within 3° and 60° was covered with a stepwidth of 0.04° and a time/step of 2.5 s.
For the measurements the samples were spread on glass plates with hexane as immersing liquid.

SQUID Magnetometry:
Measurements of the magnetic susceptibility χ(T) were conducted at applied fields of 0.1, 1 and 3 Tesla, respectively, within a temperature range of 4.2 K – 300 K on a Cryogenic Limited SQUID-magnetometer at the Institut für Festkörperphysik, Vienna University of Technology, Austria.

2.2. Synthesis of the Ligand

2.2.1. "Traditional" reaction pathway

The synthesis of heterocyclic benzimidazole-ligands was based upon the often cited method of Addison and Burke [115] of 1981, where the benzimidazole formation was achieved by heating a carboxylic acid with o-phenylenediamine in an acidic medium.

2.2.1.1. Synthesis of the Precursor Pyrazine-2,3,5,6-tetracarboxylic Acid [$(COOH)_4pz$] [116] - [118]

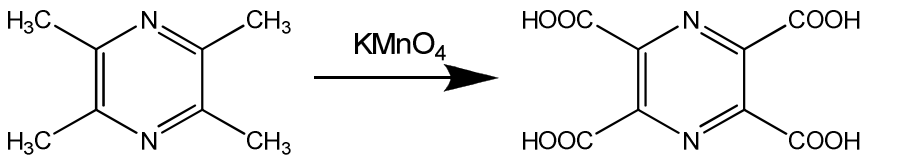

2,3,5,6-tetramethylpyrazine

molecular weight: 136.2
molecular formula: $C_8H_{12}N_2$

pyrazine-2,3,5,6-tetracarboxylic acid

molecular weight: 256.1
molecular formular: $C_8H_4N_2O_8$

11.6 g (85.3 mmol) of 2,3,5,6-tetramethylpyrazine were suspended in 200 ml of water. Then an excess of $KMnO_4$ (135.7 g = 0.87 mol) was added successively at 20 – 30°C within several hours in order to avoid runaway reactions. After the addition of the total amount of $KMnO_4$ the reaction was continued for 14 h at room temperature. A solution of 8.1 g KOH in water was prepared and added to the reaction mixture, which then was stirred at room temperature for another 0.5 h before heating it up to 40°C. Due to the exothermic process during the reaction the temperature rose up to 60°C and thus cooling was necessary to keep the temperature within the range of 40 – 50°C required by the literature. The reaction was continued whilst stirring for another 15 h at 45°C. After addition of 11 ml of ethanol the slurry was stirred for 2 more hours at 45°C in order to destroy excess-$KMnO_4$. The precipitated MnO_2 was filtered using a *Hyflo* bed. A purple colour of the filtrate indicated the existence of excess-$KMnO_4$ remnants. Thus the procedure of adding ethanol, heating and filtrating had to be continued until a colourless filtrate was obtained (summed up, 90 ml of ethanol have been added). After washing the *Hyflo* bed several times with hot water, the filtrate including the wash water was concentrated on a hot plate to a volume of 100 ml. The concentrated solution was acidified with conc. HCl to pH 2, whereupon a white solid precipitated. The solution with the precipitate was kept in the refrigerator at 5 °C for 3 days. The white precipitate was recovered by filtration and after washing it two times with 10 ml of ice cold water it was dried *in vacuo* at 100°C. For purification the precipitate was recrystallized from 20%ic HCl, whereupon a brown solution formed, which was kept in the refrigerator overnight. From this treatment a crystalline product could be obtained, which

was recovered by filtration and after washing it three times with 10 ml of ice cold water, it was dried *in vacuo* at 100°C.

Yield: 7.2 g = 33 %

^{1}H NMR (d_6 -DMSO) [ppm]: 9.25 (s, H of carboxylic acid, 4H)
(D_2O) [ppm]: no peaks except solvent peak, H-D interchange

^{13}C NMR (D_2O) [ppm]: 145.58 (C in pyrazine ring), 167.57 (C of carboxylic acid)

IR (KBr-pellet, %T) v/[cm^{-1}]: 2929 (w), 2600 (w), 1727 (s, C=O stretching mode of carboxylic acid), 1657 (s, C=N and C=C stretching modes of pyrazine ring), 1460 (m), 1242 (s), 1173 (m), 1138 (s), 780 (m)

Melting point: Found: start of decomposition at 225 °C (TGA, see Appendix 5.4)
Literature [119]: decomposition at 205 °C

2.2.1.2. Synthesis of 2,3,5,6-tetrakis(benzimidazol-2´-yl)pyrazine [(bi)$_4$pz] [115], [116], [120]

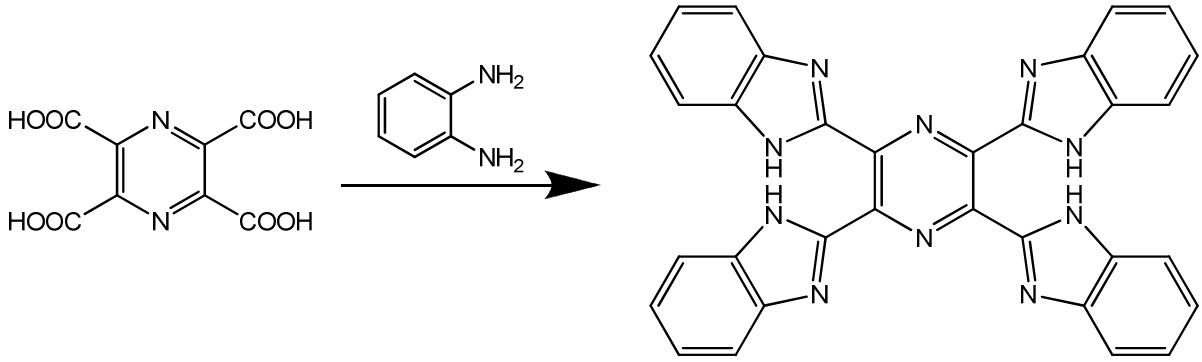

pyrazine-2,3,5,6-tetracarboxylic acid

molecular weight: 256.1
molecular formular: $C_8H_4N_2O_8$

2,3,5,6-tetrakis(benzimidazol-2´-yl)pyrazine

molecular weight: 544.6
molecular formula: $C_{32}H_{20}N_{10}$

Approximately 100 ml of highly viscous polyphosphoric acid were heated up to 100°C in order to reduce its viscosity and thus alleviating the blending of the reactants. A mixture of 10.7 g (99.0 mmol) o-phenylenediamine and 5.8 g (22.6 mmol) $(COOH)_4$pz was added. The reaction mixture was heated up to 170°C whilst stirring for 8 h. The dark brown melt was poured into 1.5 L of vigorously stirred ice cold water, which led to the precipitation of a greenish solid. After keeping the solution with the precipitate at room temperature for 3 days the precipitate was recovered by filtration. After suspending it into 400 ml of water and

neutralizing the suspension with conc. NH_3-solution to pH 7, the precipitate was recovered by filtration.

Due to the fact, that no sources in literature had given an account of $(bi)_4pz$ by the time, the purification of the ligand was quite experimental. According to a research report [116] the ligand should be soluble in DMSO and DMF, both solvents that were not truly applicable for purification due to their low volatility. Thus an experimental series was performed in order to find an appropriate solvent for purification. For this purpose a small amount of dry $(bi)_4pz$ was placed in a test tube and few millilitres (2 to 3 ml) of solvent were added. Then the samples were heated up under vigorous mixing or were treated for 5 minutes at 30°C in a supersonic bath. The results of this experimental series might be gleaned below.

- **Not or poorly soluble**: carbon tetrachloride, water
- **Partly soluble**: acetone, methylene chloride, methanol, ethanol, sodium hydroxide solution 5N, THF, ethyl acetate, toluene, DMSO, DMF, diethyl ether, acetonitrile, nitromethane, propylene carbonate. The experiments of dissolution with these solvents showed a yellow colouring of the solution but a total dissolution of the samples could not be achieved.

Based upon the purification method for benzimidazole pyridines [106] 3.9 g $(bi)_4pz$ were suspended in 150 ml of water. The suspension was stirred for 2.5 h at 40°C after alkalization with diluted NaOH solution to pH 9 – 10. This treatment assured the removal of $(COOH)_4pz$ remnants. The solid was recovered by filtration of the warm suspension and washed five times with water. Then it was suspended in 100 ml of methanol/water (1:1) and stirred for 30 minutes at 50°C. Again, the ochre solid was recovered by filtration of the warm suspension and after washing it five times with water, it was dried *in vacuo* at 100°C to give 3.5 g of purified $(bi)_4pz$. For further purification the solid was treated with toluene in a *Soxhlet* extractor for one week. The orange extract was stripped off the solvent to give a brown paste-like solid which proved to be smut. The remaining ochre solid (fraction #1) was dried *in vacuo* at 100°C. After ^{1}H-NMR analysis showed that the purification had not been entirely successful, an analysis with HPLC in methanolic solution was conducted: A saturated methanolic solution of fraction #1 was prepared and subsequently filtered. The filtrate was then analyzed by HPLC and the remaining solid by ^{1}H-NMR.
The results showed that the treatment with methanol improved the purity of the remaining solid. Thus fraction #1 was decocted in a solution of methanol basified with 10%ic NaOH, followed by filtration of the insoluble product, which then was decocted again in pure methanol. After filtration the greenish-yellow solid was dried *in vacuo* at 100°C.

The synthesis was carried out a second time with recently prepared or bought chemicals. This time the raw product was recrystallized from THF. The remaining greyish-brown solid (fraction #2) was recovered by filtration and the filtrate was stripped off the solvent to give a brown powder (fraction #3). Both fractions were dried *in vacuo* at 100°C. Fraction #2, as well as the remaining raw-product of the first synthesis, was additionally recrystallized from DMF

as an attempt for further purification, as suggested in the literature [116]. For the recrystallization from DMF did not prove to be successful, the fractions #2 and #3 were united and purified analogous to fraction #1.

Yield: 8.4 g = 68 % (raw product)

^{1}H NMR (d_6-DMSO) [ppm]: 7.31 (m – badly resolved, aromatic H, 8H), 7.71 (m – badly resolved, aromatic H, 8H)

^{13}C NMR (d-TFA) [ppm]: 116.29 (aromatic C), 131.20 (aromatic C), 134.10 (aromatic C), 137.98 (pyrazine C), 142.15 (C=N)

IR (KBr-pellet, %T) ν/[cm^{-1}]: 3405 (w, R_2N-H mode of the imidazole moiety), 3061 (w, =C-H stretching mode of aromatic rings), 1584 (m), 1452 (m), 1429 (s), 1333 (s), 1252 (m), 1228 (s), 739 (vs, mode specific for 1,2-disubstituted arenes)

UV-Vis-NIR at room temperature [nm]: 445 (shoulder), below 400 total absorbtion

Melting point: start of decomposition at 500°C, coking (TGA, see Appendix 5.4)

Elementary analysis: Found: H 3.8 %, C 63.5 %, N 22.9 %
Calculated: H 3.7 %, C 70.6 %, N 25.7 %

2.2.2. Alternative Synthesis of $(bi)_4pz$

The synthesis described in the following chapters was based upon already existing works (see references denoted at the particular chapters) which were customized.

2.2.2.1. Synthesis of the Precursors Bis(benzimidazol-2´-yl)ethane-1,2-diol $[Et(bi)_2(OH)_2]$ and Bis(benzimidazol-2´-yl)ethane-1-ol-2-on $[Et(bi)_2olon]$ [121), (122)]

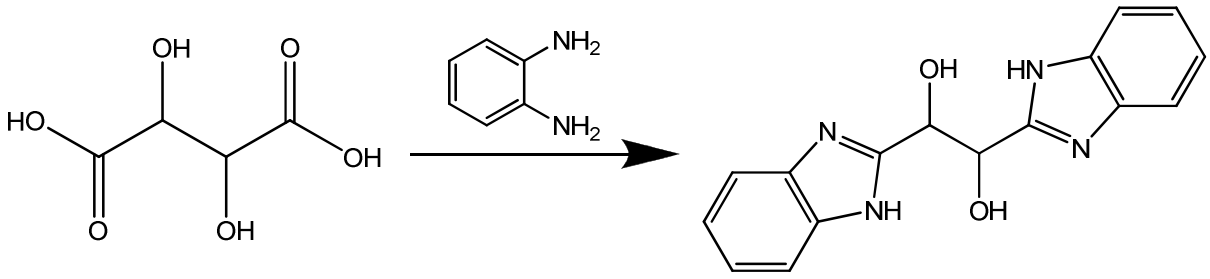

tartaric acid

molecular weight:150.1
molecular formula: $C_4H_6O_6$

bis(benzimidazol-2´-yl)ethane-1,2-diol

molecular weight: 194.3
molecular formula: $C_{16}H_{14}N_4O_2$

To 22.5 g (0.15 mol) of tartaric acid and 32.5 g (0.30 mol) of o-phenylenediamine 300 ml of 4N HCl were added. The reaction mixture was heated on the reflux for 10 h and after cooling to room temperature it was kept in the refrigerator at 5°C. The resulting crystals were recovered by filtration and the filtrate was stored in the refrigerator for further workup. After dissolving the crystals in water the product was precipitated with 5N NaOH. For purification an excess of NaOH was added to dissolve the precipitate whereupon dark particles of smut remained which were removed by filtration. The filtrate was acidified with 20%ic HCl until a crème-coloured solid precipitated which was recovered by filtration. After washing the precipitate thoroughly with cold water it was stored in the exsiccator over $CaCl_2$ for drying.

5N NaOH was added to the mother liquor from the filtration of the crystals until the forming precipitate dissolved again, leaving dark particles of smut in the solution. The smut was removed by filtration and further fractions of $Et(bi)_2(OH)_2$ were obtained by acidifying the filtrate with 20%ic HCl. Due to the darker colour of these fractions, recrystallization from water was necessary after recovering them by filtration. A total of three fractions was obtained.

Yield: 9.4 g = 21 %

^{1}H NMR (d_6-DMSO) [ppm]: Found: 5.35 (d, CH, 2H), 5.99 (d, OH, 2H – found: 1H), 7.14 (m, aromatic H, 4H), 7.51 (m, aromatic C, 4H), 12.34 (s, NH, 2H – found: 1H); D-H interchange in case of OH and NH likely

Literature [123] (300 MHz) for R,R-Et(bi)$_2$(OH)$_2$: 5.28 (d, CH, 2H), 5.92 (d, OH, 2H), 7.12 (m, aromatic H, 4H), 7.49 (m, aromatic H, 4H), 12.33 (s, NH, 2H)

IR (KBr-pellet, %T) v/[cm^{-1}]: 3440 - 3320 (s, R_2N-H modes of the imidazole moiety), 3057 (w, =C-H stretching mode of aromatic rings), 2782 (w, aliphatic -C-H mode), 1528 (m), 1455 (s), 1431 (s), 1309 (m), 1273 (s), 1111 (m), 1086 (m), 738 (vs, mode specific for 1,2-disubstituted arenes)

Melting point: Found: start of decomposition at 249 °C (analyzed with a Tottoli apparatus)

Literature [124]: 268 °C

The partial oxidation of Et(bi)$_2$(OH)$_2$ to Et(bi)$_2$olon might be accomplished with $KMnO_4$ and $K_2Cr_2O_7$, respectively. In both cases the amount of oxidizing agent needed to be calculated properly in order to prevent a total oxidation of the substance.

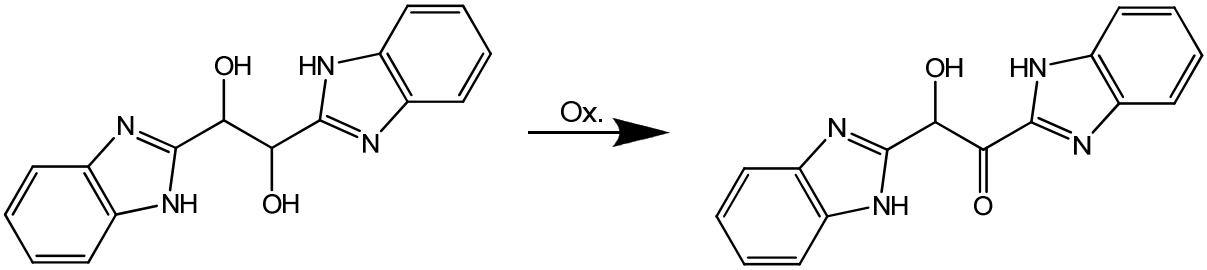

bis(benzimidazol-2´-yl)ethane-1,2-diol

molecular weight: 194.3
molecular formula: $C_{16}H_{14}N_4O_2$

bis(benzimidazol-2´-yl)ethane-1-ol-2-on

molecular weight: 192.3
molecular formula: $C_{16}H_{12}N_4O_2$

- **Oxidation with $KMnO_4$**

1.6 g (8.2 mmol) Et(bi)$_2$(OH)$_2$ were dissolved in 14.6 ml of 10%ic NaOH (aqueous solution) at 70°C. 0.46 g (2.9 mmol) $KMnO_4$ dissolved in water were added drop wise to the warm solution whilst stirring vigorously. After letting the reaction mixture cool down to room temperature over night the formed MnO_2 was removed by filtration and the filter cake was washed with water. The filtrate was acidified with 20%ic HCl to pH 4 whereupon a pale solid precipitated. The solid was recrystallized from ethanol and recovered by centrifugation.

Yield: 0.38 g = 24%

NMR and **IR** data: non-unambiguous assignment (see chapter 3.1.)

- **Oxidation with $K_2Cr_2O_7$**

1.5 g (7.7 mmol) $Et(bi)_2(OH)_2$ were dissolved in 60 ml of hot 6N H_2SO_4. 0.88g (3.0 mmol) of $K_2Cr_2O_7$ dissolved in water were added slowly to the hot solution. A change of colour from light orange to dark green and the formation of a precipitate were observed during this procedure. After recovering the pale precipitate by filtration it was recrystallized from 6N H_2SO_4. The resulting crème-coloured solid was recovered by filtration and after washing it with water it was dried *in vacuo* at 100°C to give 1.11 g. For neutralization portions of sodium-bicarbonate solution were added to the dried precipitate until foaming has stopped. After filtration the product was dissolved in ethanol for recrystallization. Unfortunately, it could not be precipitated the usual way by cooling or freezing out. Thus the solution was diluted with water and precipitation could be accomplished by acidification with 20%ic HCl. The white precipitate was recovered by filtration and after washing it with water it was dried.

Yield: 0.38 g = 25%

NMR and **IR** data: non-unambiguous assignment (see chapter 3.1.)

2.2.2.2. Cyclization of Et(bi)$_2$olon to (bi)$_4$pz [125]

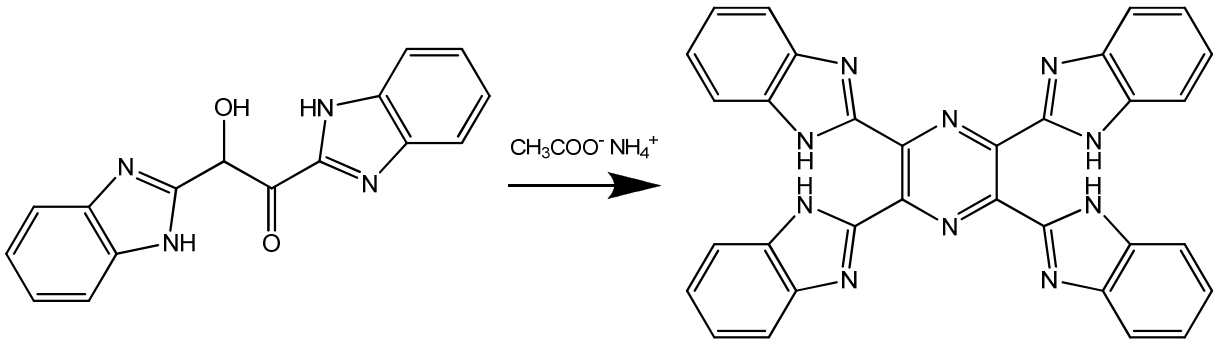

bis(benzimidazol-2´-yl)ethane-1-ol-2-on

molecular weight: 192.3
molecular formula: $C_{16}H_{12}N_4O_2$

2,3,5,6-tetrakis(benzimidazol-2´-yl)pyrazine

molecular weight: 544.6
molecular formula: $C_{32}H_{20}N_{10}$

0.2 g (0.3 mmol, 1 equivalent) Et(bi)$_2$olon were mixed with 4.5 ml glacial acetic acid and 0.5 g (6.1 mmol, 20 equivalents) ammonium acetate to be refluxed for 2 h. After cooling to room temperature a small amount of a dark solid was recovered by filtration using a membrane filter and washed with glacial acetic acid. Conc. HNO_3 was added to the dark filtrate whereupon a change of colour to greenish yellow could be observed. Upon filtration of the acidic filtrate the membrane disintegrated, thus the precipitate was recovered by centrifugation after diluting the filtrate with water. Then the precipitate was recrystallized from glacial acetic acid. The product was recovered by filtration using a membrane filter and after washing it thoroughly with water and ethanol, it was realized that it could not be removed from the membrane. Thus characterization via the usual methods (NMR, IR) was not possible and even XRD did not provide acceptable results due to the interferences caused by the nylon-membrane "substrate".

2.3. Synthesis of the Complexes

The syntheses of the complexes were performed in argon atmosphere.

2.3.1. Complexes with Iron(II)-Perchlorate

0.27 g (0.5 mmol) of $(bi)_4pz$ have been suspended in 20 ml of degassed absolute ethanol. 0.18 g (0.5 mmol) $Fe(ClO_4)_2 \cdot 6\ H_2O$ and a small amount of ascorbic acid (to prevent the oxidation of iron(II) to iron(III)) were dissolved in a few millilitres of degassed absolute ethanol. This solution was added to the suspension of the ligand, which led to an intensive green colouring of the reaction mixture. After stirring for 5 h, the resulting suspension was left to sediment over night. The precipitate was recovered by filtration, washed with ethanol and dried in an exsiccator. The green filtrate was put aside for further investigation.

IR (KBr-pellet, %T) ν/[cm^{-1}]: 3057 (w, =C-H stretching mode of aromatic rings), 1530 (m), 1492 (m), 1459 (s), 1333 (s), 1217 (m), 1107 (s), 741 (s, mode specific for 1,2-disubstituted arenes)

UV-Vis-NIR at room temperature (294 K) [nm]: 800 (broad, shoulder), 607 (broad), 489 (w, broad), 434 (w, broad), total absorption below 400 caused by ligand

Melting point: Due to the explosiveness of perchlorates upon heating or strong agitation and the consequential security measures neither a melting point analysis nor a TGA was performed.

2.3.2. Complexes with Iron(II)-Tetrafluoroborate

0.27 g (0.5 mmol) of purified fraction #1 $(bi)_4pz$ have been suspended in 20 ml of degassed absolute ethanol and acetonitrile, respectively. 0.17 g (0.5 mmol) $Fe(BF_4)_2 \cdot 6\ H_2O$ and a small amount of ascorbic acid were dissolved in a few millilitres of degassed absolute ethanol or acetonitrile. This solution was added to the suspension of the ligand, which led to an intensive green colouring of the reaction mixture. The coloured suspension was stirred over night. The dark green precipitate was recovered by filtration, washed with ethanol and dried *in vacuo* at 100°C. The green filtrate was stripped and the remaining dark solid was then also dried *in vacuo* at 100°C.

IR (KBr-pellet, %T) ν/[cm^{-1}]:

Solvent ethanol: 3290 (w, R_2N-H mode of the imidazole moiety), 3057 (w, =C-H stretching mode of aromatic rings), 1583 (m), 1535 (m), 1495 (m), 1456 (s), 1414 (m), 1339 (vs), 1221 (s), 1144 (s), 1084 (s), 742 (s, mode specific for 1,2-disubstituted arenes)

Solvent acetonitrile: 3306 (w, R_2N-H mode of the imidazole moiety), 3057 (w, =C-H stretching mode of aromatic rings), 1584 (m), 1535 (m), 1494 (m), 1459 (s), 1439 (m), 1338 (vs), 1222 (s), 1145 (s), 1083 (s), 742 (s, mode specific for 1,2-disubstituted arenes)

UV-Vis-NIR at room temperature (294 K) [nm]:

Solvent ethanol: 827 (broad, shoulder), 638 (s), 476 (shoulder), total absorption below 450 caused by the ligand

Solvent acetonitrile: 817 (broad, shoulder), 607 (s, broad), 507 (w, broad), 439 (shoulder), total absorption below 400 caused by the ligand

Melting point:

Solvent ethanol: decomposition at 428.4 °C (TGA, see Appendix 5.4)

Solvent acetonitrile: decomposition at 448.9 °C (TGA, see Appendix 5.4)

3. Results and Discussion

3.1. The Ligand (bi)4pz

The synthesis following the method of Addison and Burke [115] proved to be successful, though a rather high percentage of by-products accrued and a tedious purification was necessary to isolate the desired ligand. Due to the space consuming benzimidazole moieties, which could have easily led to a steric hindrance at higher levels of substitution at the pyrazine ring, and the harsh conditions during the reaction, which might have caused a decarboxylation of the precursor $(COOH)_4pz$ at those sites, where no benzimidazoles had been formed, the by-products most likely were mono- to triply-substituted pyrazine rings (see Fig. 3-1). ^1H NMR spectra of those compounds had been calculated using the program ChemDraw Ultra (Appendix 5.1) and the results of the predictions matched the experimental results reasonably well.

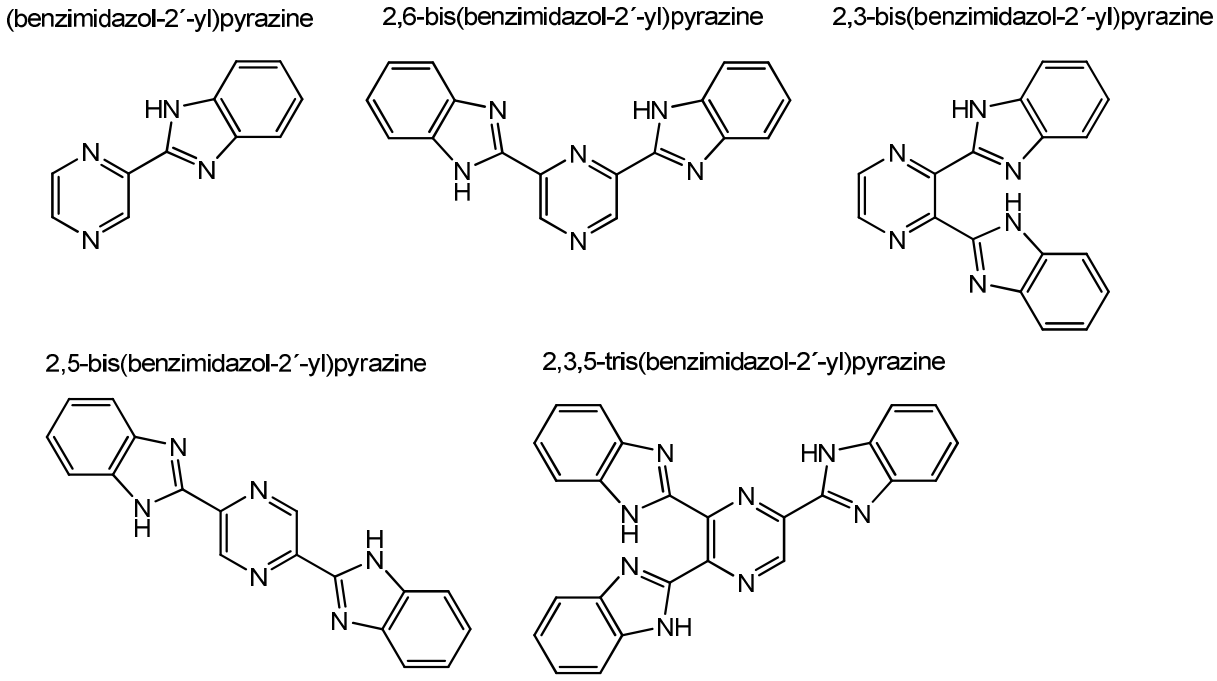

Fig. 3-1: Possible by-products with a single to triple substitution of the pyrazine ring which may occur during the synthesis of $(bi)_4pz$ following the method of Addison and Burke.

The HPLC measurement showed that the methanol-soluble fraction mainly consisted of one of the by-products (see Fig. 3-2). The solution´s impureness caused by other compounds was 10 – 12% at a maximum. Comparing the ^1H NMR spectrum of the solid obtained – after stripping the solution – with the spectra predicted by ChemDraw Ultra, the methanol-soluble fraction most likely consisted of a bi-substituted pyrazine.

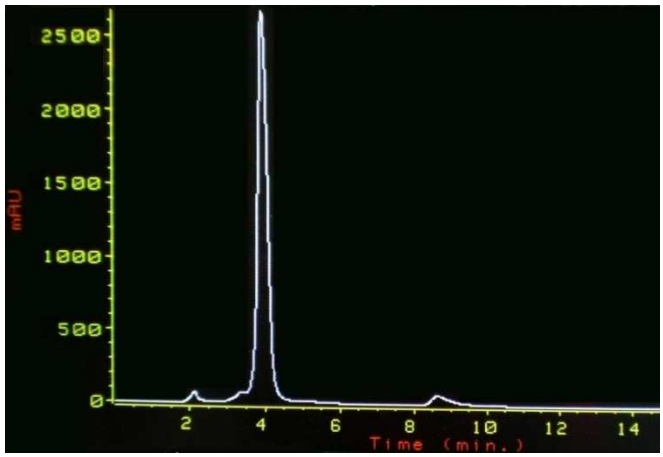

Fig. 3-2: HPLC chromatogram of the methanol-soluble fraction of the still impure ligand $(bi)_4pz$.

The alternative synthesis following the route of Taffs and Prosser [122] to $Et(bi)_2olon$ and its adjacent cyclization failed because the partial oxidation of $Et(bi)_2(OH)_2$ to $Et(bi)_2olon$ did not lead to the desired result. As shown in Fig. 3-3, the partial oxidation gave two different products depending on the oxidizing agent ($KMnO_4$ and $K_2Cr_2O_7$, respectively) used. By comparing the IR (see Fig. 3-3 and Appendix 5.3) and NMR (see Appendix 5.3) spectra of $Et(bi)_2(OH)_2$ and $Et(bi)_2olon$ oxidized with $K_2Cr_2O_7$ their similarity was obvious and thus it was reasoned, that the obtained product was the not converted starting material $Et(bi)_2(OH)_2$. The IR (see Fig. 3-3 and Appendix 5.3) and NMR (see Appendix 5.1) spectra of $Et(bi)_2olon$ oxidized with $KMnO_4$ provided inconsistent data and no unambiguous characterization was possible.

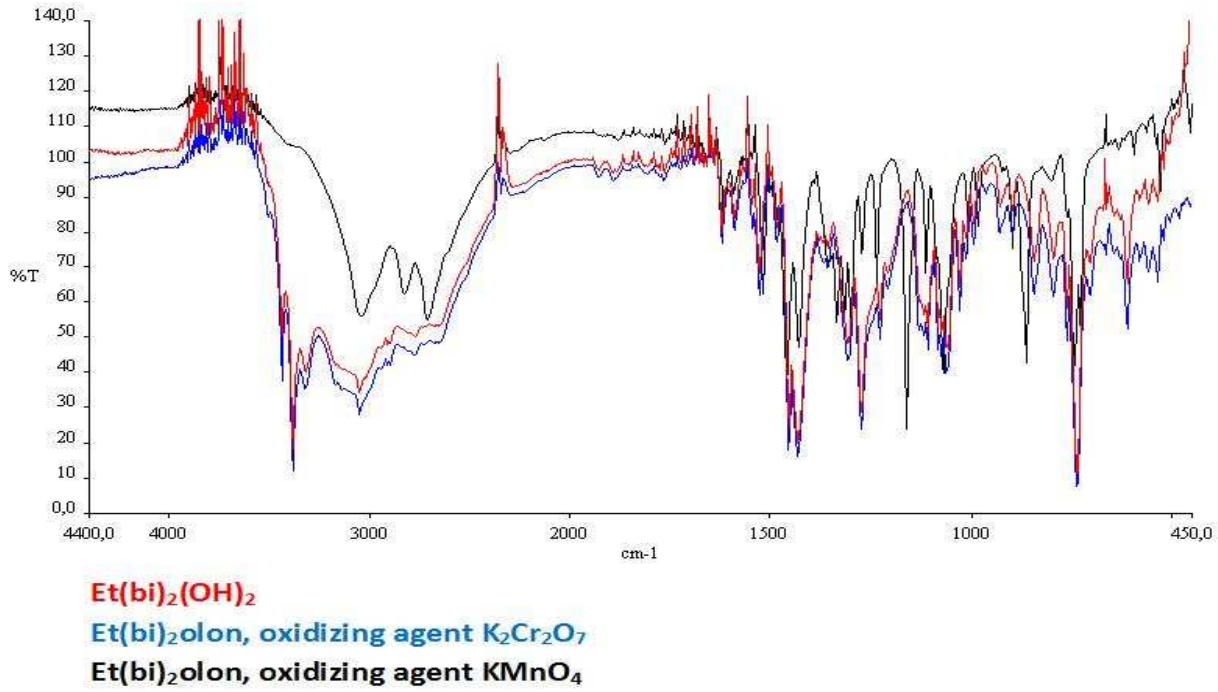

Fig. 3-3: Comparison of the IR spectra of $Et(bi)_2(OH)_2$ (red) and $Et(bi)_2olon$ (black and blue).

One problem was the uncertainty concerning the structure, where two possibilities existed due to the keto-enol tautomerism of the molecule (see Fig. 3-4). Furthermore complete oxidation of the diol to the diketone proved to be a problem during the synthesis of $Et(bi)_2olon$.

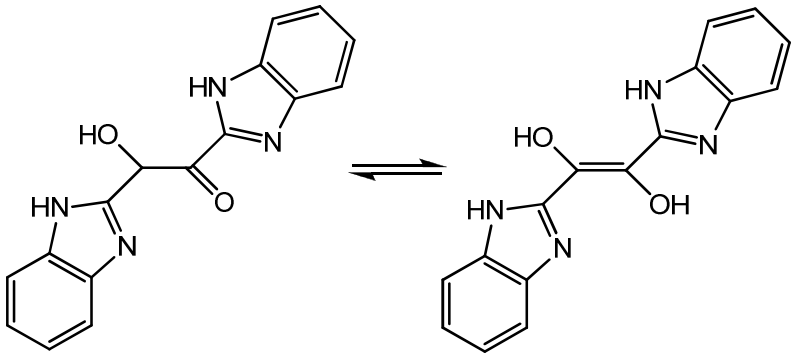

Fig. 3-4: Keto-enol tautomerism of the precursor $Et(bi)_2olon$.

A possibility to avoid the problematic oxidation step might be a Benzoin-condensation (see Fig. 3-5), a coupling reaction between two aldehydes suitable for the preparation of α-hydroxyketones. The benzimidazole-2-aldehyde needed for such a reaction could be, according to the work of Schütze [126], synthesized *via* saponification of 2-dichlormethyl-benzimidazole.
The product of the Benzoin-condensation could be then cyclisized to the desired ligand $(bi)_4pz$, as described previously in chapter 2.2.2.2.

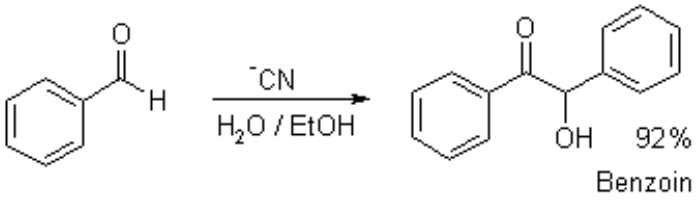

Fig. 3-5: Reaction scheme of a traditional Benzoin-condensation.

3.1.1. IR

The IR spectrum of the free ligand showed the expected R_2N-H (3405 cm^{-1}) and =C-H (3061 cm^{-1}) modes, as well as the band of 1,2-disubstituted arenes at 739 cm^{-1}. Further vibration modes below wave numbers of roughly 1600 cm^{-1} were attributed to diverse vibrations of the conjugated ring system consisting of the pyrazine ring and its benzimidazole substituents. It seemed likely that those modes were specific for the ligand, and that they might be affected by complexation at a whole (see chapter 3.2.1.).

3.1.2. UV-Vis-NIR

Below approximately 400 nm the free ligand showed the typical total absorption of arenes with conjugated π-systems.

3.1.3. XRPD

The free ligand proved to be only partly crystalline, as could be derived from the powder pattern (see Fig. 3-6), in which an amorphous bump arose at 2*θ = 15° – 35°. Nevertheless, compared to the powder pattern of the raw product the crystallinity of $(bi)_4pz$ clearly improved with purification.

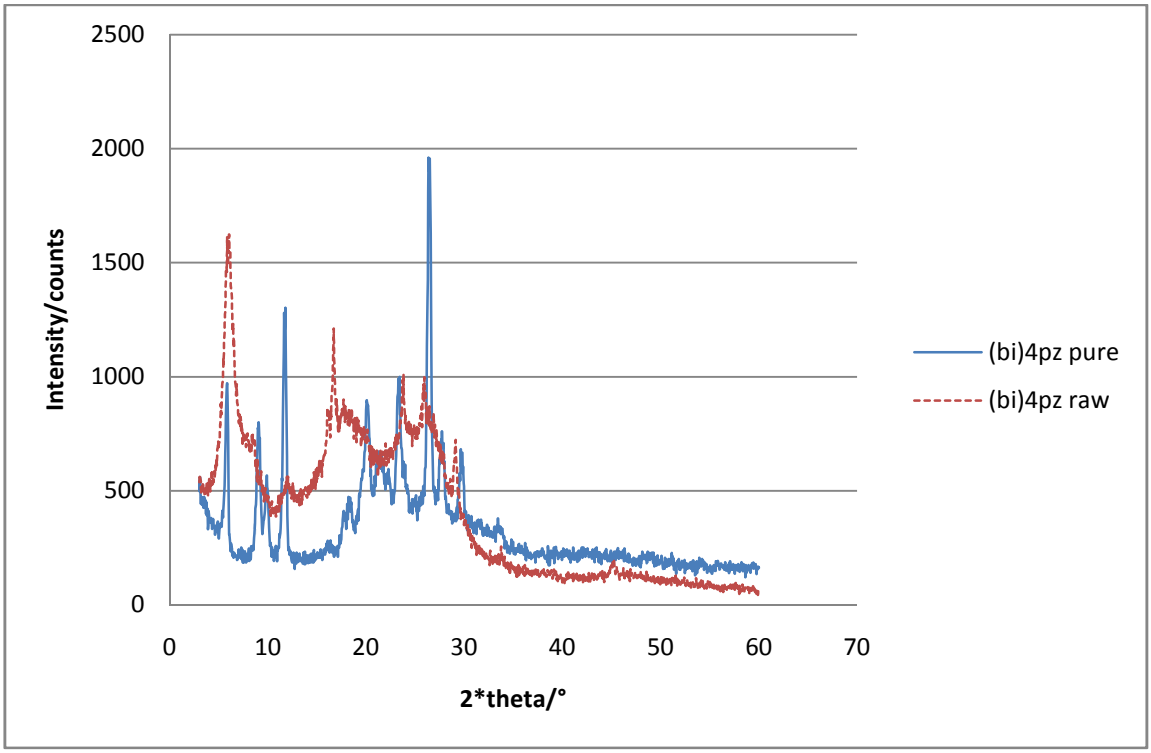

Fig. 3-6: XRPD of the ligand $(bi)_4pz$.

3.2. The Complexes

Once separated from the liquid phase, the intensively green coloured complexes proved to be stable on air.

3.2.1. IR

Despite several attempts to obtain spectra of a proper quality those of $\{Fe[(bi)_4pz]\}(ClO_4)_2$ were rather badly resolved. On that account and because the ligand used in the synthesis of $\{Fe[(bi)_4pz]\}(ClO_4)_2$ proved to be still impure, the IR spectra of $\{Fe[(bi)_4pz]\}(ClO_4)_2$ were not compared with those of the free ligand or the complex $\{Fe[(bi)_4pz]\}(BF_4)_2$ within the discussion.

The IR spectrum of the free ligand clearly differed from the spectra of the complexes (see Fig. 3-7).

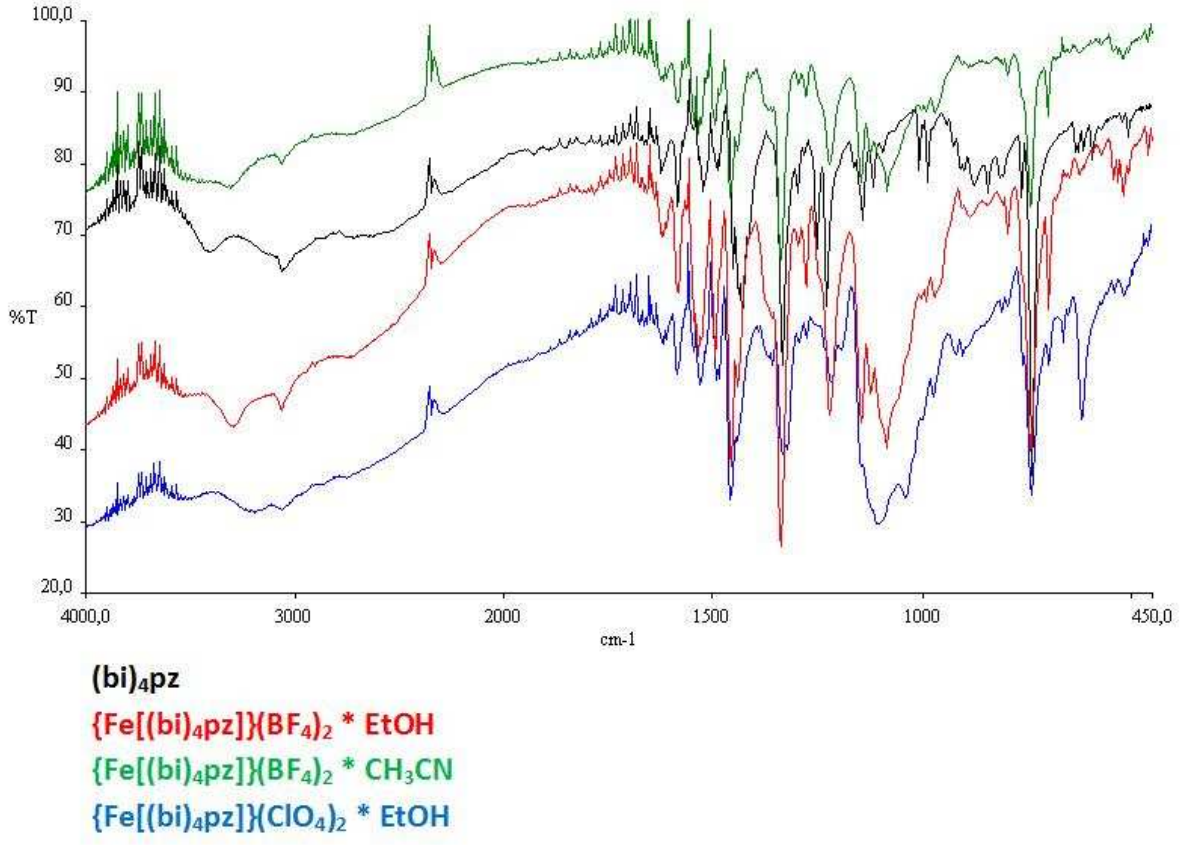

Fig. 3-7: Comparison of the IR spectra of the synthesized complexes (red, green and blue) with one of the free ligand (black).

The R_2N-H stretching modes within the free ligand (3405 cm^{-1}) were shifted to 3306 cm^{-1} within the complex synthesized in acetonitrile and to 3290 cm^{-1} within the complex

synthesized in ethanol, respectively. This shift to lower wavelengths indicated a weakening of the N-H bond due to the coordination of the iron(II), *i.e.* the withdrawal of electron density from the benzimidazole moiety to the metal. In the wave number region accounted to the ligand-specific vibration modes of the pyrazine ring and its benzimidazole substituents (*i.e.* below 1590 cm^{-1}) some slight shifts of about 4 – 10 cm^{-1} and an intensity variation of the modes were observed. Furthermore a new band arose at 1084 cm^{-1} (solvent EtOH), and 1083 cm^{-1} (solvent acetonitrile), respectively. The difference in the position of this new band of 1 cm^{-1} depending on the solvent used was negligible, for the error of measurement averaged ± 4 cm^{-1}. Due to the fact, that this vibration mode did not exist in the IR spectrum of the free ligand, it was caused by the coordination of the iron with the utmost probability.
Nevertheless a few characteristic bands of the ligand, which were not supposed to be affected by the complexation, kept their original position within the error of measurement. These bands were those of the aromatic =C-H stretching modes (free ligand: 3061 cm^{-1} vs. $\{Fe[(bi)_4pz]\}(BF_4)_2$: 3057 cm^{-1}) and the signal of 1,2-disubstituted aromatic rings of the benzimidazole moiety (free ligand: 739 cm^{-1} vs. $\{Fe[(bi)_4pz]\}(BF_4)_2$: 742 cm^{-1}).

Irrespective of the solvent used in the synthesis of the complex $\{Fe[(bi)_4pz]\}(BF_4)_2$, the major signals of its spectra equal each other within the error of measurement. The only exception (as might be seen above) was the signal of the R_2N-H band, which showed a difference in wavelength of 16 cm^{-1} depending on the solvent. This could be explained by the difference of electronegativity of the solvents´ heteroatoms oxygen in ethanol and nitrogen in acetonitrile, respectively: The higher electronegativity of the oxygen compared to the nitrogen resulted in stronger hydrogen bonds between the solvent and the hydrogen of the H-NR_2 group in the benzimidazole moiety of the ligand. This led to a further weakening of H-N bond and thus to a shift to even lower wavelengths in the IR spectrum of the complex synthesized in ethanol.

3.2.2. UV-Vis-NIR and SQUID magnetometry

Irrespective of the grade of purity of the ligand, type of solvent or metal-salt used for complexation no SC could be observed by means of electronic spectroscopy within the available temperature range of 123 K to 373 K. This result did not coercively signify, that the ligand system at hand might not allow a spin transition at all, for the temperature needed to accomplish the transition could be higher than 373 K. In this context several examples of SC compounds with transition temperatures over 400 K were reported in the literature [(3), (127)] and considering the results of the TGA (see Appendix 5.4), heating up the $\{Fe[(bi)_4pz]\}(BF_4)_2$ complexes to similar temperatures should not affect their stability.

Measurements of the magnetic properties of the $\{Fe[(bi)_4pz]\}(BF_4)_2$ complexes (see Appendix 5.5) with a SQUID-magnetometer within a range of 4.2 K and 300 K confirmed the results

obtained at the UV-Vis-NIR spectroscopy. The $\{Fe[(bi)_4pz]\}(ClO_4)_2$ complex was not investigated due to security reasons.

At magnetic fields of 1 T and 3 T $\{Fe[(bi)_4pz]\}(BF_4)_2$ * CH_3CN showed a dominating rate of diamagnetism above temperatures of about 150 K and 270 K, respectively. The low spin state of this complex was more distinct than within $\{Fe[(bi)_4pz]\}(BF_4)_2$ * EtOH, which proved to be paramagnetic irrespective to the parameters applied during the measurement. Nevertheless, the effective magnetic moment was estimated to be around 1 µB and thus $\{Fe[(bi)_4pz]\}(BF_4)_2$ * EtOH could also be accounted to the low spin state, for the magnetic moment of the high spin state would not be expected to be lower than 5.4 µB. Traces of iron(III) within the sample might explain the paramagnetism of $\{Fe[(bi)_4pz]\}(BF_4)_2$ * EtOH. Oxidation of iron(II) to iron(III) during the complex synthesis or its recovery as well as already existing traces of iron(III) within the metal salt used for synthesis could be considered as the corresponding sources for this paramagnetic metal of d^5 electron configuration.

3.2.3. XRPD

The diffraction patterns of the ligand proved to be different from those of the complexes (see Fig. 3-8). Therefore it suggested itself that the method chosen for complexation had been appropriate and with a complete conversion of the free ligand to the complex. Furthermore it was shown that the solvent used in the synthesis of the complexes influenced their later structure.

Looking at the powder diffraction pattern of the perchlorate complex $\{Fe[(bi)_4pz]\}(ClO_4)_2$*EtOH (see Fig. 3-9) the lower grade of crystallinity stood out. This was not surprising, for a not completely purified fraction of the ligand had been used at the synthesis of this particular complex and – as it had been pointed out previously (see chapter 3.1.3) – the crystallinity of the ligand improved with the grade of purification.
The conclusion that the solvent used at the synthesis of the complexes influenced their later structure was affirmed by the comparison of the diffraction patterns of $\{Fe[(bi)_4pz]\}(BF_4)_2$*EtOH and $\{Fe[(bi)_4pz]\}(ClO_4)_2$*EtOH (see Fig. 3-9). Despite the higher degree of crystallinity within the tetrafluoroborate sample, the major signals of both complexes were positioned similarly.

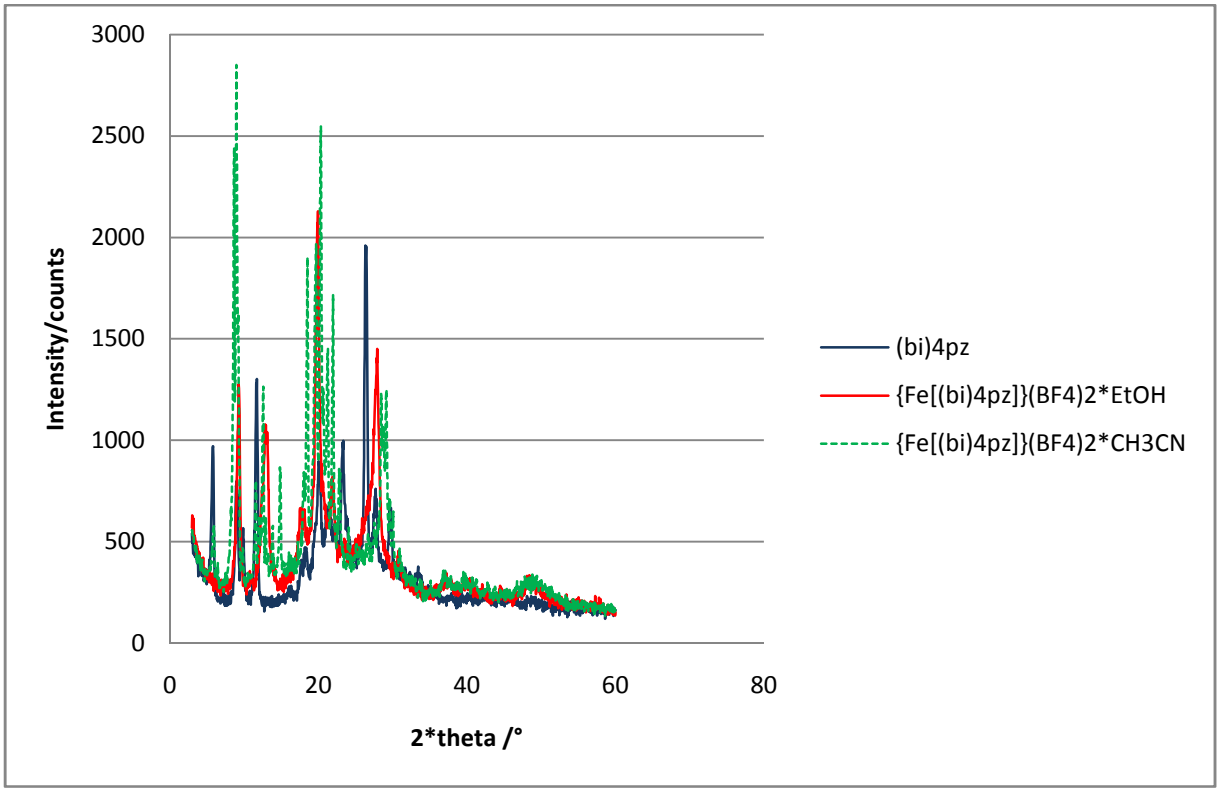

Fig. 3-8: XRPD of the tetrafluoroborate complexes compared with the free ligand.

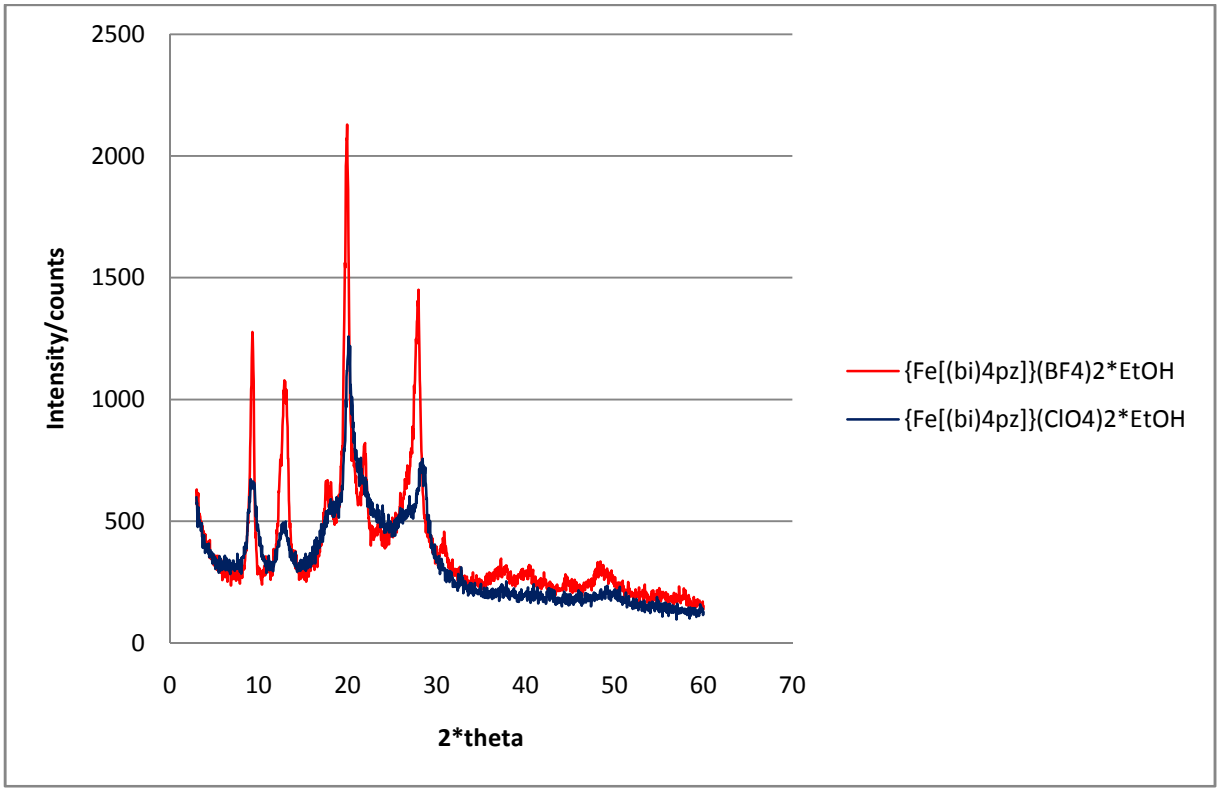

Fig. 3-9: XRPD of the complexes $\{Fe[(bi)_4pz]\}(BF_4)_2$*EtOH and $\{Fe[(bi)_4pz]\}(ClO_4)_2$*EtOH.

4. Outlook

As already mentioned in chapter 3.1., the synthesis of pure $(bi)_4pz$ proved to be troublesome and only low yields of the desired product were obtained. Thus a ligand synthesis following the suggested Benzoine condensation route with a subsequent cyclization of the condensation product might be an interesting alternative to be tested.

Since the temperature dependent UV-Vis-NIR measurements have been limited within a temperature range of 123 – 372 K and no SC has been observed in that range, it surely would be advisable to conduct continuative measurements using instruments that allow the heating to higher temperatures.
According to Kolnaar et al. [128] the variation of counter ions allows shifting of the transition temperature by as much as 100K. Subject to the condition that the ligand (bi)4pz allows a thermally induced spin transition, the modification of counter ions and solvents [129] obviously provides a promising opportunity to tune the transition temperature of the system. In order to verify the possibility of thermally induced SC in the ligand field given by $(bi)_4pz$ theoretic calculations may be conducted within the scope of further research projects.

Complexations with different transition metals which show aptness to spin transition, such as iron(III), cobalt(II) and manganese(III) [2], or syntheses of mixed-metal complexes could be subject to diverse experimental series with the objective of gaining a better understanding for the ligand system at hand.

5. Appendix

5.1. NMR

^{1}H NMR $(COOH)_4pz$ / d_6-DMSO

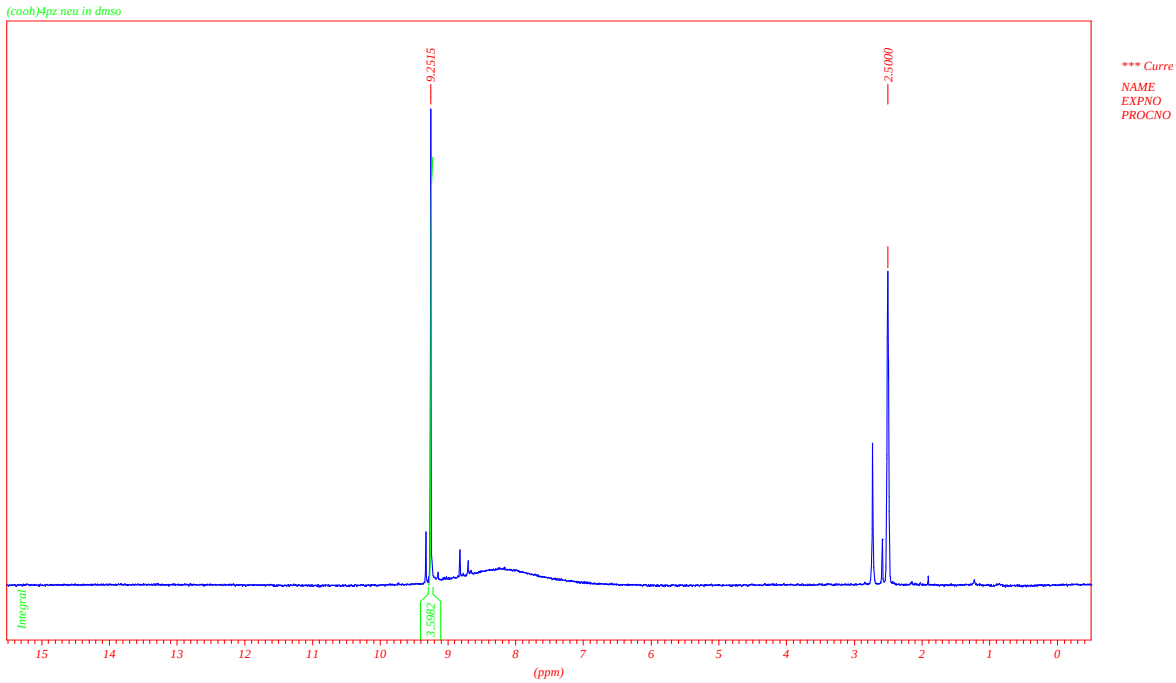

^{1}H NMR $(COOH)_4pz$ / D_2O

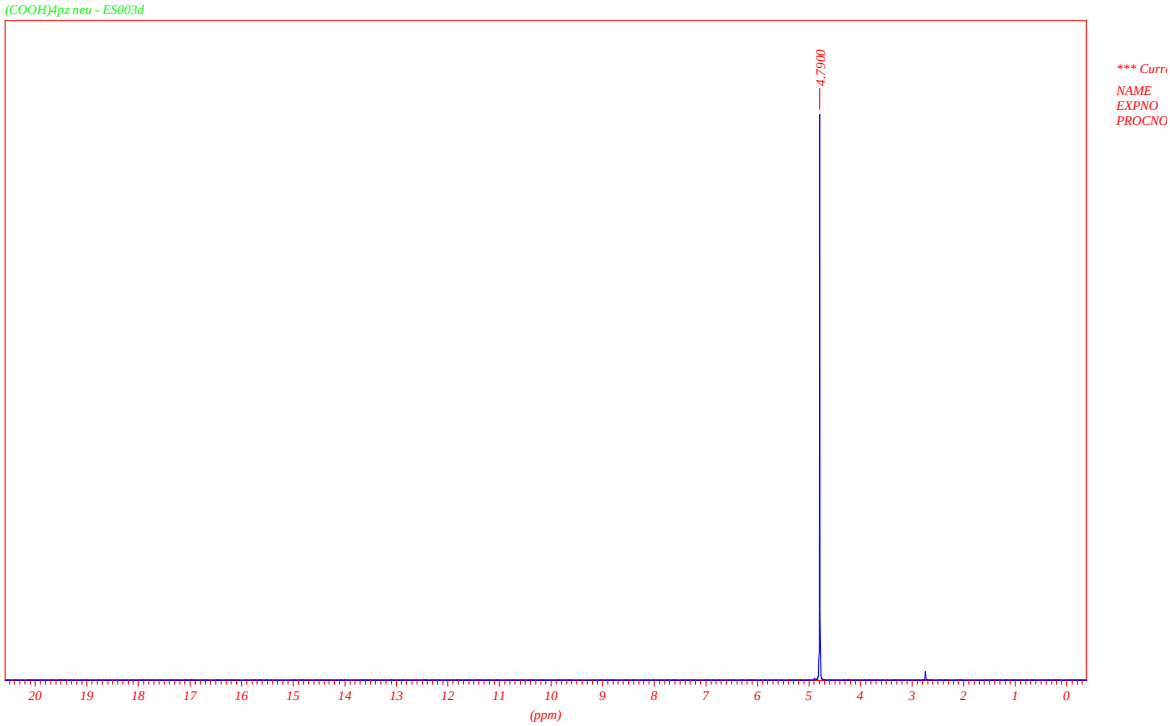

^{13}C NMR $(COOH)_4pz$ / D_2O

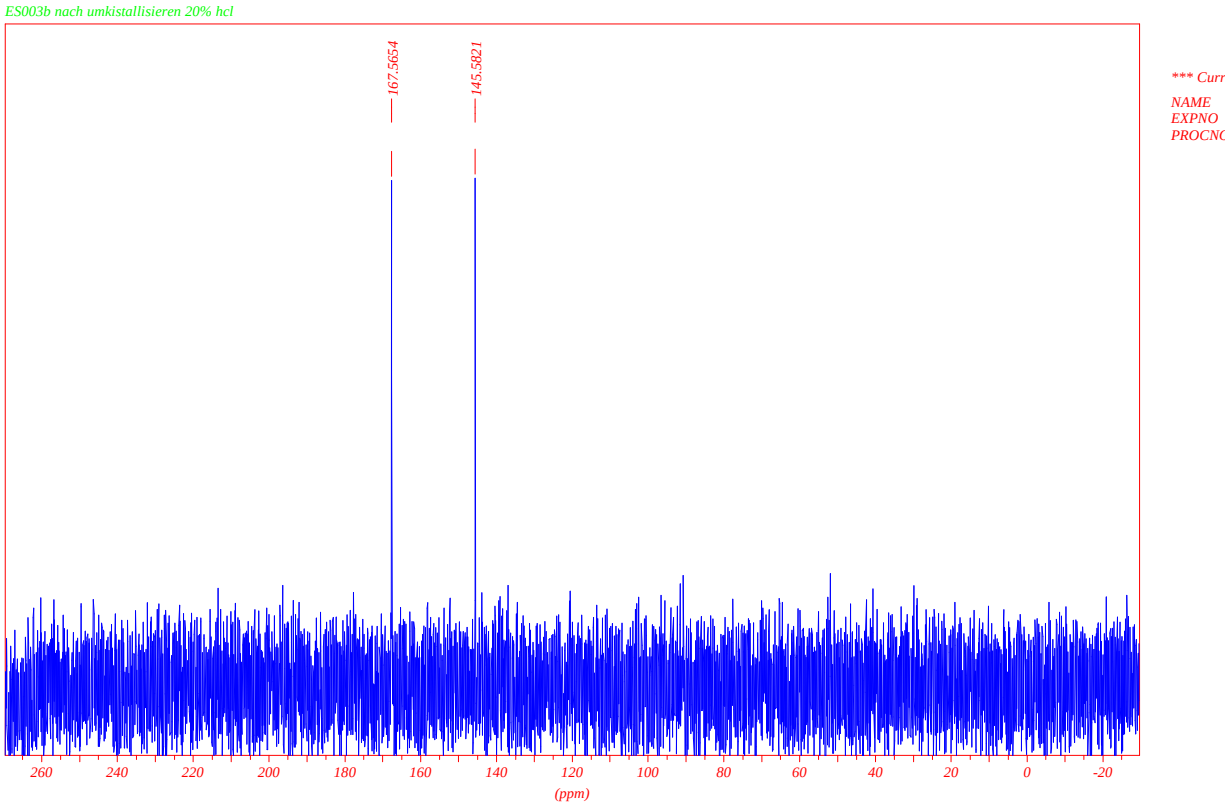

^{1}H NMR $(bi)_4pz$ / d_6-DMSO, raw product

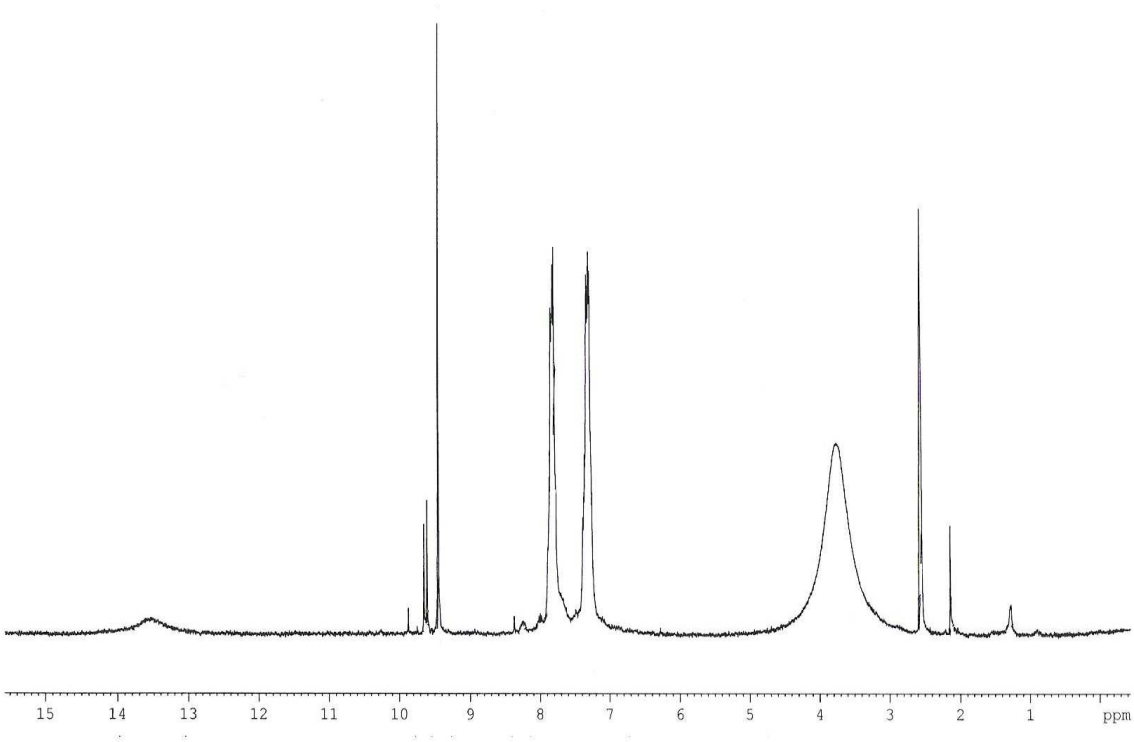

^{1}H NMR (bi)$_4$pz / d$_6$-DMSO, purified

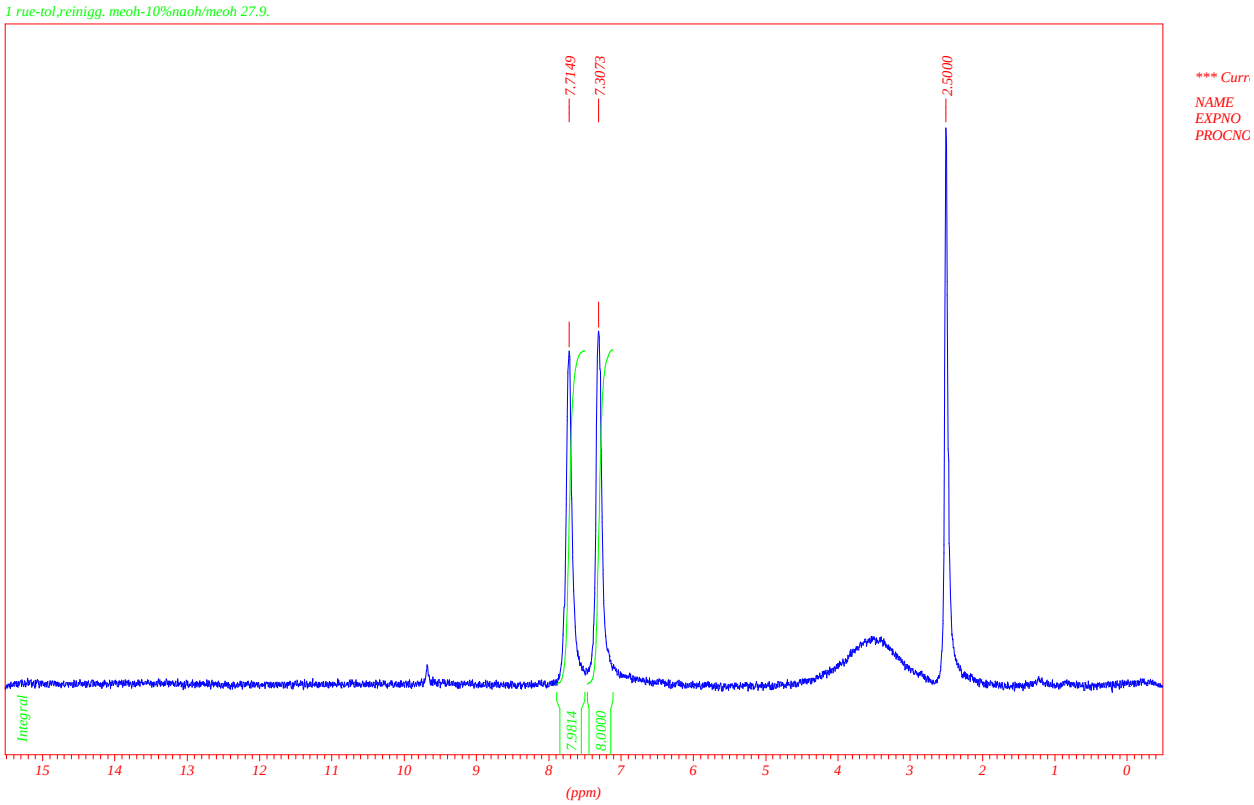

^{13}C NMR (bi)$_4$pz / d-TFA

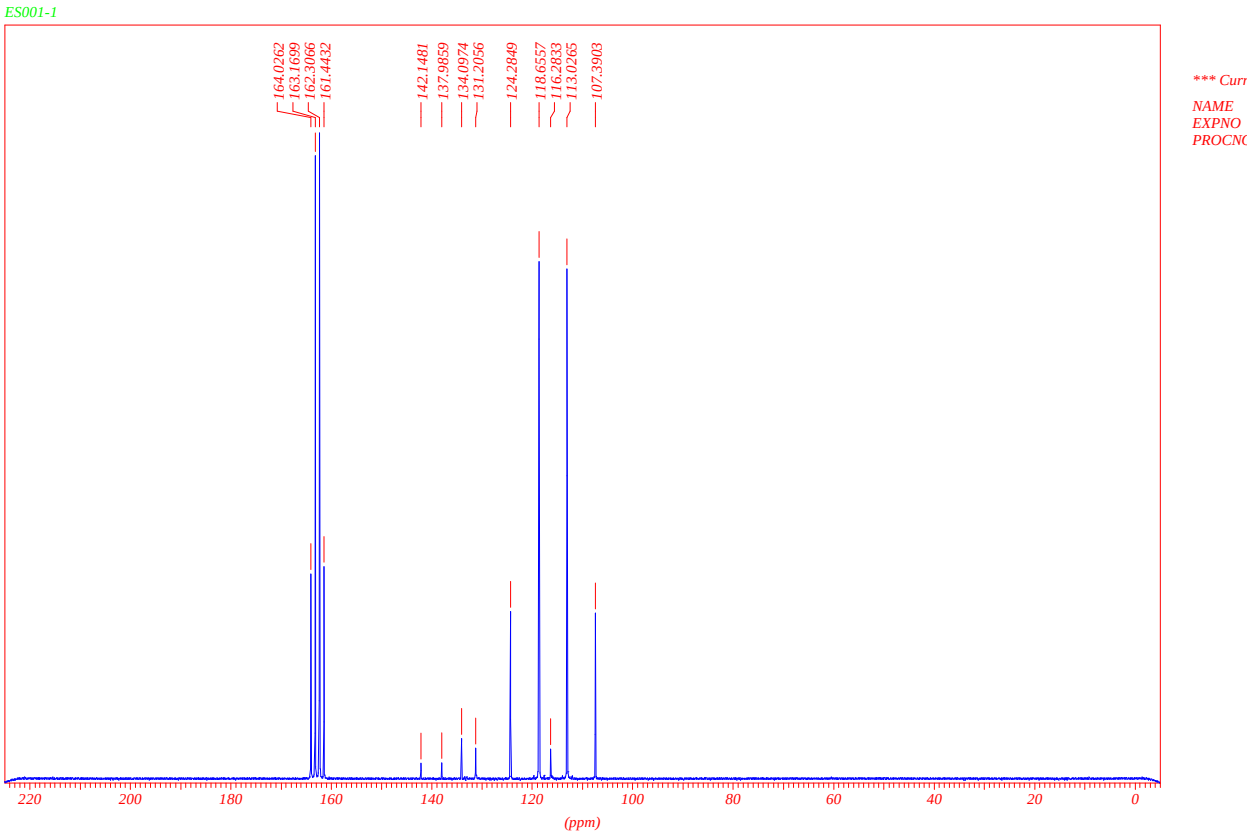

^{1}H NMR Et(bi)$_2$(OH)$_2$ / d$_6$-DMSO

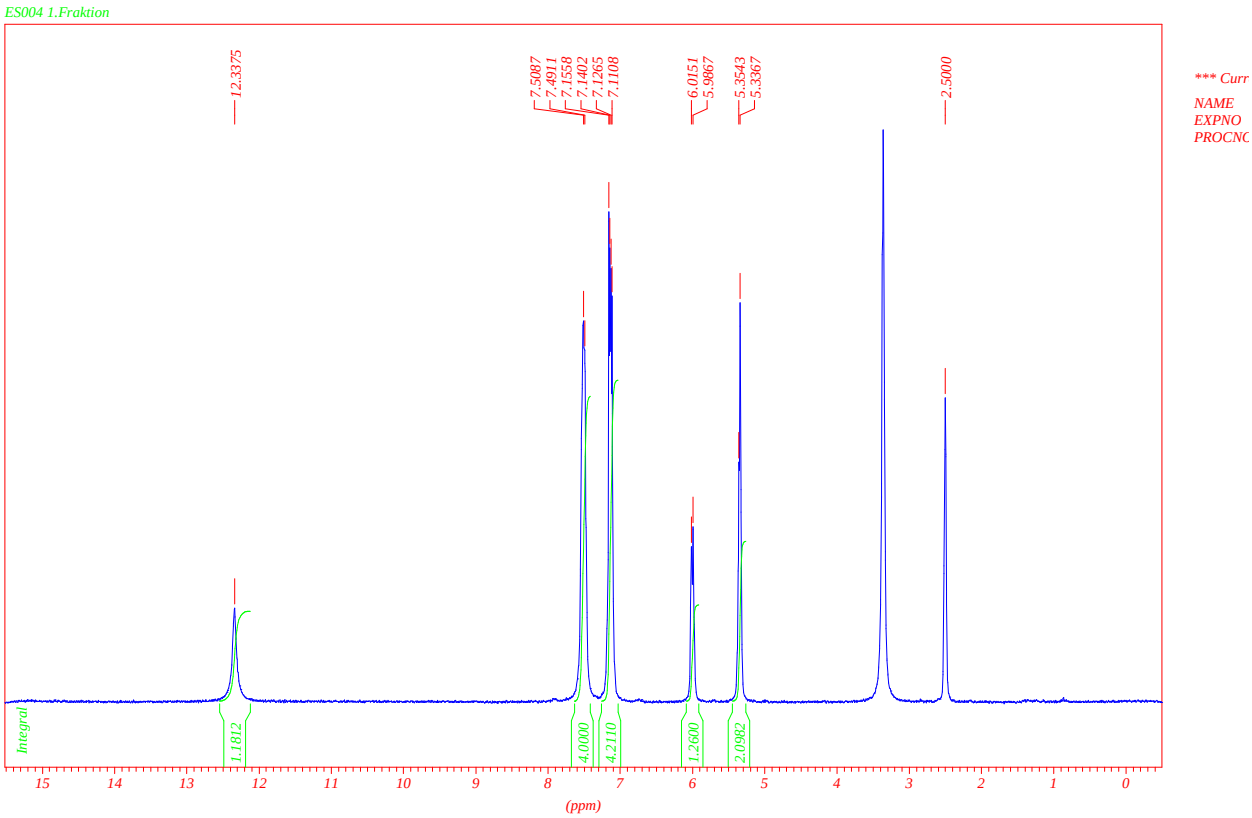

^{1}H NMR Et(bi)$_2$olon/ d$_6$-DMSO, oxidizing agent KMnO$_4$

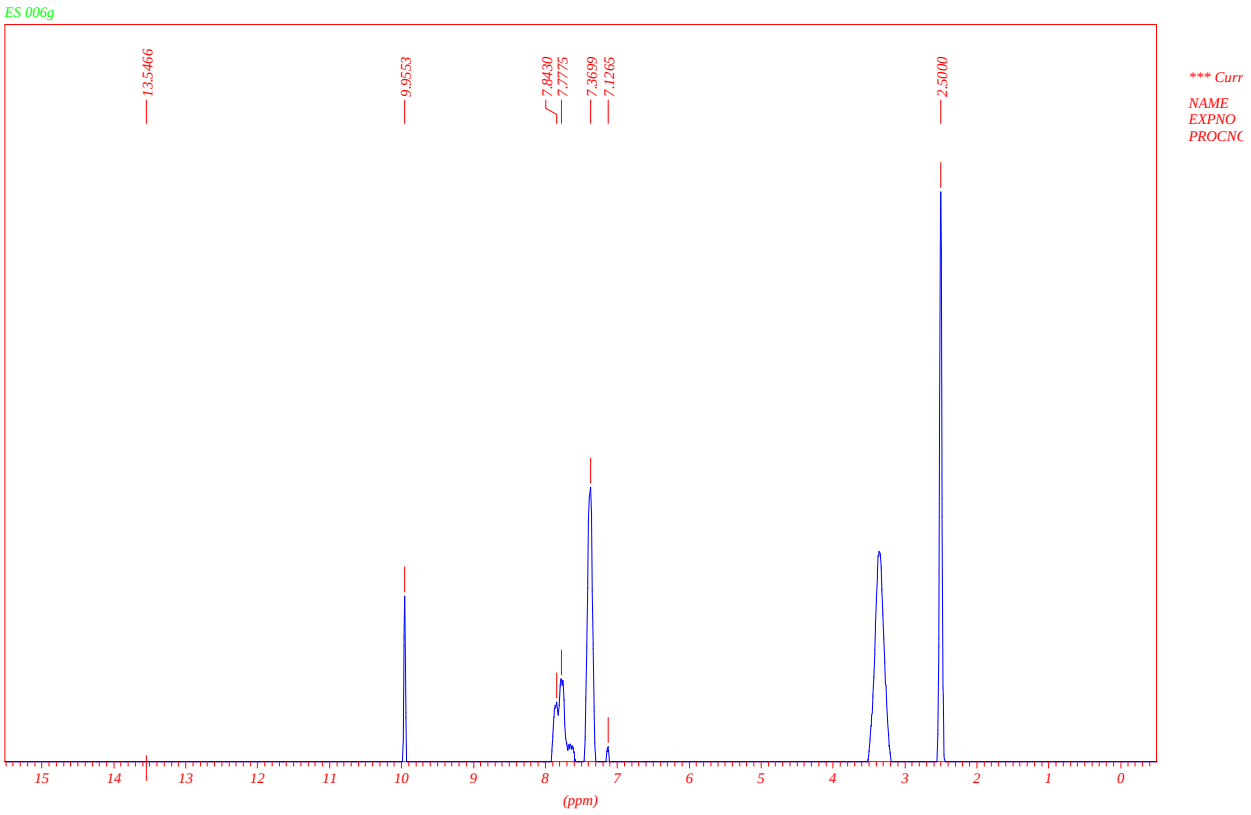

^{1}H NMR Et(bi)$_2$olon/ d$_6$-DMSO, oxidizing agent $K_2Cr_2O_7$

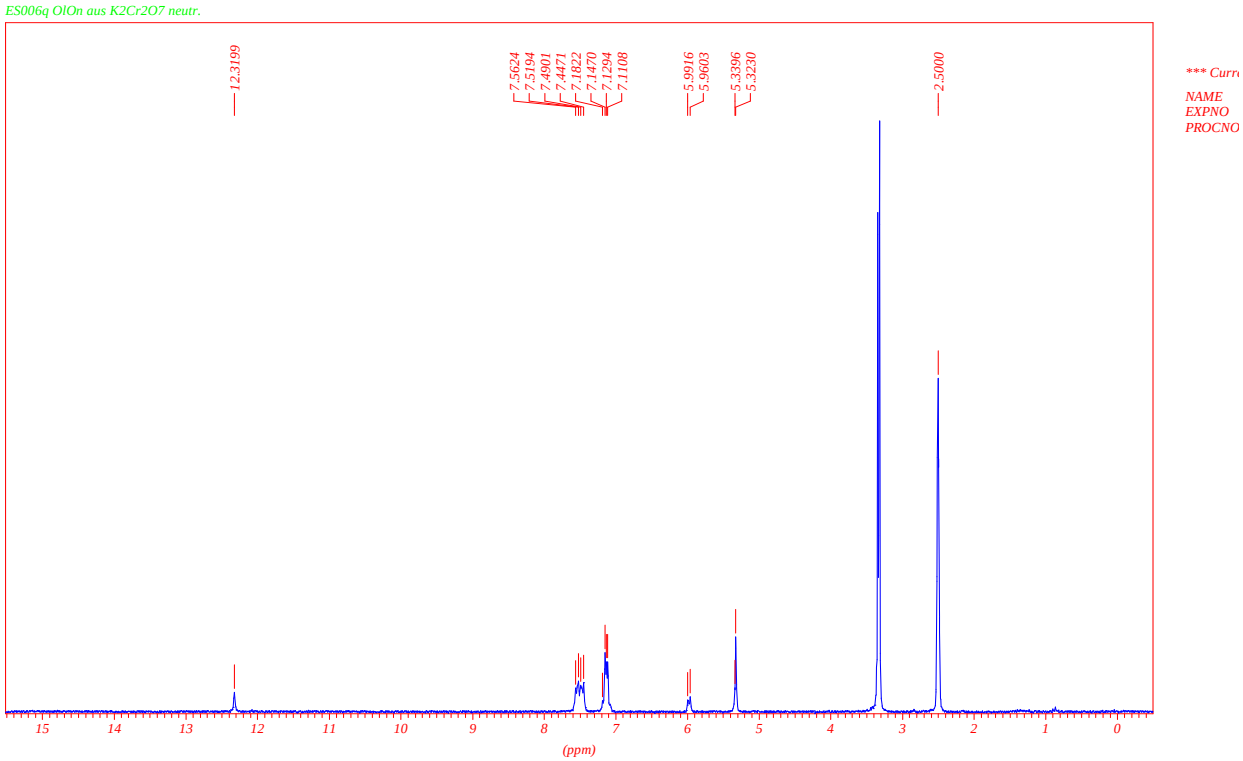

ChemNMR ^{1}H Estimation of 2,3,5,6-tetrakis(benzimidazol-2´-yl)pyrazine

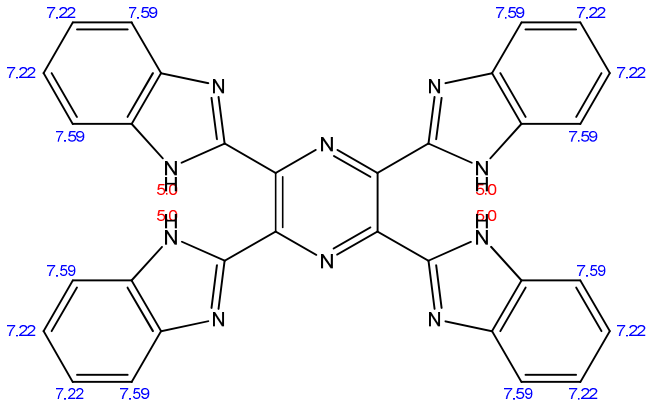

Estimation quality is indicated by color: good, medium, rough

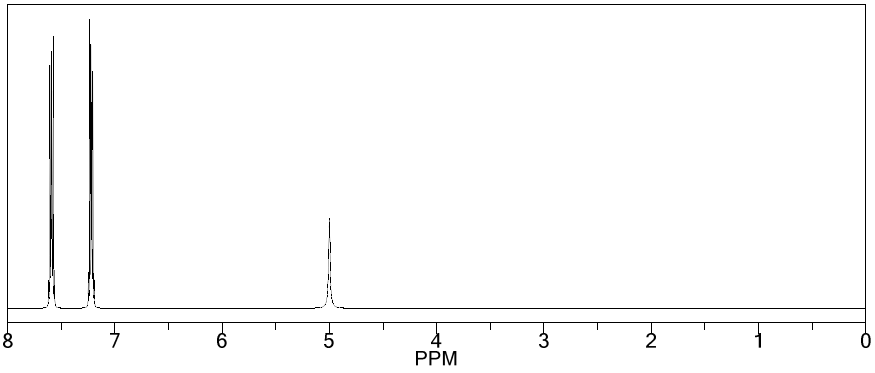

ChemNMR ^{13}C Estimation of 2,3,5,6-tetrakis(benzimidazol-2´-yl)pyrazine

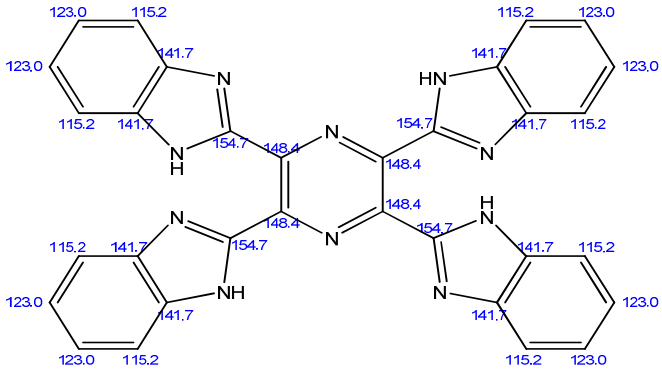

Estimation quality is indicated by color: good, medium, rough

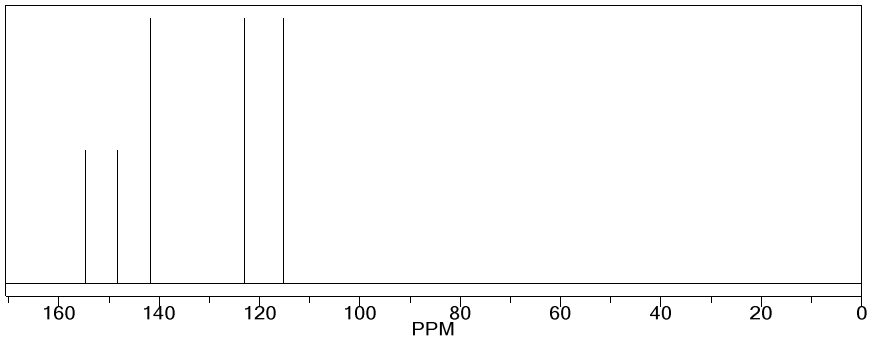

ChemNMR ^{1}H Estimation of (benzimidazol-2´-yl)pyrazine

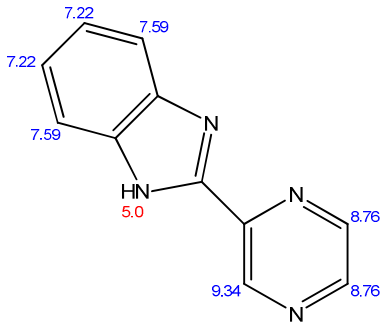

Estimation quality is indicated by color: good, medium, rough

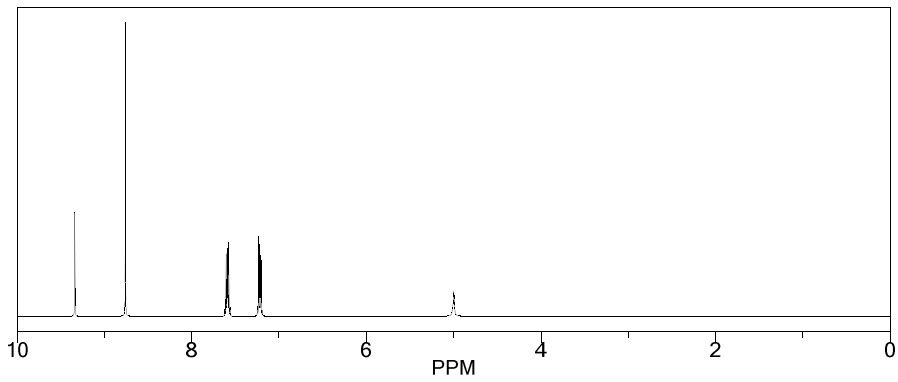

ChemNMR ^{1}H Estimation of 2,5-bis(benzimidazol-2´-yl)pyrazine

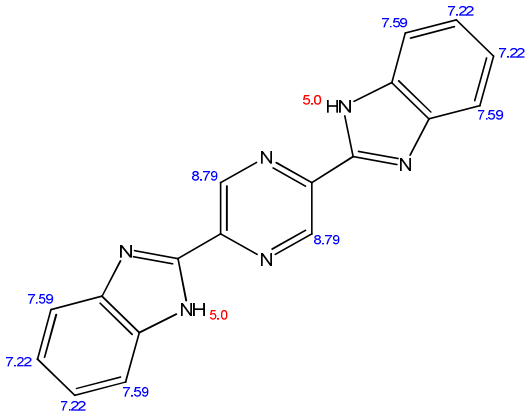

Estimation quality is indicated by color: good, medium, rough

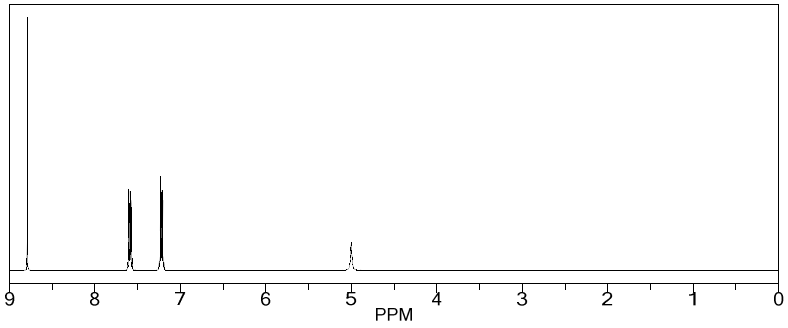

ChemNMR ^{1}H Estimation of 2,6-bis(benzimidazol-2´-yl)pyrazine

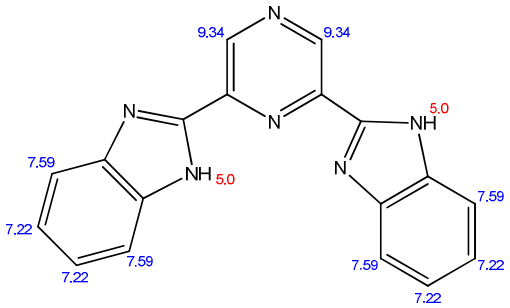

Estimation quality is indicated by color: good, medium, rough

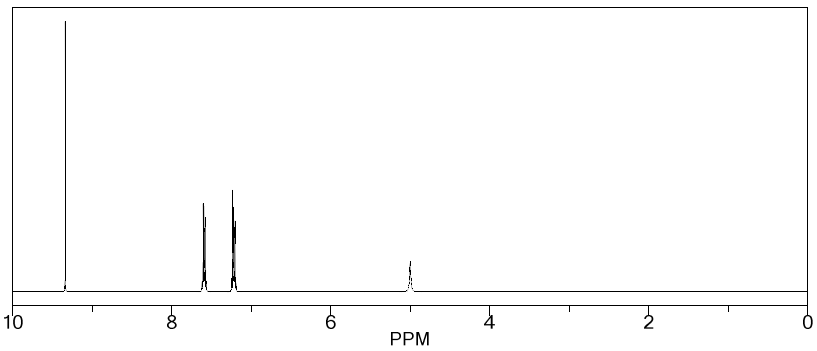

ChemNMR ^{1}H Estimation of 2,3-bis(benzimidazol-2′-yl)pyrazine

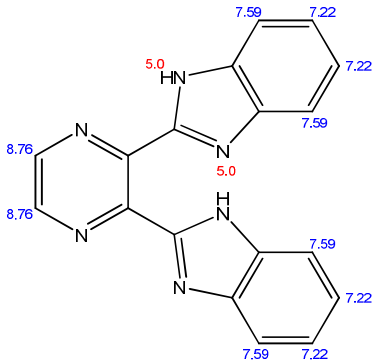

Estimation quality is indicated by color: good, medium, rough

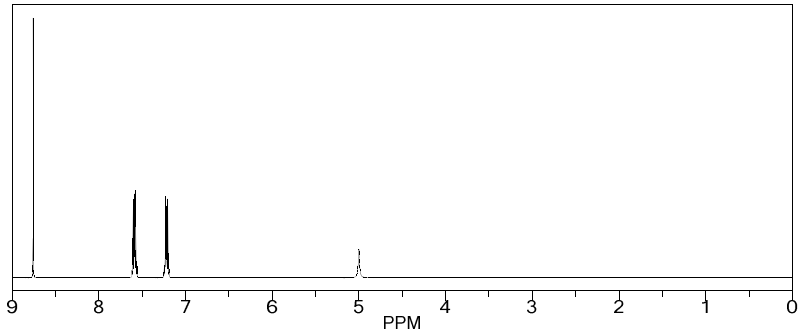

ChemNMR ^{1}H Estimation of 2,3,5-tris(benzimidazol-2′-yl)pyrazine

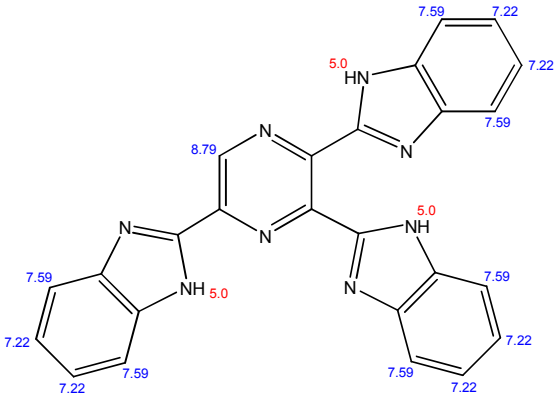

Estimation quality is indicated by color: good, medium, rough

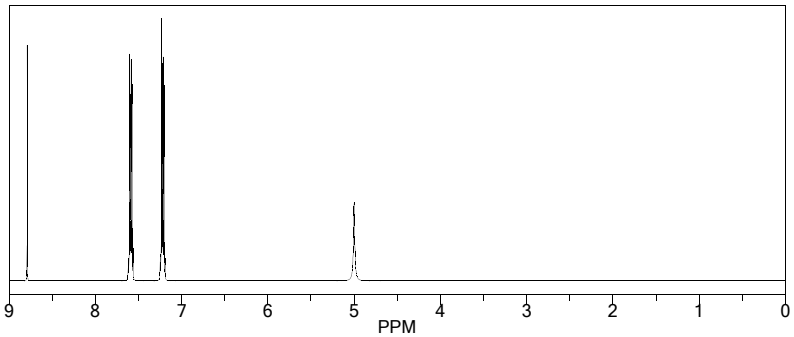

5.2. UV-Vis-NIR

$(bi)_4pz$

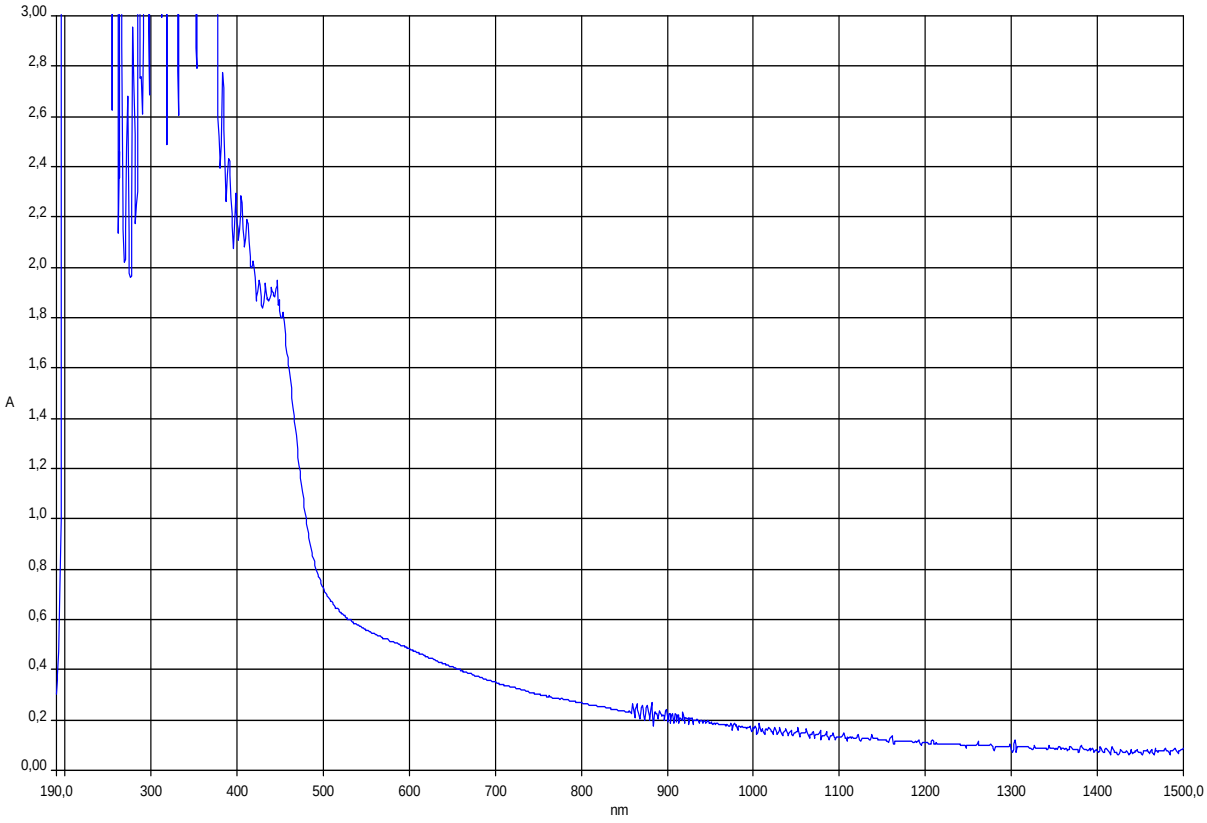

$\{Fe[(bi)_4pz]\}(BF_4)_2$ * EtOH

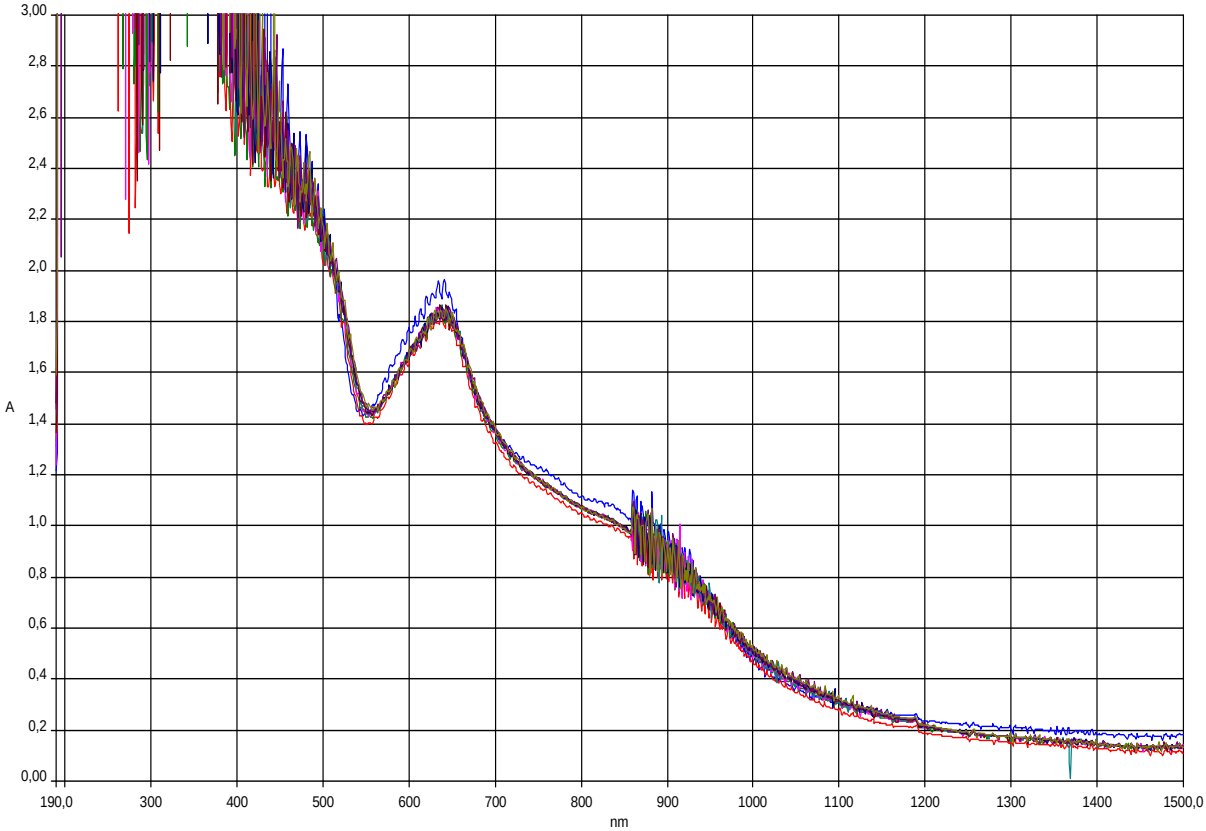

{Fe[(bi)$_4$pz]}(BF$_4$)$_2$ * CH$_3$CN

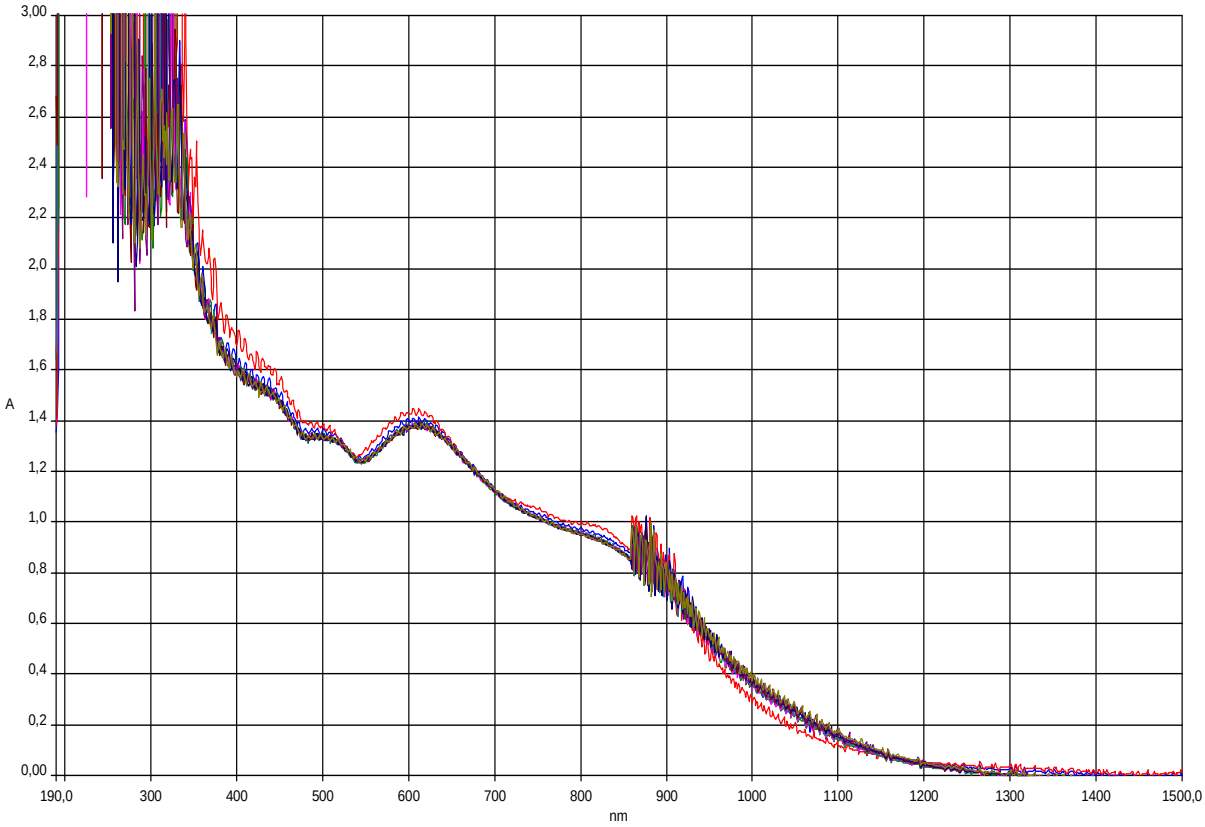

{Fe[(bi)$_4$pz]}(ClO$_4$)$_2$ * EtOH

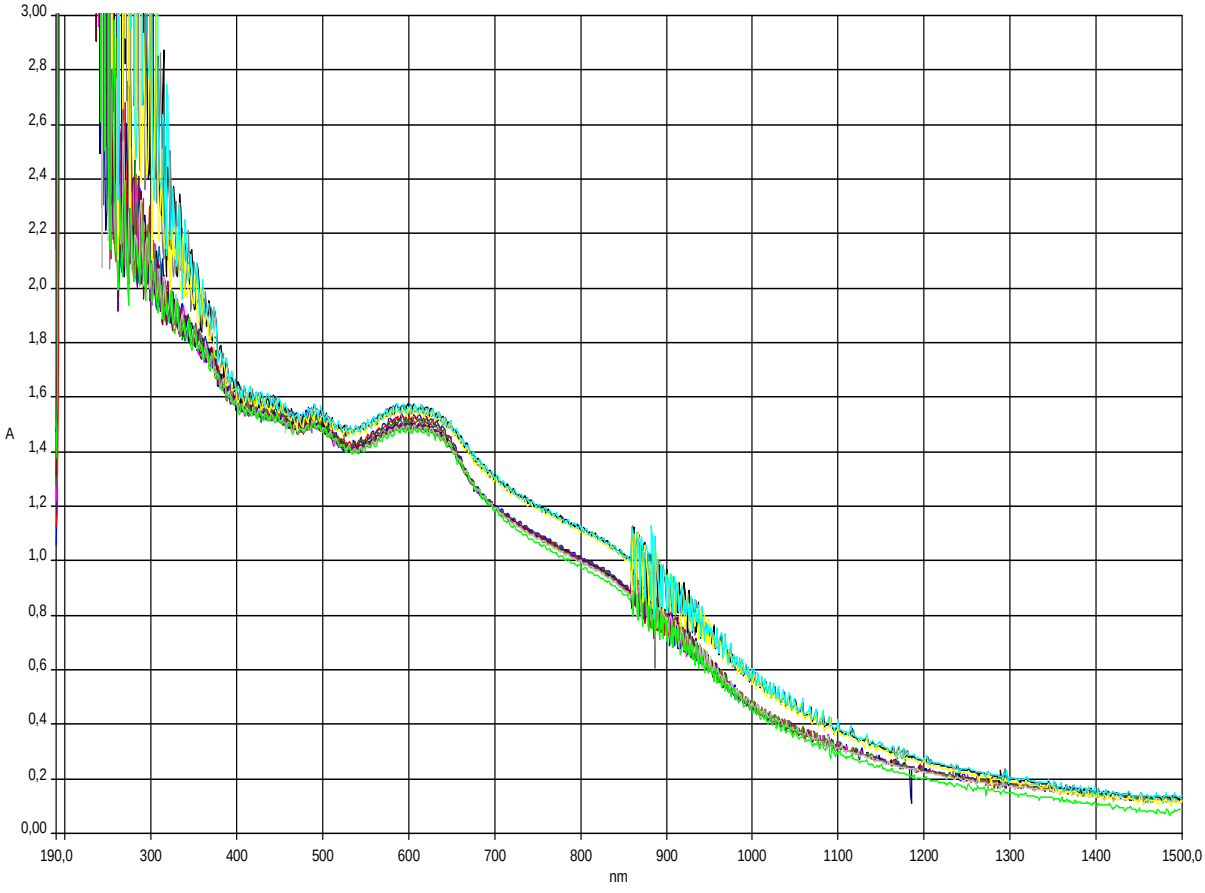

5.3. IR

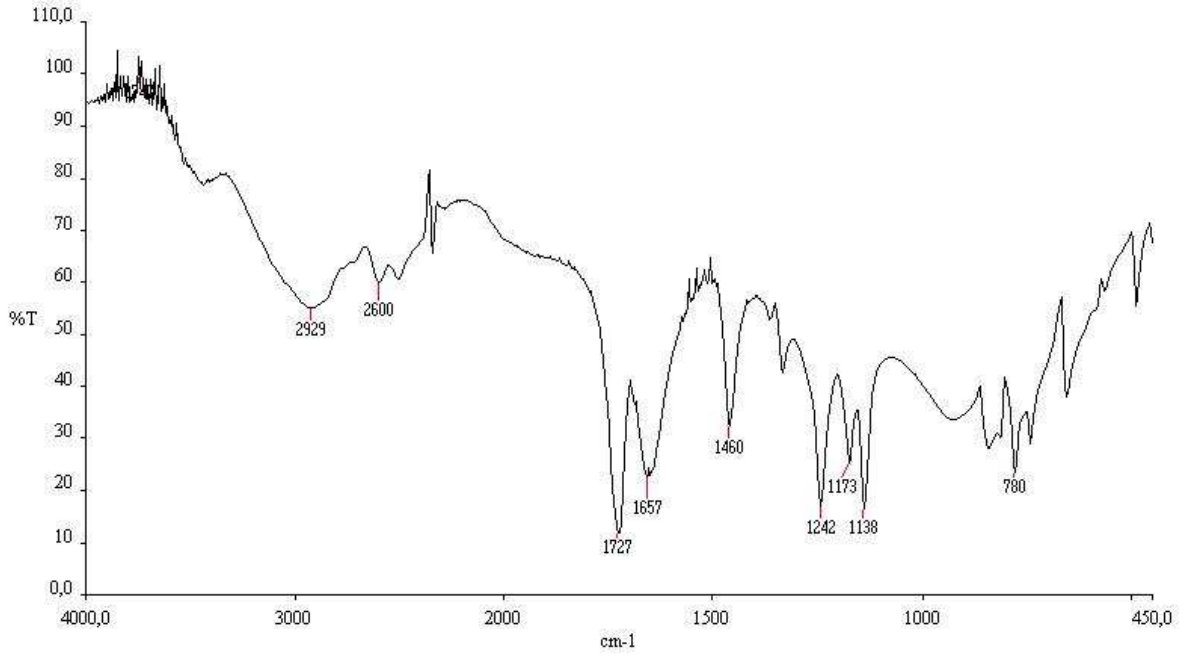

$(COOH)_4pz$

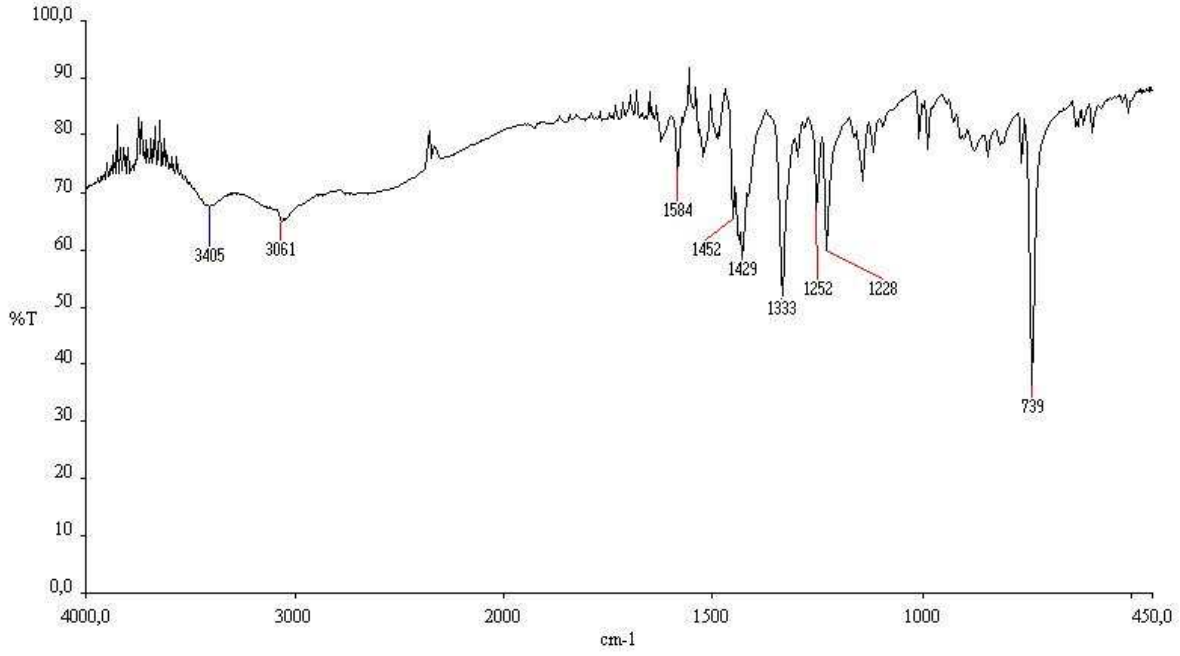

$(bi)_4pz$

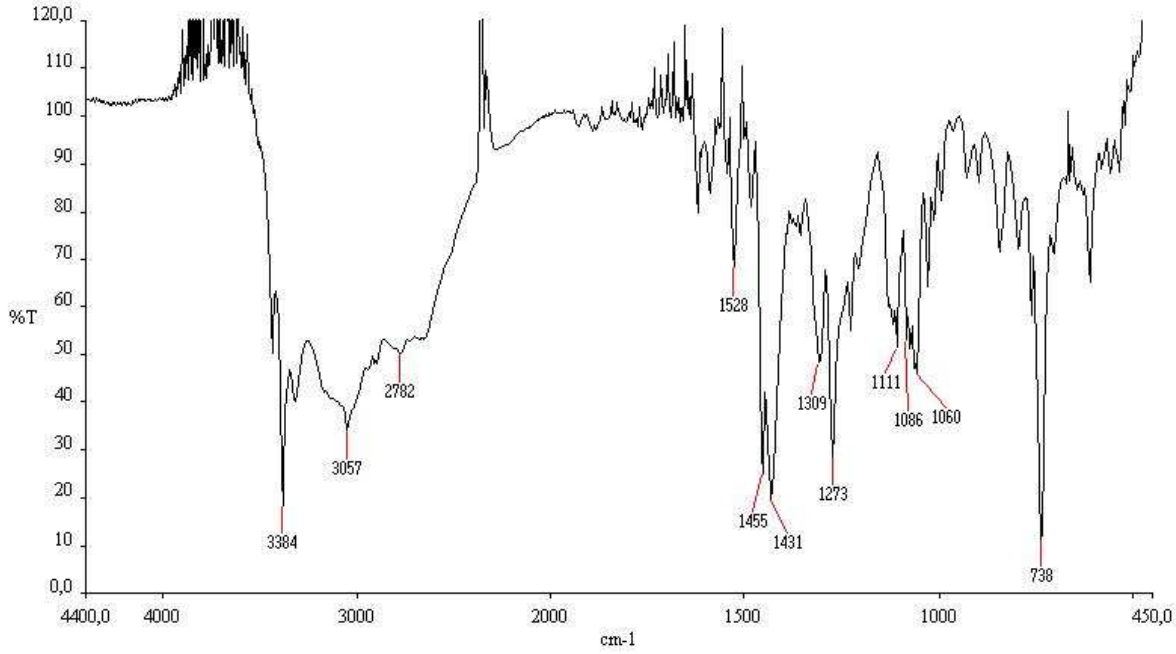

Et(bi)$_2$(OH)$_2$

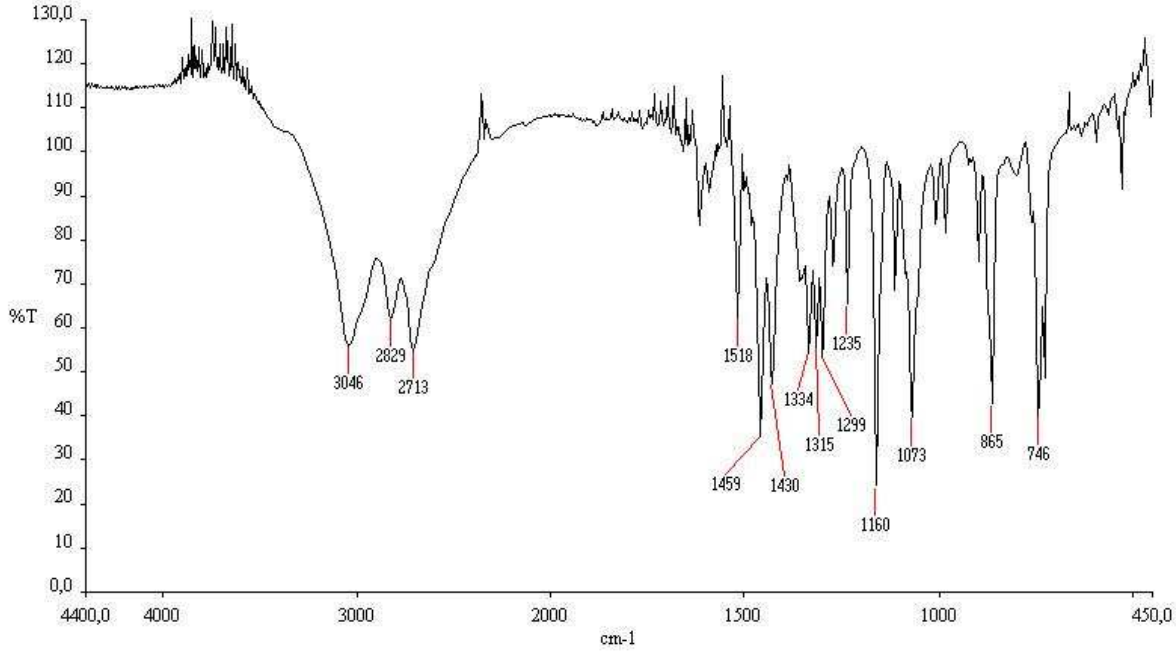

Et(bi)$_2$olon, oxidizing agent KMnO$_4$

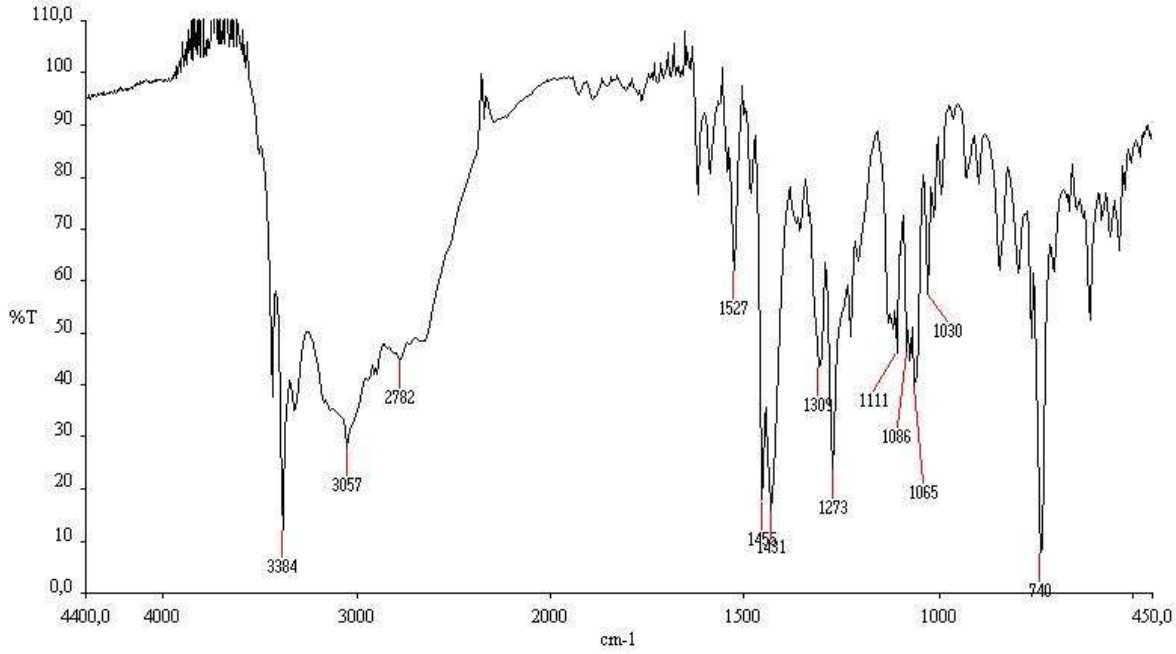

Et(bi)$_2$olon, oxidizing agent $K_2Cr_2O_7$

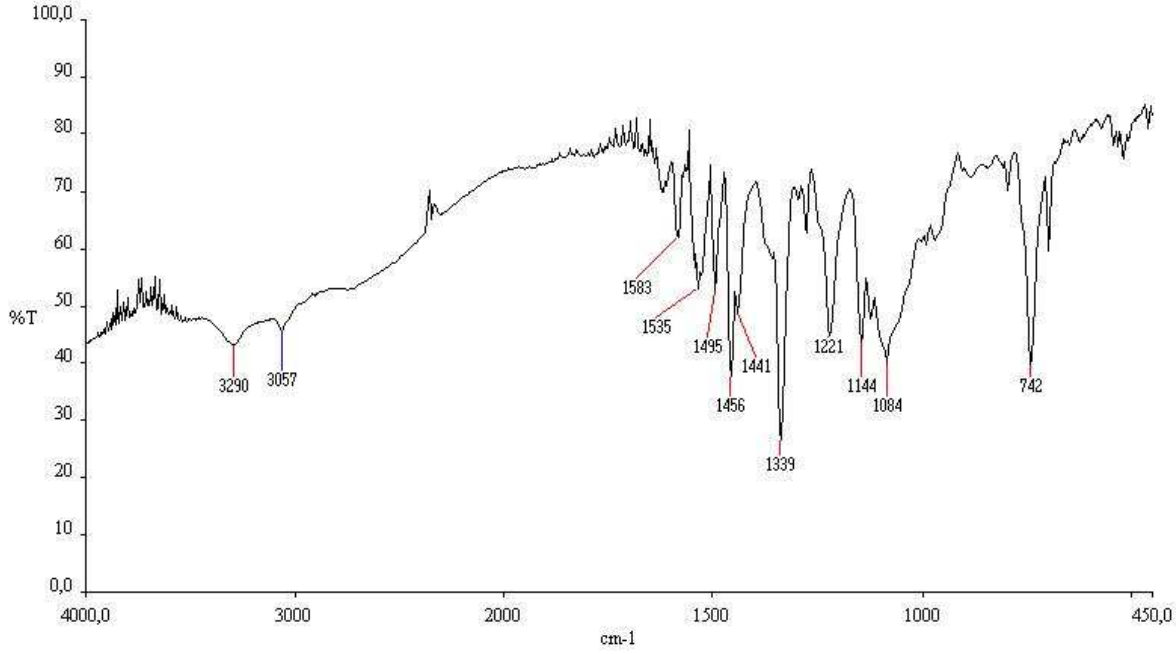

{Fe[(bi)$_4$pz]}(BF$_4$)$_2$ * EtOH

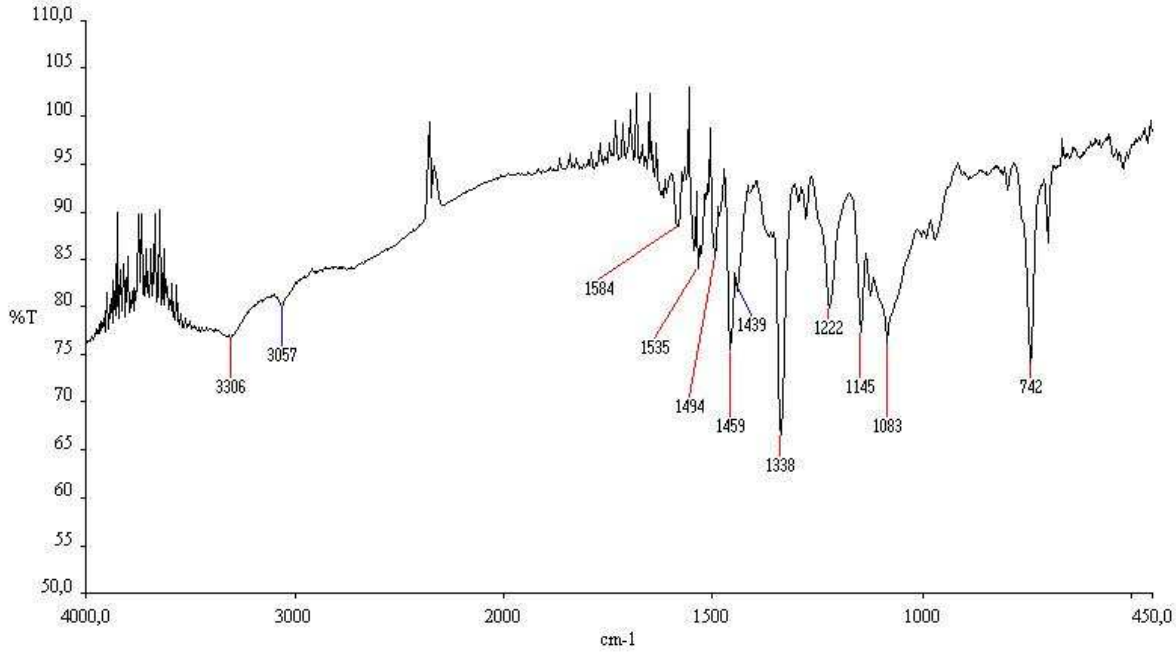

{Fe[(bi)$_4$pz]}(BF$_4$)$_2$ * CH$_3$CN

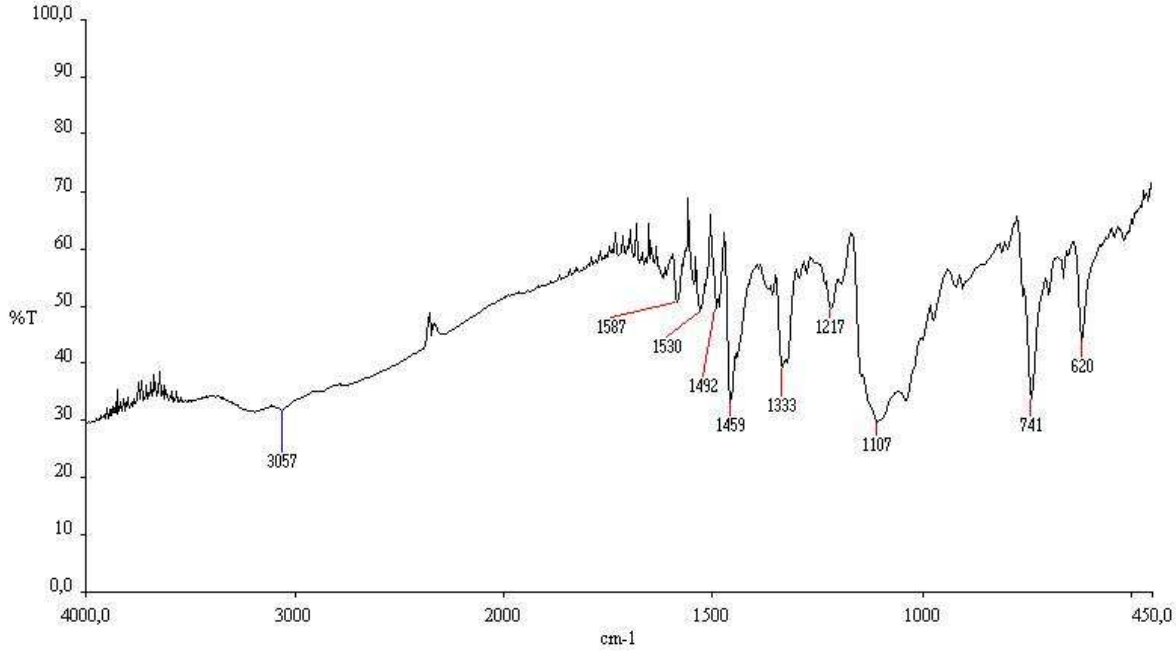

{Fe[(bi)$_4$pz]}(ClO$_4$)$_2$ * EtOH

5.4. TGA

$(COOH)_4pz$

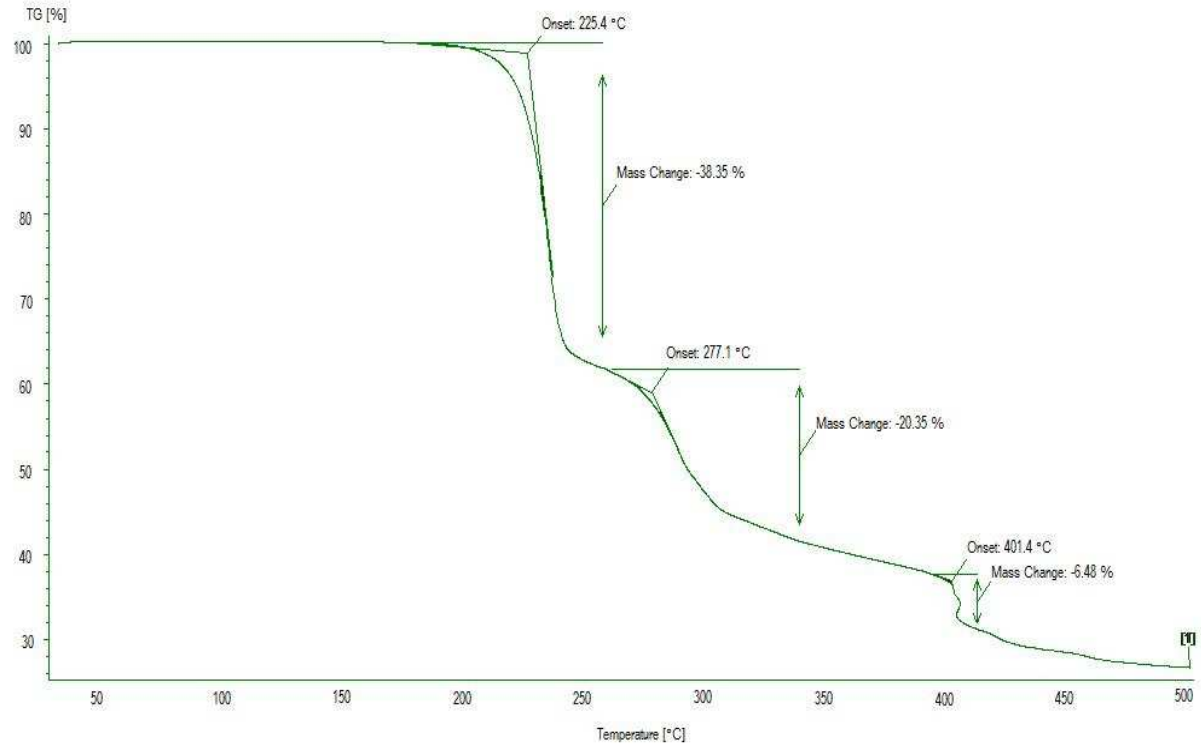

$(bi)_4pz$

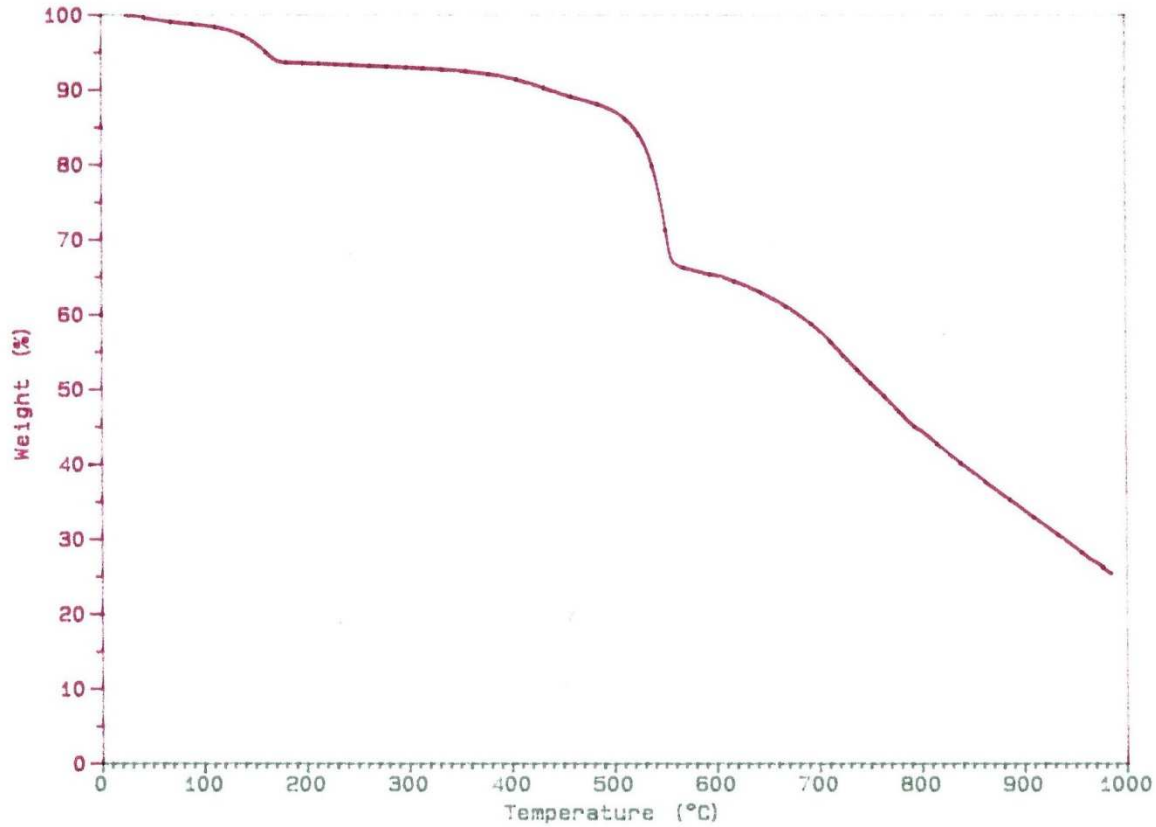

{Fe[(bi)$_4$pz]}(BF$_4$)$_2$ * EtOH

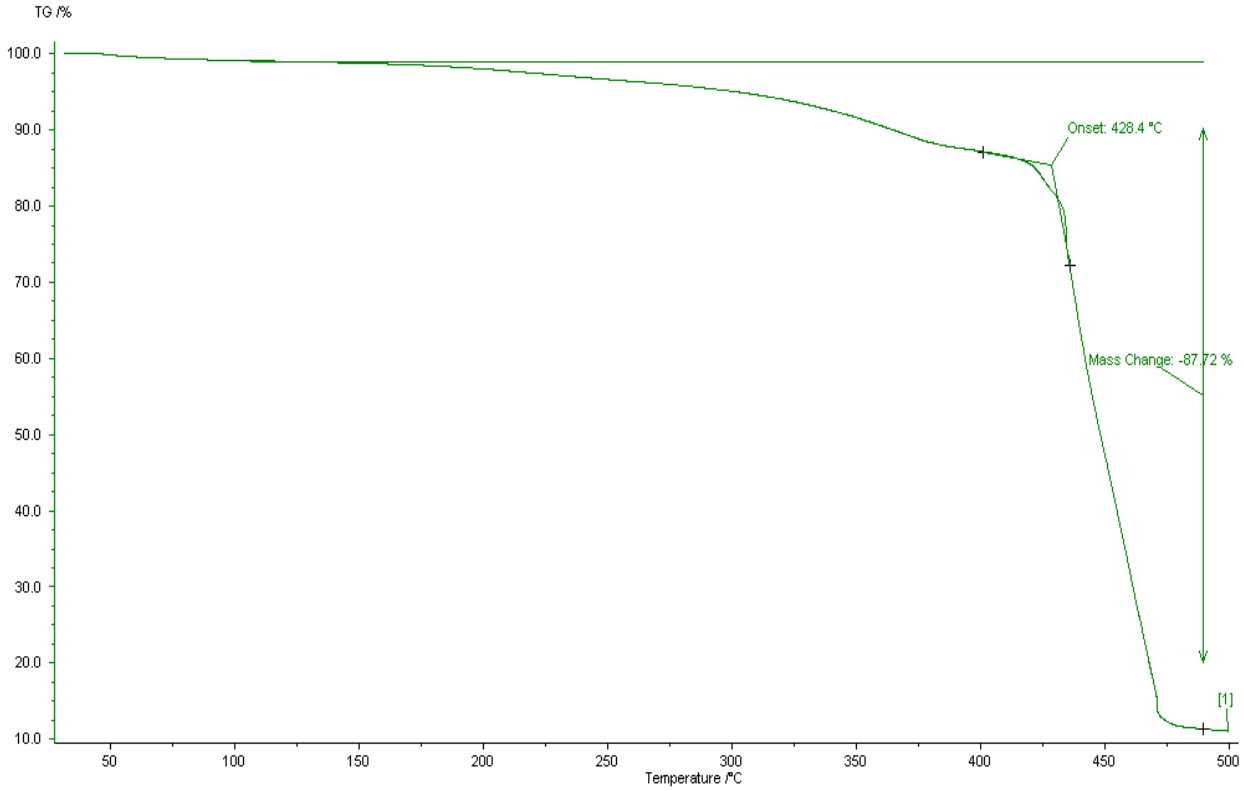

{Fe[(bi)$_4$pz]}(BF$_4$)$_2$ * CH$_3$CN

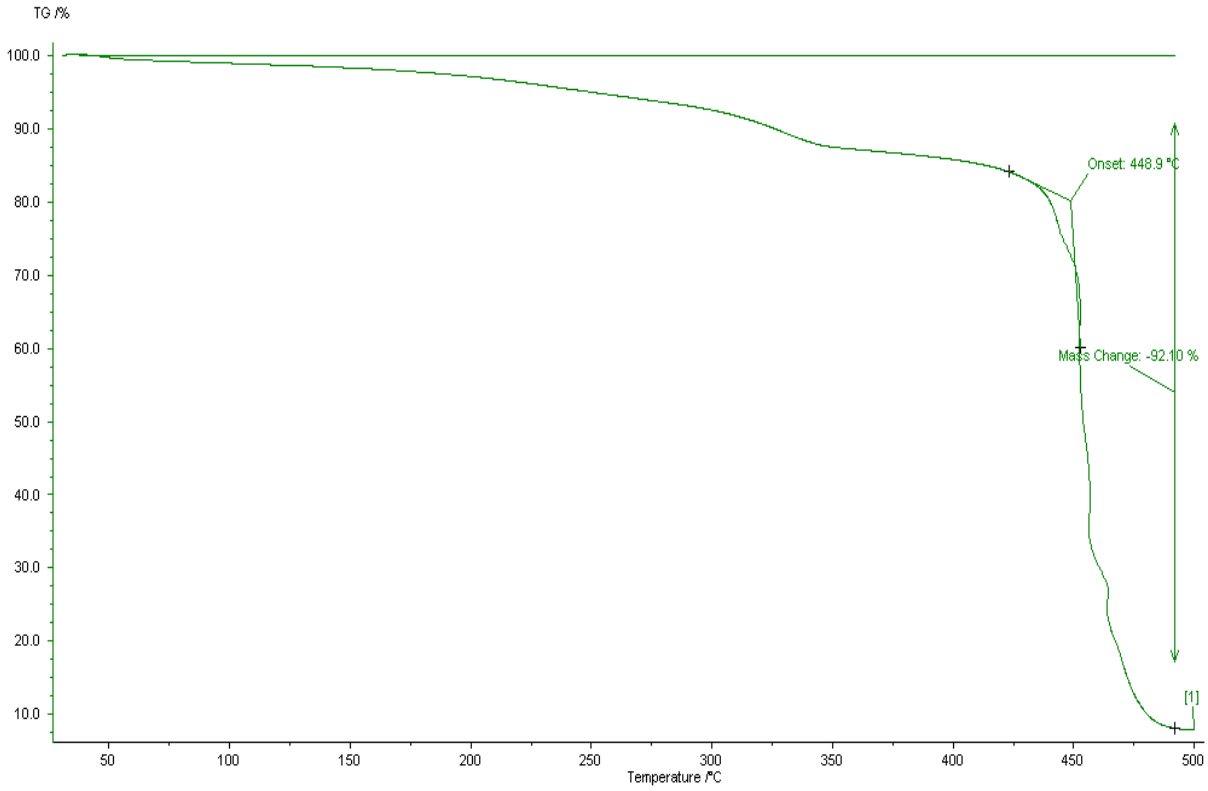

5.5 SQUID Magnetometry

{Fe[(bi)$_4$pz]}(BF$_4$)$_2$ * EtOH

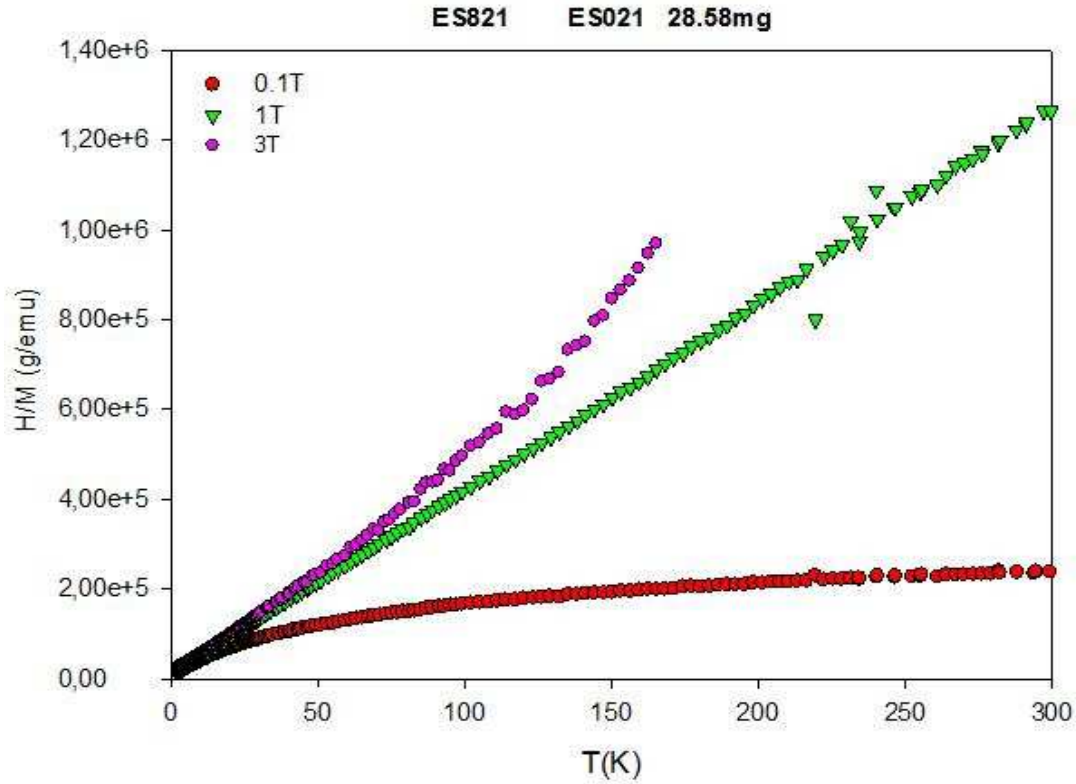

{Fe[(bi)$_4$pz]}(BF$_4$)$_2$ * CH$_3$CN

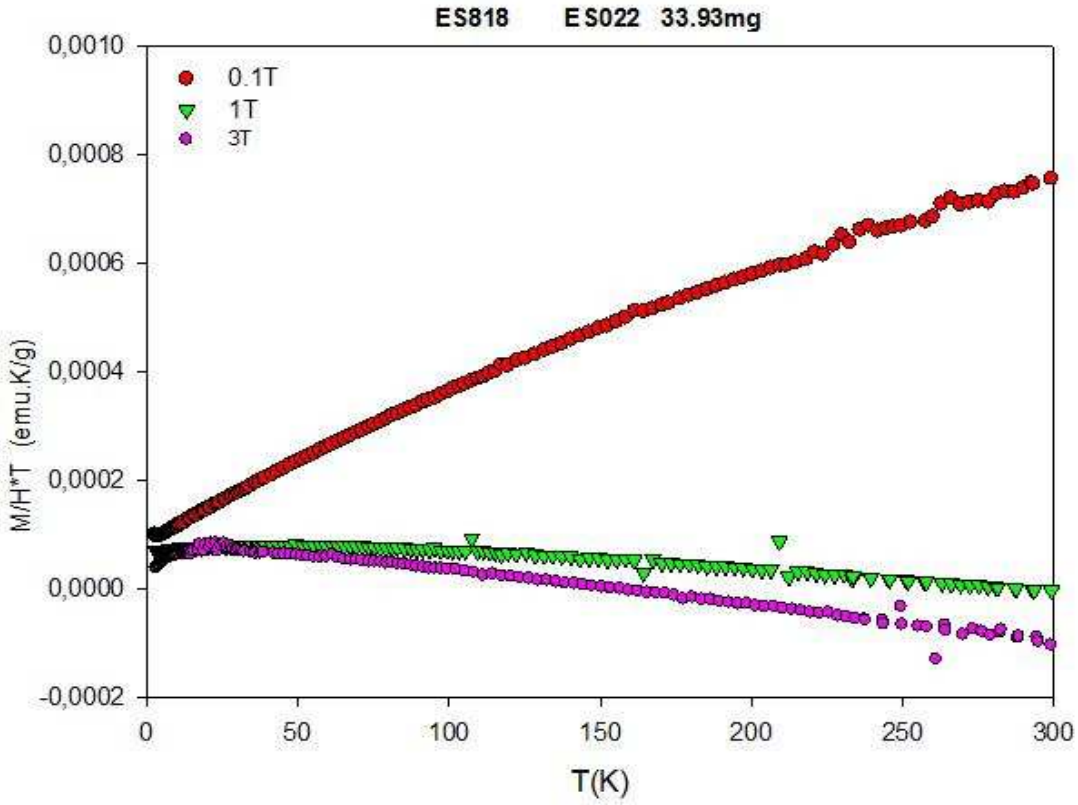

5.6. XRPD Data

Legend: 1 = $(bi)_4pz$ raw, 2 = $(bi)_4pz$ pure, 3 = $\{Fe[(bi)_4pz]\}(BF_4)_2$ * EtOH, 4 = $\{Fe[(bi)_4pz]\}(BF_4)_2$ * CH_3CN, 5 = $\{Fe[(bi)_4pz]\}(ClO_4)_2$ * EtOH

2θ / °	1	2	3	4	5
	Intensity / counts				
3,00	538,24	540,00	570,00	556,00	598,00
3,04	571,21	496,00	630,00	556,00	570,00
3,08	561,69	560,00	610,00	532,00	576,00
3,12	547,56	472,00	570,00	540,00	516,00
3,16	538,24	442,00	592,00	530,00	476,00
3,20	484,00	472,00	614,00	526,00	558,00
3,24	501,76	448,00	550,00	524,00	512,00
3,28	529,00	470,00	510,00	494,00	500,00
3,32	510,76	436,00	530,00	490,00	506,00
3,36	538,24	458,00	530,00	494,00	482,00
3,40	529,00	468,00	522,00	470,00	480,00
3,44	497,29	424,00	518,00	460,00	492,00
3,48	510,76	472,00	500,00	456,00	480,00
3,52	484,00	426,00	490,00	480,00	460,00
3,56	479,61	438,00	498,00	474,00	470,00
3,60	506,25	460,00	486,00	414,00	492,00
3,64	479,61	440,00	436,00	452,00	436,00
3,68	519,84	398,00	480,00	434,00	438,00
3,72	506,25	450,00	454,00	396,00	390,00
3,76	538,24	392,00	462,00	432,00	434,00
3,80	524,41	422,00	426,00	402,00	428,00
3,84	524,41	398,00	456,00	400,00	430,00
3,88	479,61	330,00	440,00	424,00	442,00
3,92	533,61	346,00	444,00	412,00	402,00
3,96	515,29	410,00	418,00	422,00	370,00
4,00	552,25	384,00	446,00	440,00	380,00
4,04	524,41	378,00	414,00	408,00	400,00
4,08	542,89	374,00	408,00	384,00	382,00
4,12	497,29	366,00	416,00	410,00	402,00
4,16	552,25	358,00	412,00	364,00	386,00
4,20	524,41	380,00	380,00	352,00	404,00
4,24	524,41	364,00	386,00	414,00	390,00
4,28	590,49	356,00	416,00	372,00	372,00
4,32	547,56	332,00	402,00	382,00	378,00
4,36	529,00	358,00	372,00	412,00	366,00
4,40	556,96	376,00	376,00	402,00	408,00
4,44	538,24	360,00	364,00	344,00	352,00
4,48	576,00	348,00	350,00	344,00	364,00
4,52	585,64	342,00	422,00	354,00	352,00
4,56	556,96	342,00	364,00	346,00	378,00
4,60	576,00	306,00	348,00	354,00	380,00
4,64	610,09	316,00	356,00	352,00	364,00
4,68	585,64	324,00	352,00	338,00	366,00
4,72	635,04	322,00	344,00	304,00	372,00
4,76	640,09	348,00	368,00	372,00	340,00
4,80	610,09	352,00	330,00	356,00	326,00
4,84	681,21	344,00	360,00	344,00	354,00
4,88	691,69	364,00	350,00	348,00	366,00

4,92	718,24	314,00	334,00	342,00	364,00
4,96	681,21	310,00	320,00	328,00	328,00
5,00	707,56	290,00	338,00	350,00	334,00
5,04	712,89	332,00	358,00	324,00	342,00
5,08	750,76	342,00	316,00	342,00	352,00
5,12	789,61	350,00	334,00	356,00	304,00
5,16	789,61	340,00	332,00	352,00	318,00
5,20	882,09	356,00	358,00	362,00	344,00
5,24	835,21	350,00	320,00	362,00	328,00
5,28	906,01	342,00	314,00	352,00	334,00
5,32	936,36	388,00	300,00	352,00	338,00
5,36	973,44	412,00	344,00	356,00	328,00
5,40	985,96	382,00	358,00	374,00	322,00
5,44	1082,41	418,00	318,00	360,00	298,00
5,48	1056,25	438,00	322,00	378,00	304,00
5,52	1142,44	468,00	318,00	360,00	288,00
5,56	1197,16	522,00	300,00	376,00	298,00
5,60	1274,49	584,00	318,00	402,00	356,00
5,64	1288,81	664,00	316,00	396,00	322,00
5,68	1339,56	716,00	296,00	448,00	294,00
5,72	1474,56	828,00	288,00	462,00	346,00
5,76	1482,25	928,00	342,00	448,00	328,00
5,80	1459,24	962,00	292,00	526,00	330,00
5,84	1616,04	970,00	308,00	538,00	334,00
5,88	1489,96	916,00	306,00	566,00	332,00
5,92	1489,96	754,00	258,00	570,00	300,00
5,96	1552,36	560,00	296,00	578,00	320,00
6,00	1544,49	416,00	266,00	516,00	320,00
6,04	1624,09	308,00	278,00	428,00	324,00
6,08	1552,36	308,00	316,00	352,00	324,00
6,12	1552,36	274,00	288,00	328,00	352,00
6,16	1544,49	252,00	284,00	360,00	314,00
6,20	1398,76	234,00	312,00	358,00	358,00
6,24	1391,29	268,00	274,00	340,00	308,00
6,28	1369,00	250,00	270,00	330,00	298,00
6,32	1324,96	246,00	284,00	356,00	308,00
6,36	1260,25	214,00	290,00	330,00	348,00
6,40	1197,16	226,00	314,00	318,00	340,00
6,44	1232,01	230,00	308,00	358,00	308,00
6,48	1128,96	206,00	252,00	396,00	330,00
6,52	1169,64	228,00	286,00	344,00	310,00
6,56	1108,89	222,00	302,00	328,00	298,00
6,60	1043,29	224,00	298,00	324,00	324,00
6,64	979,69	212,00	294,00	300,00	322,00
6,68	967,21	212,00	312,00	282,00	334,00
6,72	961,00	212,00	286,00	272,00	340,00
6,76	918,09	216,00	288,00	292,00	292,00
6,80	967,21	206,00	284,00	268,00	282,00
6,84	888,04	196,00	274,00	294,00	300,00
6,88	882,09	198,00	236,00	290,00	318,00
6,92	876,16	208,00	272,00	276,00	310,00
6,96	841,00	208,00	312,00	292,00	316,00
7,00	817,96	242,00	294,00	300,00	326,00
7,04	795,24	206,00	300,00	296,00	302,00
7,08	835,21	212,00	278,00	286,00	314,00
7,12	806,56	220,00	262,00	306,00	336,00
7,16	784,00	230,00	306,00	304,00	338,00

7,20	823,69	216,00	282,00	310,00	316,00
7,24	800,89	218,00	290,00	304,00	316,00
7,28	756,25	250,00	264,00	252,00	304,00
7,32	795,24	198,00	264,00	276,00	296,00
7,36	767,29	242,00	286,00	302,00	310,00
7,40	696,96	212,00	286,00	278,00	318,00
7,44	750,76	184,00	298,00	330,00	322,00
7,48	750,76	208,00	256,00	294,00	316,00
7,52	712,89	184,00	282,00	346,00	304,00
7,56	718,24	206,00	296,00	316,00	316,00
7,60	739,84	204,00	302,00	342,00	366,00
7,64	750,76	234,00	286,00	300,00	330,00
7,68	729,00	214,00	272,00	332,00	308,00
7,72	734,41	224,00	262,00	290,00	306,00
7,76	691,69	184,00	280,00	330,00	306,00
7,80	718,24	206,00	316,00	346,00	336,00
7,84	756,25	212,00	258,00	358,00	334,00
7,88	739,84	208,00	244,00	370,00	292,00
7,92	750,76	192,00	276,00	388,00	340,00
7,96	734,41	204,00	282,00	424,00	328,00
8,00	718,24	214,00	272,00	428,00	338,00
8,04	712,89	246,00	284,00	420,00	284,00
8,08	676,00	192,00	312,00	448,00	350,00
8,12	686,44	216,00	280,00	524,00	318,00
8,16	707,56	214,00	268,00	574,00	346,00
8,20	670,81	196,00	304,00	572,00	354,00
8,24	702,25	204,00	302,00	672,00	350,00
8,28	691,69	256,00	314,00	604,00	354,00
8,32	670,81	246,00	302,00	658,00	350,00
8,36	750,76	242,00	316,00	710,00	394,00
8,40	707,56	238,00	304,00	720,00	366,00
8,44	745,29	254,00	330,00	958,00	392,00
8,48	707,56	258,00	340,00	1032,00	368,00
8,52	712,89	240,00	368,00	1240,00	410,00
8,56	723,61	292,00	404,00	1424,00	408,00
8,60	729,00	308,00	378,00	1890,00	386,00
8,64	718,24	332,00	400,00	2276,00	392,00
8,68	681,21	356,00	416,00	2444,00	438,00
8,72	605,16	422,00	474,00	1710,00	442,00
8,76	635,04	438,00	460,00	1192,00	498,00
8,80	610,09	472,00	498,00	1208,00	536,00
8,84	615,04	572,00	492,00	1328,00	532,00
8,88	538,24	626,00	550,00	1558,00	548,00
8,92	640,09	710,00	616,00	1976,00	536,00
8,96	571,21	776,00	654,00	2482,00	600,00
9,00	556,96	768,00	700,00	2850,00	578,00
9,04	538,24	800,00	802,00	2660,00	604,00
9,08	529,00	790,00	848,00	2120,00	638,00
9,12	529,00	702,00	960,00	1806,00	672,00
9,16	561,69	730,00	1042,00	1520,00	632,00
9,20	552,25	614,00	1058,00	1592,00	638,00
9,24	529,00	528,00	1172,00	1626,00	642,00
9,28	585,64	442,00	1276,00	1328,00	654,00
9,32	542,89	396,00	1256,00	1016,00	652,00
9,36	501,76	374,00	1198,00	884,00	662,00
9,40	497,29	332,00	1122,00	864,00	634,00
9,44	529,00	310,00	1076,00	676,00	656,00

9,48	529,00	342,00	864,00	474,00	654,00
9,52	479,61	356,00	736,00	402,00	656,00
9,56	515,29	376,00	604,00	354,00	646,00
9,60	453,69	374,00	524,00	362,00	610,00
9,64	479,61	396,00	432,00	370,00	544,00
9,68	492,84	412,00	452,00	370,00	518,00
9,72	510,76	442,00	384,00	424,00	560,00
9,76	501,76	464,00	368,00	406,00	522,00
9,80	479,61	520,00	342,00	468,00	472,00
9,84	462,25	530,00	302,00	458,00	462,00
9,88	479,61	566,00	282,00	460,00	470,00
9,92	475,24	516,00	314,00	384,00	486,00
9,96	445,21	508,00	314,00	352,00	472,00
10,00	475,24	472,00	286,00	312,00	456,00
10,04	470,89	406,00	300,00	308,00	426,00
10,08	453,69	384,00	294,00	290,00	412,00
10,12	453,69	338,00	306,00	308,00	398,00
10,16	428,49	278,00	290,00	324,00	434,00
10,20	420,25	258,00	282,00	280,00	410,00
10,24	424,36	272,00	270,00	294,00	406,00
10,28	380,25	266,00	262,00	306,00	384,00
10,32	441,00	254,00	266,00	304,00	354,00
10,36	441,00	210,00	240,00	312,00	398,00
10,40	453,69	250,00	268,00	300,00	346,00
10,44	424,36	222,00	298,00	340,00	352,00
10,48	424,36	222,00	280,00	346,00	340,00
10,52	392,04	238,00	274,00	336,00	358,00
10,56	412,09	226,00	288,00	302,00	336,00
10,60	416,16	192,00	296,00	338,00	338,00
10,64	424,36	212,00	316,00	332,00	344,00
10,68	404,01	238,00	306,00	340,00	338,00
10,72	408,04	210,00	278,00	324,00	318,00
10,76	428,49	220,00	314,00	328,00	328,00
10,80	388,09	258,00	356,00	342,00	312,00
10,84	388,09	208,00	306,00	338,00	334,00
10,88	432,64	232,00	322,00	318,00	286,00
10,92	428,49	190,00	306,00	342,00	332,00
10,96	432,64	254,00	312,00	326,00	326,00
11,00	408,04	238,00	326,00	334,00	316,00
11,04	484,00	250,00	318,00	334,00	314,00
11,08	462,25	250,00	308,00	326,00	318,00
11,12	453,69	250,00	298,00	342,00	358,00
11,16	408,04	310,00	298,00	346,00	338,00
11,20	445,21	296,00	294,00	350,00	298,00
11,24	441,00	314,00	288,00	354,00	334,00
11,28	457,96	334,00	300,00	372,00	316,00
11,32	484,00	370,00	284,00	422,00	316,00
11,36	445,21	454,00	260,00	456,00	330,00
11,40	462,25	554,00	312,00	456,00	300,00
11,44	457,96	542,00	280,00	506,00	306,00
11,48	488,41	664,00	318,00	542,00	300,00
11,52	488,41	814,00	276,00	618,00	320,00
11,56	475,24	1022,00	310,00	762,00	332,00
11,60	475,24	1110,00	320,00	800,00	296,00
11,64	484,00	1280,00	310,00	682,00	294,00
11,68	519,84	1208,00	386,00	502,00	322,00
11,72	524,41	1206,00	336,00	390,00	318,00

11,76	484,00	1302,00	346,00	398,00	326,00
11,80	515,29	1124,00	358,00	394,00	338,00
11,84	538,24	984,00	350,00	418,00	356,00
11,88	519,84	874,00	376,00	426,00	332,00
11,92	561,69	650,00	370,00	456,00	382,00
11,96	519,84	390,00	406,00	550,00	350,00
12,00	515,29	336,00	398,00	586,00	374,00
12,04	561,69	292,00	464,00	626,00	342,00
12,08	501,76	238,00	448,00	576,00	372,00
12,12	529,00	250,00	490,00	518,00	394,00
12,16	506,25	236,00	480,00	488,00	394,00
12,20	510,76	218,00	524,00	484,00	416,00
12,24	484,00	236,00	622,00	534,00	418,00
12,28	510,76	230,00	620,00	534,00	396,00
12,32	506,25	230,00	648,00	556,00	418,00
12,36	524,41	206,00	684,00	520,00	428,00
12,40	466,56	196,00	708,00	654,00	450,00
12,44	501,76	190,00	752,00	748,00	430,00
12,48	510,76	184,00	728,00	918,00	426,00
12,52	533,61	190,00	772,00	1084,00	450,00
12,56	538,24	194,00	728,00	1200,00	466,00
12,60	470,89	228,00	794,00	1264,00	488,00
12,64	453,69	204,00	832,00	990,00	450,00
12,68	501,76	214,00	892,00	612,00	470,00
12,72	484,00	156,00	918,00	482,00	472,00
12,76	470,89	206,00	932,00	458,00	494,00
12,80	479,61	186,00	1036,00	398,00	474,00
12,84	488,41	192,00	1024,00	478,00	486,00
12,88	475,24	180,00	1078,00	546,00	476,00
12,92	449,44	228,00	1012,00	556,00	470,00
12,96	449,44	192,00	1074,00	620,00	452,00
13,00	479,61	208,00	986,00	508,00	474,00
13,04	449,44	194,00	1018,00	394,00	498,00
13,08	479,61	188,00	984,00	392,00	442,00
13,12	488,41	194,00	1040,00	390,00	462,00
13,16	457,96	220,00	1004,00	420,00	444,00
13,20	436,81	224,00	932,00	420,00	432,00
13,24	492,84	206,00	886,00	430,00	418,00
13,28	449,44	202,00	758,00	446,00	420,00
13,32	515,29	202,00	756,00	364,00	404,00
13,36	466,56	190,00	692,00	330,00	428,00
13,40	441,00	190,00	586,00	340,00	402,00
13,44	488,41	196,00	558,00	354,00	382,00
13,48	457,96	206,00	492,00	348,00	396,00
13,52	484,00	180,00	474,00	370,00	352,00
13,56	501,76	182,00	492,00	350,00	354,00
13,60	501,76	228,00	434,00	374,00	376,00
13,64	484,00	196,00	388,00	364,00	384,00
13,68	497,29	178,00	406,00	378,00	350,00
13,72	497,29	184,00	362,00	440,00	338,00
13,76	506,25	232,00	374,00	492,00	364,00
13,80	506,25	178,00	370,00	498,00	370,00
13,84	515,29	190,00	368,00	558,00	340,00
13,88	492,84	184,00	376,00	578,00	348,00
13,92	475,24	184,00	380,00	546,00	328,00
13,96	479,61	216,00	366,00	408,00	328,00
14,00	470,89	206,00	334,00	366,00	324,00

14,04	506,25	198,00	332,00	422,00	360,00
14,08	488,41	182,00	338,00	354,00	314,00
14,12	519,84	216,00	378,00	338,00	324,00
14,16	484,00	206,00	306,00	344,00	374,00
14,20	497,29	202,00	342,00	342,00	326,00
14,24	519,84	184,00	362,00	330,00	328,00
14,28	506,25	184,00	320,00	354,00	302,00
14,32	533,61	204,00	314,00	344,00	292,00
14,36	488,41	222,00	310,00	366,00	312,00
14,40	547,56	196,00	300,00	384,00	320,00
14,44	506,25	186,00	290,00	376,00	314,00
14,48	533,61	214,00	294,00	386,00	320,00
14,52	529,00	224,00	306,00	378,00	320,00
14,56	510,76	188,00	260,00	420,00	296,00
14,60	538,24	184,00	300,00	420,00	328,00
14,64	529,00	214,00	274,00	448,00	330,00
14,68	580,81	240,00	276,00	468,00	296,00
14,72	547,56	190,00	264,00	542,00	340,00
14,76	552,25	220,00	276,00	594,00	302,00
14,80	552,25	196,00	278,00	718,00	324,00
14,84	506,25	204,00	284,00	866,00	316,00
14,88	595,36	200,00	318,00	848,00	338,00
14,92	538,24	212,00	272,00	852,00	336,00
14,96	595,36	220,00	270,00	636,00	304,00
15,00	552,25	204,00	310,00	542,00	312,00
15,04	610,09	230,00	270,00	474,00	330,00
15,08	561,69	214,00	278,00	392,00	342,00
15,12	566,44	206,00	288,00	388,00	348,00
15,16	595,36	210,00	260,00	364,00	338,00
15,20	595,36	206,00	282,00	382,00	336,00
15,24	630,01	206,00	340,00	402,00	300,00
15,28	600,25	228,00	280,00	372,00	366,00
15,32	600,25	208,00	296,00	396,00	296,00
15,36	585,64	242,00	252,00	380,00	348,00
15,40	605,16	222,00	294,00	344,00	332,00
15,44	630,01	206,00	294,00	394,00	348,00
15,48	561,69	224,00	288,00	346,00	344,00
15,52	620,01	196,00	296,00	374,00	306,00
15,56	610,09	204,00	304,00	360,00	354,00
15,60	625,00	216,00	334,00	352,00	334,00
15,64	645,16	222,00	272,00	366,00	330,00
15,68	655,36	242,00	298,00	332,00	330,00
15,72	645,16	228,00	316,00	338,00	342,00
15,76	655,36	228,00	332,00	340,00	368,00
15,80	665,64	220,00	314,00	370,00	310,00
15,84	665,64	236,00	296,00	330,00	366,00
15,88	707,56	250,00	356,00	394,00	324,00
15,92	707,56	234,00	332,00	380,00	328,00
15,96	729,00	268,00	336,00	390,00	346,00
16,00	767,29	242,00	362,00	386,00	326,00
16,04	864,36	274,00	342,00	450,00	324,00
16,08	817,96	280,00	336,00	414,00	394,00
16,12	841,00	274,00	344,00	372,00	348,00
16,16	841,00	270,00	314,00	350,00	358,00
16,20	852,64	252,00	326,00	378,00	394,00
16,24	829,44	254,00	340,00	386,00	360,00
16,28	784,00	228,00	300,00	410,00	368,00

16,32	734,41	246,00	328,00	430,00	422,00
16,36	767,29	282,00	350,00	426,00	326,00
16,40	852,64	238,00	328,00	418,00	382,00
16,44	823,69	264,00	324,00	394,00	384,00
16,48	912,04	252,00	334,00	356,00	432,00
16,52	942,49	258,00	354,00	416,00	384,00
16,56	967,21	226,00	346,00	358,00	394,00
16,60	1011,24	258,00	312,00	382,00	366,00
16,64	1089,00	252,00	354,00	412,00	386,00
16,68	1211,04	224,00	382,00	384,00	416,00
16,72	1102,24	210,00	376,00	354,00	402,00
16,76	1043,29	232,00	366,00	338,00	388,00
16,80	1024,00	252,00	356,00	338,00	404,00
16,84	930,25	220,00	380,00	390,00	390,00
16,88	894,01	228,00	374,00	420,00	460,00
16,92	864,36	242,00	428,00	374,00	410,00
16,96	823,69	248,00	402,00	376,00	430,00
17,00	900,00	238,00	422,00	384,00	444,00
17,04	841,00	222,00	400,00	360,00	488,00
17,08	800,89	258,00	444,00	346,00	442,00
17,12	778,41	210,00	440,00	362,00	480,00
17,16	756,25	248,00	444,00	374,00	438,00
17,20	823,69	250,00	480,00	412,00	416,00
17,24	756,25	250,00	464,00	436,00	434,00
17,28	806,56	304,00	534,00	498,00	486,00
17,32	795,24	298,00	506,00	416,00	488,00
17,36	795,24	266,00	538,00	436,00	446,00
17,40	835,21	276,00	550,00	400,00	502,00
17,44	823,69	284,00	538,00	392,00	468,00
17,48	846,81	308,00	572,00	446,00	516,00
17,52	858,49	334,00	650,00	440,00	508,00
17,56	841,00	342,00	664,00	428,00	540,00
17,60	864,36	374,00	612,00	438,00	476,00
17,64	823,69	386,00	646,00	450,00	500,00
17,68	888,04	406,00	666,00	518,00	528,00
17,72	900,00	410,00	610,00	480,00	490,00
17,76	835,21	398,00	668,00	554,00	538,00
17,80	876,16	370,00	586,00	560,00	540,00
17,84	800,89	402,00	606,00	488,00	546,00
17,88	870,25	398,00	556,00	594,00	540,00
17,92	823,69	354,00	642,00	642,00	544,00
17,96	817,96	332,00	608,00	722,00	562,00
18,00	823,69	362,00	642,00	808,00	570,00
18,04	812,25	390,00	626,00	808,00	530,00
18,08	841,00	442,00	640,00	842,00	534,00
18,12	789,61	374,00	660,00	814,00	590,00
18,16	789,61	420,00	656,00	708,00	536,00
18,20	812,25	472,00	606,00	704,00	536,00
18,24	858,49	410,00	586,00	744,00	560,00
18,28	778,41	420,00	544,00	726,00	530,00
18,32	852,64	412,00	520,00	882,00	568,00
18,36	823,69	470,00	548,00	1090,00	516,00
18,40	800,89	408,00	508,00	1170,00	546,00
18,44	841,00	434,00	528,00	1222,00	580,00
18,48	806,56	448,00	520,00	1508,00	518,00
18,52	852,64	418,00	568,00	1702,00	548,00
18,56	846,81	402,00	486,00	1902,00	524,00

18,60	812,25	362,00	538,00	1690,00	540,00
18,64	795,24	368,00	536,00	1198,00	544,00
18,68	806,56	342,00	508,00	804,00	560,00
18,72	784,00	334,00	494,00	588,00	546,00
18,76	729,00	326,00	546,00	598,00	598,00
18,80	806,56	336,00	548,00	582,00	536,00
18,84	817,96	336,00	538,00	590,00	582,00
18,88	784,00	314,00	556,00	576,00	578,00
18,92	817,96	360,00	556,00	586,00	552,00
18,96	778,41	368,00	574,00	580,00	578,00
19,00	712,89	388,00	608,00	576,00	514,00
19,04	829,44	354,00	556,00	612,00	576,00
19,08	823,69	390,00	566,00	660,00	594,00
19,12	756,25	394,00	606,00	740,00	568,00
19,16	784,00	416,00	648,00	802,00	594,00
19,20	800,89	368,00	662,00	842,00	608,00
19,24	806,56	406,00	724,00	878,00	588,00
19,28	778,41	478,00	722,00	892,00	614,00
19,32	756,25	488,00	788,00	900,00	580,00
19,36	772,84	474,00	772,00	1000,00	644,00
19,40	761,76	502,00	808,00	1232,00	630,00
19,44	784,00	504,00	806,00	1302,00	638,00
19,48	691,69	534,00	932,00	1402,00	672,00
19,52	778,41	554,00	1042,00	1468,00	728,00
19,56	761,76	550,00	1172,00	1638,00	748,00
19,60	723,61	558,00	1250,00	1736,00	796,00
19,64	750,76	592,00	1328,00	1806,00	786,00
19,68	761,76	592,00	1560,00	1876,00	816,00
19,72	734,41	586,00	1540,00	1968,00	830,00
19,76	778,41	584,00	1712,00	1922,00	910,00
19,80	745,29	638,00	1958,00	1572,00	998,00
19,84	772,84	668,00	1982,00	1220,00	968,00
19,88	734,41	678,00	2070,00	1072,00	1092,00
19,92	712,89	780,00	2066,00	968,00	1118,00
19,96	718,24	780,00	2128,00	928,00	1116,00
20,00	739,84	854,00	1972,00	894,00	1158,00
20,04	702,25	896,00	1862,00	1014,00	1186,00
20,08	723,61	886,00	1652,00	1082,00	1258,00
20,12	767,29	882,00	1520,00	1288,00	1236,00
20,16	718,24	866,00	1352,00	1488,00	1198,00
20,20	723,61	874,00	1210,00	1664,00	1208,00
20,24	723,61	824,00	1118,00	1944,00	1144,00
20,28	696,96	778,00	1002,00	2402,00	1218,00
20,32	676,00	734,00	978,00	2484,00	1026,00
20,36	635,04	726,00	914,00	2548,00	1060,00
20,40	660,49	632,00	880,00	2272,00	990,00
20,44	702,25	564,00	748,00	1772,00	938,00
20,48	605,16	590,00	880,00	1400,00	1010,00
20,52	691,69	506,00	778,00	1166,00	988,00
20,56	691,69	514,00	794,00	1124,00	974,00
20,60	681,21	486,00	766,00	1086,00	884,00
20,64	630,01	522,00	796,00	1202,00	906,00
20,68	686,44	476,00	786,00	1258,00	832,00
20,72	615,04	488,00	726,00	1216,00	822,00
20,76	686,44	494,00	738,00	1132,00	862,00
20,80	620,01	480,00	710,00	982,00	790,00
20,84	670,81	498,00	696,00	874,00	780,00

20,88	676,00	564,00	658,00	832,00	792,00
20,92	635,04	518,00	674,00	836,00	752,00
20,96	630,01	534,00	684,00	864,00	792,00
21,00	650,25	612,00	614,00	856,00	770,00
21,04	630,01	616,00	630,00	914,00	724,00
21,08	681,21	604,00	608,00	964,00	716,00
21,12	635,04	616,00	578,00	1064,00	702,00
21,16	645,16	632,00	566,00	1108,00	756,00
21,20	561,69	610,00	582,00	1190,00	704,00
21,24	650,25	618,00	592,00	1412,00	724,00
21,28	655,36	672,00	580,00	1424,00	696,00
21,32	600,25	624,00	600,00	1450,00	644,00
21,36	605,16	610,00	600,00	1152,00	650,00
21,40	620,01	668,00	574,00	884,00	710,00
21,44	681,21	614,00	618,00	650,00	676,00
21,48	605,16	596,00	566,00	616,00	760,00
21,52	650,25	656,00	636,00	560,00	688,00
21,56	640,09	638,00	608,00	574,00	714,00
21,60	625,00	646,00	670,00	606,00	654,00
21,64	660,49	604,00	668,00	638,00	664,00
21,68	670,81	582,00	716,00	650,00	688,00
21,72	625,00	598,00	672,00	670,00	684,00
21,76	615,04	612,00	726,00	708,00	674,00
21,80	605,16	558,00	766,00	798,00	660,00
21,84	655,36	530,00	810,00	974,00	658,00
21,88	650,25	568,00	776,00	1136,00	610,00
21,92	660,49	572,00	816,00	1354,00	670,00
21,96	707,56	504,00	820,00	1548,00	634,00
22,00	676,00	538,00	734,00	1718,00	678,00
22,04	610,09	552,00	774,00	1442,00	602,00
22,08	635,04	558,00	736,00	1104,00	634,00
22,12	681,21	566,00	626,00	728,00	634,00
22,16	655,36	552,00	670,00	664,00	662,00
22,20	655,36	582,00	606,00	578,00	560,00
22,24	645,16	530,00	596,00	554,00	618,00
22,28	625,00	594,00	570,00	574,00	562,00
22,32	676,00	564,00	534,00	534,00	582,00
22,36	686,44	552,00	512,00	492,00	610,00
22,40	645,16	536,00	514,00	492,00	580,00
22,44	676,00	530,00	474,00	470,00	556,00
22,48	686,44	514,00	492,00	506,00	594,00
22,52	670,81	486,00	466,00	504,00	560,00
22,56	660,49	458,00	462,00	558,00	588,00
22,60	686,44	440,00	400,00	626,00	526,00
22,64	650,25	476,00	430,00	540,00	580,00
22,68	670,81	502,00	482,00	598,00	544,00
22,72	635,04	468,00	426,00	662,00	528,00
22,76	686,44	460,00	460,00	796,00	526,00
22,80	686,44	446,00	478,00	814,00	574,00
22,84	686,44	478,00	462,00	858,00	546,00
22,88	712,89	496,00	436,00	770,00	518,00
22,92	696,96	502,00	424,00	822,00	542,00
22,96	681,21	546,00	432,00	850,00	548,00
23,00	734,41	598,00	442,00	682,00	532,00
23,04	702,25	652,00	448,00	590,00	542,00
23,08	745,29	702,00	438,00	504,00	540,00
23,12	723,61	764,00	468,00	486,00	530,00

23,16	723,61	852,00	464,00	498,00	514,00
23,20	734,41	910,00	452,00	462,00	516,00
23,24	707,56	926,00	446,00	488,00	532,00
23,28	718,24	990,00	474,00	448,00	496,00
23,32	718,24	968,00	442,00	468,00	566,00
23,36	734,41	958,00	458,00	408,00	518,00
23,40	772,84	998,00	488,00	382,00	528,00
23,44	812,25	836,00	474,00	368,00	494,00
23,48	795,24	830,00	464,00	380,00	540,00
23,52	812,25	748,00	514,00	440,00	504,00
23,56	841,00	688,00	460,00	384,00	544,00
23,60	823,69	686,00	456,00	396,00	514,00
23,64	894,01	678,00	470,00	406,00	514,00
23,68	936,36	642,00	504,00	372,00	474,00
23,72	985,96	560,00	448,00	374,00	506,00
23,76	900,00	590,00	424,00	360,00	494,00
23,80	1011,24	626,00	422,00	384,00	502,00
23,84	888,04	580,00	436,00	388,00	486,00
23,88	888,04	612,00	400,00	382,00	494,00
23,92	841,00	552,00	422,00	438,00	476,00
23,96	795,24	614,00	458,00	412,00	564,00
24,00	829,44	536,00	418,00	488,00	496,00
24,04	795,24	514,00	432,00	496,00	528,00
24,08	789,61	518,00	396,00	546,00	520,00
24,12	756,25	506,00	442,00	570,00	452,00
24,16	789,61	526,00	446,00	464,00	474,00
24,20	756,25	488,00	388,00	490,00	466,00
24,24	772,84	506,00	440,00	444,00	458,00
24,28	772,84	490,00	430,00	370,00	460,00
24,32	800,89	480,00	394,00	434,00	454,00
24,36	800,89	408,00	400,00	378,00	490,00
24,40	745,29	422,00	424,00	362,00	476,00
24,44	784,00	404,00	460,00	352,00	474,00
24,48	750,76	408,00	404,00	406,00	464,00
24,52	789,61	412,00	450,00	376,00	468,00
24,56	761,76	412,00	426,00	416,00	474,00
24,60	750,76	444,00	408,00	422,00	526,00
24,64	756,25	428,00	408,00	400,00	500,00
24,68	696,96	462,00	406,00	422,00	454,00
24,72	767,29	400,00	482,00	374,00	468,00
24,76	756,25	460,00	442,00	362,00	482,00
24,80	745,29	432,00	438,00	388,00	498,00
24,84	750,76	430,00	464,00	376,00	462,00
24,88	789,61	450,00	486,00	402,00	492,00
24,92	784,00	438,00	476,00	434,00	484,00
24,96	739,84	464,00	464,00	434,00	470,00
25,00	767,29	448,00	476,00	430,00	436,00
25,04	729,00	454,00	514,00	466,00	456,00
25,08	750,76	480,00	434,00	478,00	476,00
25,12	756,25	410,00	442,00	466,00	486,00
25,16	778,41	408,00	462,00	488,00	450,00
25,20	729,00	370,00	446,00	464,00	440,00
25,24	772,84	450,00	466,00	432,00	454,00
25,28	772,84	440,00	444,00	414,00	502,00
25,32	750,76	442,00	450,00	442,00	446,00
25,36	761,76	410,00	500,00	440,00	440,00
25,40	795,24	422,00	534,00	390,00	496,00

25,44	789,61	472,00	510,00	474,00	510,00
25,48	784,00	466,00	456,00	472,00	464,00
25,52	829,44	434,00	454,00	468,00	490,00
25,56	812,25	440,00	496,00	432,00	492,00
25,60	806,56	454,00	486,00	452,00	496,00
25,64	870,25	492,00	514,00	424,00	472,00
25,68	778,41	440,00	516,00	444,00	516,00
25,72	870,25	462,00	528,00	432,00	474,00
25,76	924,16	444,00	488,00	422,00	522,00
25,80	930,25	482,00	524,00	404,00	514,00
25,84	967,21	520,00	558,00	410,00	518,00
25,88	894,01	490,00	558,00	438,00	538,00
25,92	998,56	478,00	616,00	406,00	554,00
25,96	912,04	528,00	544,00	458,00	496,00
26,00	912,04	594,00	578,00	430,00	522,00
26,04	936,36	604,00	542,00	398,00	534,00
26,08	870,25	684,00	574,00	416,00	516,00
26,12	795,24	830,00	570,00	390,00	514,00
26,16	841,00	912,00	552,00	412,00	548,00
26,20	864,36	1134,00	590,00	456,00	490,00
26,24	795,24	1344,00	594,00	388,00	512,00
26,28	852,64	1424,00	590,00	412,00	512,00
26,32	835,21	1808,00	610,00	414,00	508,00
26,36	852,64	1960,00	618,00	440,00	508,00
26,40	784,00	1900,00	608,00	440,00	510,00
26,44	870,25	1956,00	672,00	488,00	506,00
26,48	858,49	1956,00	672,00	458,00	510,00
26,52	795,24	1842,00	636,00	456,00	544,00
26,56	761,76	1628,00	672,00	426,00	512,00
26,60	789,61	1338,00	634,00	468,00	512,00
26,64	806,56	1080,00	702,00	512,00	516,00
26,68	756,25	880,00	682,00	536,00	542,00
26,72	767,29	758,00	728,00	534,00	518,00
26,76	772,84	646,00	684,00	536,00	524,00
26,80	756,25	580,00	694,00	518,00	552,00
26,84	778,41	504,00	712,00	486,00	564,00
26,88	841,00	516,00	654,00	426,00	564,00
26,92	734,41	494,00	686,00	406,00	528,00
26,96	756,25	516,00	706,00	422,00	602,00
27,00	789,61	480,00	722,00	428,00	558,00
27,04	750,76	460,00	726,00	418,00	552,00
27,08	729,00	440,00	784,00	492,00	536,00
27,12	696,96	500,00	764,00	430,00	560,00
27,16	767,29	456,00	798,00	428,00	516,00
27,20	734,41	500,00	790,00	404,00	536,00
27,24	696,96	466,00	778,00	436,00	516,00
27,28	707,56	474,00	888,00	448,00	516,00
27,32	691,69	458,00	866,00	442,00	562,00
27,36	676,00	546,00	878,00	468,00	510,00
27,40	712,89	504,00	838,00	490,00	562,00
27,44	676,00	600,00	938,00	488,00	558,00
27,48	686,44	638,00	1056,00	504,00	568,00
27,52	640,09	618,00	1026,00	554,00	538,00
27,56	707,56	662,00	1080,00	594,00	566,00
27,60	665,64	700,00	1140,00	576,00	554,00
27,64	635,04	724,00	1182,00	516,00	558,00
27,68	670,81	688,00	1248,00	522,00	564,00

27,72	625,00	760,00	1228,00	496,00	612,00
27,76	670,81	712,00	1262,00	520,00	574,00
27,80	610,09	708,00	1318,00	470,00	628,00
27,84	645,16	686,00	1326,00	528,00	608,00
27,88	640,09	708,00	1404,00	532,00	632,00
27,92	660,49	616,00	1382,00	548,00	634,00
27,96	605,16	630,00	1450,00	558,00	636,00
28,00	561,69	554,00	1338,00	540,00	624,00
28,04	580,81	474,00	1260,00	574,00	712,00
28,08	556,96	464,00	1182,00	560,00	644,00
28,12	561,69	474,00	1080,00	612,00	694,00
28,16	529,00	428,00	1046,00	616,00	738,00
28,20	515,29	404,00	972,00	572,00	700,00
28,24	538,24	402,00	904,00	636,00	708,00
28,28	501,76	414,00	788,00	688,00	710,00
28,32	533,61	424,00	768,00	694,00	744,00
28,36	510,76	424,00	702,00	858,00	702,00
28,40	510,76	440,00	688,00	1044,00	698,00
28,44	479,61	398,00	620,00	1100,00	756,00
28,48	506,25	396,00	608,00	1230,00	708,00
28,52	515,29	400,00	600,00	1218,00	644,00
28,56	552,25	410,00	560,00	1146,00	728,00
28,60	484,00	404,00	530,00	1004,00	684,00
28,64	497,29	398,00	512,00	998,00	696,00
28,68	475,24	372,00	524,00	950,00	696,00
28,72	524,41	408,00	496,00	1070,00	720,00
28,76	515,29	356,00	510,00	1050,00	652,00
28,80	479,61	394,00	454,00	1064,00	652,00
28,84	556,96	396,00	496,00	1058,00	624,00
28,88	576,00	364,00	480,00	938,00	590,00
28,92	625,00	368,00	504,00	866,00	592,00
28,96	630,01	396,00	444,00	846,00	506,00
29,00	625,00	384,00	434,00	852,00	524,00
29,04	681,21	382,00	454,00	926,00	520,00
29,08	707,56	374,00	458,00	1006,00	454,00
29,12	723,61	402,00	456,00	1192,00	524,00
29,16	645,16	366,00	418,00	1248,00	482,00
29,20	610,09	406,00	414,00	1242,00	502,00
29,24	600,25	428,00	448,00	1004,00	466,00
29,28	547,56	376,00	424,00	940,00	500,00
29,32	519,84	458,00	394,00	722,00	434,00
29,36	475,24	460,00	442,00	654,00	440,00
29,40	510,76	490,00	398,00	606,00	432,00
29,44	506,25	486,00	416,00	546,00	388,00
29,48	475,24	524,00	402,00	570,00	408,00
29,52	445,21	576,00	430,00	592,00	382,00
29,56	404,01	544,00	372,00	612,00	380,00
29,60	424,36	576,00	370,00	708,00	366,00
29,64	376,36	682,00	390,00	666,00	368,00
29,68	404,01	604,00	370,00	710,00	370,00
29,72	396,01	662,00	378,00	572,00	348,00
29,76	376,36	666,00	362,00	550,00	396,00
29,80	376,36	666,00	366,00	524,00	404,00
29,84	396,01	576,00	326,00	480,00	372,00
29,88	372,49	606,00	344,00	506,00	344,00
29,92	396,01	532,00	358,00	512,00	354,00
29,96	349,69	520,00	382,00	560,00	348,00

30,00	357,21	448,00	396,00	586,00	330,00
30,04	376,36	396,00	360,00	576,00	346,00
30,08	342,25	412,00	338,00	648,00	346,00
30,12	368,64	388,00	356,00	610,00	352,00
30,16	342,25	408,00	316,00	522,00	346,00
30,20	342,25	376,00	362,00	478,00	330,00
30,24	334,89	386,00	366,00	460,00	306,00
30,28	338,56	326,00	358,00	426,00	356,00
30,32	334,89	368,00	354,00	380,00	314,00
30,36	349,69	370,00	368,00	354,00	332,00
30,40	299,29	362,00	384,00	350,00	282,00
30,44	295,84	392,00	378,00	382,00	326,00
30,48	295,84	378,00	400,00	368,00	316,00
30,52	338,56	344,00	378,00	326,00	338,00
30,56	302,76	346,00	374,00	314,00	344,00
30,60	282,24	342,00	404,00	328,00	334,00
30,64	320,41	342,00	402,00	354,00	314,00
30,68	285,61	344,00	370,00	326,00	298,00
30,72	265,69	388,00	430,00	368,00	324,00
30,76	249,64	338,00	424,00	356,00	310,00
30,80	306,25	334,00	372,00	390,00	306,00
30,84	299,29	352,00	456,00	414,00	298,00
30,88	292,41	352,00	412,00	412,00	300,00
30,92	278,89	330,00	422,00	440,00	306,00
30,96	295,84	314,00	396,00	468,00	256,00
31,00	265,69	332,00	358,00	426,00	260,00
31,04	268,96	360,00	396,00	444,00	292,00
31,08	282,24	326,00	388,00	356,00	296,00
31,12	249,64	332,00	374,00	352,00	250,00
31,16	259,21	340,00	366,00	344,00	300,00
31,20	272,25	324,00	330,00	350,00	286,00
31,24	219,04	310,00	338,00	402,00	296,00
31,28	256,00	356,00	348,00	358,00	278,00
31,32	256,00	368,00	336,00	364,00	294,00
31,36	228,01	342,00	310,00	356,00	274,00
31,40	219,04	346,00	338,00	370,00	290,00
31,44	265,69	372,00	312,00	358,00	256,00
31,48	265,69	346,00	310,00	324,00	250,00
31,52	249,64	352,00	298,00	332,00	294,00
31,56	219,04	362,00	320,00	340,00	290,00
31,60	234,09	350,00	326,00	356,00	268,00
31,64	246,49	332,00	270,00	350,00	290,00
31,68	246,49	372,00	306,00	316,00	288,00
31,72	225,00	332,00	322,00	322,00	260,00
31,76	249,64	358,00	296,00	312,00	272,00
31,80	252,81	340,00	342,00	324,00	264,00
31,84	210,25	326,00	294,00	284,00	230,00
31,88	222,01	304,00	280,00	338,00	230,00
31,92	213,16	336,00	284,00	290,00	248,00
31,96	222,01	302,00	296,00	314,00	258,00
32,00	231,04	332,00	276,00	322,00	254,00
32,04	225,00	324,00	286,00	320,00	250,00
32,08	201,64	320,00	304,00	330,00	230,00
32,12	207,36	336,00	302,00	296,00	238,00
32,16	210,25	306,00	278,00	304,00	230,00
32,20	231,04	324,00	302,00	312,00	246,00
32,24	204,49	332,00	292,00	306,00	244,00

32,28	222,01	304,00	300,00	336,00	242,00
32,32	216,09	350,00	282,00	318,00	232,00
32,36	210,25	302,00	274,00	312,00	214,00
32,40	204,49	334,00	256,00	308,00	214,00
32,44	207,36	326,00	302,00	276,00	282,00
32,48	201,64	338,00	306,00	318,00	254,00
32,52	198,81	316,00	298,00	290,00	228,00
32,56	174,24	308,00	286,00	310,00	242,00
32,60	225,00	298,00	312,00	308,00	254,00
32,64	237,16	304,00	282,00	332,00	236,00
32,68	225,00	308,00	270,00	294,00	246,00
32,72	210,25	322,00	252,00	318,00	238,00
32,76	201,64	308,00	284,00	300,00	310,00
32,80	184,96	308,00	298,00	282,00	278,00
32,84	207,36	310,00	270,00	318,00	276,00
32,88	174,24	294,00	238,00	318,00	250,00
32,92	216,09	304,00	260,00	308,00	270,00
32,96	182,25	316,00	248,00	308,00	260,00
33,00	207,36	296,00	272,00	294,00	204,00
33,04	196,00	336,00	272,00	286,00	232,00
33,08	198,81	342,00	262,00	318,00	234,00
33,12	219,04	328,00	250,00	298,00	218,00
33,16	182,25	332,00	276,00	250,00	230,00
33,20	201,64	276,00	258,00	266,00	250,00
33,24	179,56	326,00	238,00	268,00	252,00
33,28	193,21	326,00	230,00	276,00	238,00
33,32	213,16	346,00	226,00	238,00	238,00
33,36	179,56	318,00	250,00	230,00	232,00
33,40	187,69	354,00	272,00	224,00	234,00
33,44	190,44	378,00	252,00	236,00	218,00
33,48	222,01	338,00	254,00	246,00	212,00
33,52	193,21	336,00	250,00	252,00	220,00
33,56	176,89	318,00	232,00	262,00	194,00
33,60	196,00	342,00	232,00	288,00	208,00
33,64	184,96	328,00	256,00	286,00	202,00
33,68	225,00	342,00	244,00	314,00	238,00
33,72	234,09	310,00	248,00	290,00	222,00
33,76	256,00	334,00	240,00	300,00	246,00
33,80	213,16	334,00	240,00	268,00	220,00
33,84	228,01	330,00	254,00	274,00	214,00
33,88	196,00	332,00	226,00	306,00	216,00
33,92	210,25	314,00	270,00	256,00	204,00
33,96	193,21	302,00	214,00	296,00	244,00
34,00	174,24	290,00	258,00	260,00	214,00
34,04	171,61	300,00	240,00	236,00	218,00
34,08	182,25	296,00	290,00	236,00	206,00
34,12	210,25	246,00	262,00	200,00	194,00
34,16	174,24	278,00	246,00	234,00	206,00
34,20	169,00	258,00	230,00	224,00	196,00
34,24	158,76	250,00	236,00	236,00	220,00
34,28	166,41	276,00	236,00	260,00	222,00
34,32	166,41	264,00	250,00	244,00	246,00
34,36	163,84	228,00	256,00	230,00	216,00
34,40	184,96	258,00	258,00	210,00	206,00
34,44	166,41	244,00	244,00	240,00	220,00
34,48	156,25	258,00	278,00	208,00	210,00
34,52	182,25	234,00	246,00	234,00	216,00

34,56	156,25	250,00	240,00	216,00	212,00
34,60	146,41	228,00	262,00	256,00	202,00
34,64	129,96	224,00	236,00	238,00	202,00
34,68	161,29	238,00	242,00	242,00	200,00
34,72	184,96	244,00	232,00	230,00	208,00
34,76	176,89	254,00	236,00	266,00	208,00
34,80	171,61	286,00	264,00	236,00	208,00
34,84	171,61	236,00	256,00	246,00	222,00
34,88	153,76	242,00	236,00	266,00	200,00
34,92	151,29	244,00	218,00	256,00	230,00
34,96	158,76	276,00	238,00	252,00	204,00
35,00	166,41	244,00	254,00	260,00	242,00
35,04	151,29	222,00	258,00	268,00	192,00
35,08	161,29	246,00	256,00	270,00	208,00
35,12	169,00	236,00	234,00	308,00	204,00
35,16	134,56	240,00	222,00	252,00	208,00
35,20	136,89	220,00	230,00	284,00	196,00
35,24	153,76	234,00	240,00	240,00	188,00
35,28	161,29	246,00	232,00	250,00	200,00
35,32	123,21	248,00	234,00	260,00	192,00
35,36	163,84	234,00	250,00	232,00	226,00
35,40	123,21	248,00	244,00	270,00	192,00
35,44	156,25	232,00	236,00	228,00	186,00
35,48	151,29	248,00	214,00	244,00	202,00
35,52	174,24	260,00	274,00	258,00	210,00
35,56	129,96	266,00	242,00	256,00	186,00
35,60	144,00	242,00	270,00	258,00	212,00
35,64	163,84	244,00	252,00	240,00	186,00
35,68	132,25	228,00	284,00	264,00	226,00
35,72	134,56	244,00	244,00	232,00	184,00
35,76	153,76	226,00	258,00	244,00	194,00
35,80	136,89	254,00	240,00	244,00	202,00
35,84	153,76	258,00	244,00	254,00	184,00
35,88	153,76	238,00	262,00	234,00	196,00
35,92	151,29	232,00	290,00	248,00	212,00
35,96	166,41	240,00	272,00	260,00	198,00
36,00	134,56	226,00	272,00	252,00	190,00
36,04	153,76	242,00	284,00	242,00	196,00
36,08	139,24	218,00	242,00	258,00	208,00
36,12	127,69	234,00	274,00	258,00	188,00
36,16	174,24	244,00	264,00	268,00	218,00
36,20	129,96	270,00	270,00	242,00	198,00
36,24	161,29	198,00	270,00	280,00	180,00
36,28	158,76	194,00	268,00	272,00	222,00
36,32	139,24	220,00	288,00	252,00	212,00
36,36	146,41	250,00	256,00	228,00	188,00
36,40	148,84	228,00	276,00	288,00	192,00
36,44	158,76	238,00	288,00	274,00	184,00
36,48	144,00	220,00	256,00	260,00	200,00
36,52	144,00	218,00	272,00	266,00	198,00
36,56	134,56	212,00	302,00	274,00	202,00
36,60	151,29	206,00	276,00	310,00	200,00
36,64	146,41	208,00	298,00	302,00	220,00
36,68	132,25	228,00	296,00	288,00	188,00
36,72	134,56	228,00	296,00	312,00	194,00
36,76	148,84	222,00	306,00	334,00	196,00
36,80	153,76	200,00	286,00	360,00	202,00

36,84	144,00	220,00	306,00	302,00	208,00
36,88	118,81	214,00	262,00	356,00	200,00
36,92	123,21	216,00	312,00	330,00	212,00
36,96	148,84	208,00	296,00	318,00	224,00
37,00	129,96	208,00	298,00	334,00	202,00
37,04	132,25	214,00	278,00	324,00	172,00
37,08	148,84	212,00	314,00	356,00	214,00
37,12	127,69	216,00	288,00	308,00	208,00
37,16	139,24	228,00	274,00	338,00	186,00
37,20	136,89	206,00	338,00	314,00	232,00
37,24	144,00	184,00	346,00	324,00	218,00
37,28	153,76	228,00	292,00	310,00	216,00
37,32	134,56	228,00	280,00	274,00	240,00
37,36	148,84	214,00	270,00	312,00	224,00
37,40	129,96	234,00	292,00	310,00	210,00
37,44	136,89	226,00	296,00	280,00	236,00
37,48	151,29	212,00	298,00	320,00	216,00
37,52	129,96	232,00	284,00	292,00	186,00
37,56	144,00	220,00	304,00	294,00	220,00
37,60	136,89	208,00	312,00	296,00	226,00
37,64	123,21	220,00	280,00	274,00	200,00
37,68	127,69	232,00	314,00	316,00	214,00
37,72	132,25	222,00	302,00	302,00	200,00
37,76	123,21	228,00	308,00	314,00	194,00
37,80	136,89	232,00	292,00	294,00	206,00
37,84	144,00	214,00	318,00	330,00	252,00
37,88	141,61	242,00	316,00	294,00	232,00
37,92	148,84	246,00	298,00	300,00	204,00
37,96	141,61	246,00	304,00	254,00	218,00
38,00	146,41	224,00	264,00	274,00	188,00
38,04	156,25	230,00	276,00	274,00	222,00
38,08	158,76	234,00	282,00	278,00	186,00
38,12	136,89	214,00	282,00	266,00	184,00
38,16	127,69	208,00	268,00	288,00	210,00
38,20	134,56	204,00	262,00	266,00	184,00
38,24	141,61	202,00	244,00	280,00	178,00
38,28	134,56	214,00	290,00	266,00	194,00
38,32	125,44	204,00	294,00	264,00	192,00
38,36	123,21	200,00	278,00	286,00	200,00
38,40	127,69	212,00	262,00	272,00	196,00
38,44	129,96	186,00	256,00	274,00	204,00
38,48	151,29	224,00	268,00	284,00	212,00
38,52	146,41	256,00	236,00	262,00	208,00
38,56	144,00	236,00	266,00	294,00	200,00
38,60	141,61	172,00	262,00	286,00	216,00
38,64	123,21	214,00	256,00	312,00	190,00
38,68	144,00	232,00	254,00	308,00	224,00
38,72	127,69	174,00	278,00	298,00	198,00
38,76	136,89	216,00	248,00	288,00	186,00
38,80	132,25	230,00	244,00	260,00	208,00
38,84	134,56	236,00	232,00	292,00	184,00
38,88	151,29	214,00	270,00	304,00	212,00
38,92	127,69	208,00	250,00	256,00	190,00
38,96	114,49	230,00	266,00	306,00	200,00
39,00	114,49	204,00	274,00	278,00	196,00
39,04	121,00	222,00	262,00	282,00	170,00
39,08	148,84	206,00	242,00	276,00	186,00

39,12	153,76	250,00	266,00	290,00	194,00
39,16	148,84	182,00	280,00	256,00	192,00
39,20	134,56	206,00	266,00	282,00	196,00
39,24	127,69	216,00	282,00	286,00	168,00
39,28	123,21	216,00	276,00	244,00	170,00
39,32	146,41	254,00	274,00	312,00	188,00
39,36	127,69	226,00	272,00	320,00	208,00
39,40	110,25	236,00	274,00	308,00	198,00
39,44	129,96	230,00	294,00	294,00	206,00
39,48	108,16	228,00	294,00	296,00	196,00
39,52	104,04	216,00	264,00	350,00	220,00
39,56	123,21	200,00	302,00	286,00	176,00
39,60	132,25	226,00	262,00	300,00	180,00
39,64	114,49	224,00	262,00	294,00	186,00
39,68	116,64	218,00	290,00	302,00	180,00
39,72	116,64	210,00	304,00	276,00	186,00
39,76	118,81	226,00	260,00	286,00	192,00
39,80	132,25	214,00	280,00	350,00	196,00
39,84	127,69	230,00	272,00	268,00	200,00
39,88	129,96	234,00	274,00	296,00	190,00
39,92	129,96	222,00	290,00	280,00	194,00
39,96	98,01	196,00	292,00	324,00	202,00
40,00	112,36	224,00	290,00	306,00	202,00
40,04	108,16	210,00	294,00	284,00	200,00
40,08	102,01	246,00	296,00	318,00	210,00
40,12	114,49	210,00	298,00	302,00	198,00
40,16	114,49	240,00	274,00	288,00	180,00
40,20	90,25	226,00	264,00	266,00	174,00
40,24	112,36	212,00	288,00	262,00	210,00
40,28	112,36	214,00	262,00	296,00	228,00
40,32	108,16	218,00	280,00	272,00	190,00
40,36	123,21	220,00	316,00	290,00	190,00
40,40	132,25	214,00	304,00	286,00	194,00
40,44	118,81	242,00	320,00	288,00	202,00
40,48	110,25	232,00	286,00	244,00	206,00
40,52	127,69	236,00	276,00	274,00	202,00
40,56	141,61	218,00	316,00	246,00	164,00
40,60	132,25	228,00	288,00	278,00	202,00
40,64	112,36	204,00	294,00	320,00	178,00
40,68	129,96	226,00	278,00	322,00	206,00
40,72	118,81	236,00	244,00	296,00	212,00
40,76	118,81	196,00	256,00	286,00	210,00
40,80	132,25	214,00	280,00	332,00	222,00
40,84	127,69	184,00	300,00	272,00	192,00
40,88	118,81	212,00	228,00	288,00	174,00
40,92	127,69	224,00	250,00	296,00	240,00
40,96	132,25	200,00	252,00	276,00	192,00
41,00	121,00	210,00	264,00	282,00	212,00
41,04	121,00	200,00	258,00	286,00	176,00
41,08	104,04	250,00	252,00	296,00	192,00
41,12	139,24	212,00	272,00	282,00	192,00
41,16	125,44	198,00	250,00	282,00	208,00
41,20	125,44	200,00	250,00	280,00	190,00
41,24	121,00	198,00	230,00	314,00	184,00
41,28	106,09	204,00	256,00	286,00	206,00
41,32	112,36	214,00	252,00	286,00	228,00
41,36	116,64	210,00	244,00	310,00	184,00

41,40	121,00	224,00	248,00	298,00	184,00
41,44	136,89	228,00	246,00	258,00	162,00
41,48	110,25	194,00	224,00	270,00	204,00
41,52	129,96	188,00	240,00	252,00	184,00
41,56	112,36	194,00	260,00	262,00	180,00
41,60	114,49	192,00	244,00	262,00	184,00
41,64	106,09	236,00	234,00	240,00	180,00
41,68	127,69	204,00	254,00	234,00	178,00
41,72	125,44	196,00	266,00	246,00	210,00
41,76	108,16	212,00	246,00	244,00	184,00
41,80	129,96	208,00	222,00	216,00	186,00
41,84	136,89	238,00	242,00	250,00	190,00
41,88	132,25	208,00	262,00	250,00	182,00
41,92	118,81	232,00	246,00	232,00	198,00
41,96	112,36	250,00	232,00	224,00	170,00
42,00	132,25	236,00	244,00	248,00	168,00
42,04	134,56	206,00	260,00	268,00	188,00
42,08	96,04	244,00	290,00	256,00	176,00
42,12	129,96	250,00	268,00	252,00	170,00
42,16	132,25	226,00	252,00	236,00	186,00
42,20	121,00	234,00	240,00	242,00	186,00
42,24	112,36	220,00	254,00	264,00	182,00
42,28	123,21	240,00	260,00	238,00	160,00
42,32	104,04	210,00	242,00	224,00	164,00
42,36	118,81	236,00	244,00	228,00	174,00
42,40	108,16	242,00	224,00	264,00	210,00
42,44	114,49	224,00	240,00	276,00	190,00
42,48	112,36	244,00	228,00	248,00	190,00
42,52	102,01	226,00	222,00	272,00	198,00
42,56	121,00	246,00	216,00	252,00	222,00
42,60	114,49	232,00	242,00	256,00	222,00
42,64	102,01	218,00	238,00	262,00	214,00
42,68	139,24	208,00	248,00	266,00	224,00
42,72	121,00	214,00	238,00	266,00	174,00
42,76	110,25	212,00	252,00	298,00	214,00
42,80	102,01	230,00	206,00	270,00	182,00
42,84	129,96	222,00	236,00	288,00	198,00
42,88	127,69	222,00	224,00	270,00	202,00
42,92	116,64	226,00	232,00	258,00	200,00
42,96	118,81	212,00	242,00	284,00	220,00
43,00	141,61	202,00	214,00	252,00	202,00
43,04	139,24	218,00	238,00	270,00	182,00
43,08	127,69	242,00	200,00	242,00	182,00
43,12	129,96	208,00	196,00	222,00	168,00
43,16	121,00	214,00	232,00	250,00	214,00
43,20	108,16	208,00	216,00	228,00	180,00
43,24	134,56	220,00	222,00	226,00	214,00
43,28	121,00	186,00	216,00	242,00	174,00
43,32	129,96	222,00	206,00	246,00	190,00
43,36	134,56	246,00	196,00	228,00	158,00
43,40	121,00	216,00	212,00	246,00	156,00
43,44	114,49	210,00	216,00	232,00	168,00
43,48	110,25	250,00	236,00	246,00	162,00
43,52	118,81	224,00	214,00	244,00	172,00
43,56	123,21	208,00	240,00	212,00	182,00
43,60	110,25	220,00	220,00	266,00	162,00
43,64	132,25	230,00	214,00	240,00	186,00

43,68	125,44	186,00	226,00	230,00	184,00
43,72	139,24	202,00	220,00	248,00	164,00
43,76	134,56	192,00	214,00	222,00	184,00
43,80	132,25	230,00	224,00	278,00	174,00
43,84	141,61	184,00	224,00	262,00	174,00
43,88	139,24	222,00	216,00	268,00	182,00
43,92	132,25	220,00	218,00	254,00	172,00
43,96	116,64	178,00	216,00	248,00	166,00
44,00	125,44	206,00	216,00	236,00	166,00
44,04	148,84	202,00	222,00	248,00	174,00
44,08	114,49	208,00	226,00	240,00	150,00
44,12	132,25	218,00	220,00	218,00	186,00
44,16	123,21	208,00	216,00	238,00	174,00
44,20	121,00	206,00	238,00	238,00	196,00
44,24	100,00	226,00	244,00	232,00	194,00
44,28	141,61	214,00	232,00	202,00	198,00
44,32	121,00	200,00	222,00	230,00	168,00
44,36	132,25	234,00	254,00	230,00	210,00
44,40	129,96	204,00	266,00	236,00	172,00
44,44	121,00	244,00	240,00	222,00	170,00
44,48	127,69	210,00	282,00	262,00	162,00
44,52	121,00	206,00	228,00	228,00	168,00
44,56	114,49	220,00	216,00	226,00	200,00
44,60	116,64	190,00	250,00	248,00	190,00
44,64	139,24	206,00	244,00	220,00	160,00
44,68	125,44	198,00	272,00	258,00	186,00
44,72	129,96	202,00	240,00	252,00	184,00
44,76	136,89	200,00	266,00	230,00	176,00
44,80	151,29	196,00	238,00	228,00	198,00
44,84	136,89	190,00	236,00	246,00	154,00
44,88	163,84	220,00	246,00	228,00	190,00
44,92	166,41	236,00	254,00	238,00	178,00
44,96	166,41	206,00	250,00	224,00	156,00
45,00	179,56	214,00	246,00	242,00	158,00
45,04	174,24	204,00	212,00	260,00	200,00
45,08	163,84	182,00	232,00	260,00	168,00
45,12	196,00	214,00	230,00	234,00	164,00
45,16	174,24	192,00	216,00	212,00	166,00
45,20	198,81	224,00	262,00	248,00	182,00
45,24	198,81	226,00	226,00	232,00	172,00
45,28	169,00	232,00	206,00	240,00	176,00
45,32	166,41	232,00	210,00	230,00	188,00
45,36	158,76	208,00	214,00	260,00	188,00
45,40	134,56	226,00	228,00	266,00	156,00
45,44	144,00	196,00	234,00	226,00	166,00
45,48	163,84	230,00	216,00	226,00	174,00
45,52	163,84	222,00	260,00	254,00	166,00
45,56	146,41	238,00	212,00	234,00	192,00
45,60	144,00	226,00	228,00	240,00	174,00
45,64	136,89	248,00	230,00	240,00	168,00
45,68	141,61	204,00	218,00	226,00	184,00
45,72	136,89	220,00	250,00	254,00	198,00
45,76	129,96	202,00	218,00	248,00	178,00
45,80	110,25	232,00	234,00	262,00	186,00
45,84	108,16	214,00	236,00	246,00	176,00
45,88	136,89	228,00	210,00	220,00	184,00
45,92	129,96	208,00	204,00	252,00	174,00

45,96	129,96	230,00	226,00	240,00	216,00
46,00	139,24	222,00	202,00	234,00	188,00
46,04	129,96	204,00	208,00	258,00	168,00
46,08	129,96	228,00	240,00	254,00	178,00
46,12	136,89	220,00	234,00	214,00	178,00
46,16	136,89	238,00	184,00	242,00	208,00
46,20	161,29	208,00	224,00	242,00	162,00
46,24	127,69	224,00	222,00	228,00	198,00
46,28	127,69	190,00	202,00	228,00	204,00
46,32	106,09	246,00	222,00	238,00	152,00
46,36	132,25	226,00	192,00	262,00	178,00
46,40	136,89	198,00	234,00	248,00	178,00
46,44	121,00	212,00	214,00	248,00	170,00
46,48	129,96	214,00	212,00	242,00	162,00
46,52	127,69	190,00	218,00	272,00	164,00
46,56	148,84	200,00	248,00	244,00	168,00
46,60	127,69	192,00	228,00	270,00	172,00
46,64	146,41	190,00	222,00	276,00	188,00
46,68	121,00	208,00	218,00	262,00	198,00
46,72	136,89	224,00	224,00	280,00	204,00
46,76	141,61	184,00	242,00	306,00	178,00
46,80	129,96	202,00	234,00	270,00	166,00
46,84	104,04	218,00	242,00	274,00	182,00
46,88	116,64	188,00	252,00	266,00	202,00
46,92	156,25	196,00	232,00	230,00	194,00
46,96	127,69	190,00	232,00	254,00	196,00
47,00	127,69	196,00	228,00	252,00	200,00
47,04	139,24	194,00	230,00	244,00	172,00
47,08	129,96	182,00	260,00	286,00	194,00
47,12	127,69	198,00	248,00	270,00	172,00
47,16	127,69	170,00	252,00	276,00	176,00
47,20	116,64	182,00	234,00	244,00	196,00
47,24	118,81	206,00	246,00	252,00	172,00
47,28	123,21	176,00	254,00	304,00	182,00
47,32	127,69	194,00	246,00	256,00	196,00
47,36	134,56	202,00	230,00	238,00	150,00
47,40	146,41	182,00	264,00	234,00	164,00
47,44	134,56	200,00	216,00	252,00	190,00
47,48	123,21	170,00	264,00	260,00	188,00
47,52	127,69	174,00	244,00	250,00	188,00
47,56	114,49	200,00	258,00	260,00	176,00
47,60	106,09	192,00	246,00	302,00	196,00
47,64	116,64	180,00	234,00	286,00	186,00
47,68	125,44	184,00	280,00	268,00	206,00
47,72	129,96	202,00	268,00	290,00	194,00
47,76	129,96	188,00	240,00	264,00	172,00
47,80	123,21	212,00	296,00	328,00	204,00
47,84	125,44	212,00	260,00	300,00	204,00
47,88	112,36	168,00	270,00	288,00	186,00
47,92	118,81	212,00	304,00	302,00	200,00
47,96	144,00	164,00	278,00	316,00	192,00
48,00	121,00	182,00	290,00	292,00	180,00
48,04	123,21	182,00	304,00	316,00	178,00
48,08	129,96	194,00	310,00	292,00	190,00
48,12	108,16	232,00	332,00	296,00	182,00
48,16	106,09	200,00	270,00	270,00	194,00
48,20	125,44	200,00	270,00	302,00	192,00

48,24	121,00	208,00	278,00	282,00	186,00
48,28	127,69	214,00	290,00	320,00	196,00
48,32	121,00	218,00	286,00	292,00	182,00
48,36	112,36	202,00	314,00	292,00	210,00
48,40	106,09	200,00	334,00	264,00	214,00
48,44	114,49	200,00	326,00	320,00	192,00
48,48	114,49	218,00	308,00	324,00	220,00
48,52	104,04	212,00	318,00	316,00	210,00
48,56	144,00	192,00	276,00	292,00	190,00
48,60	116,64	182,00	306,00	284,00	178,00
48,64	127,69	186,00	288,00	246,00	202,00
48,68	129,96	232,00	304,00	282,00	202,00
48,72	106,09	198,00	320,00	320,00	200,00
48,76	116,64	212,00	310,00	308,00	188,00
48,80	108,16	200,00	300,00	326,00	206,00
48,84	108,16	208,00	260,00	338,00	210,00
48,88	116,64	226,00	274,00	296,00	202,00
48,92	110,25	196,00	294,00	258,00	208,00
48,96	123,21	222,00	296,00	292,00	182,00
49,00	106,09	218,00	282,00	312,00	230,00
49,04	108,16	220,00	292,00	308,00	210,00
49,08	102,01	204,00	292,00	322,00	206,00
49,12	108,16	228,00	282,00	268,00	204,00
49,16	108,16	208,00	306,00	298,00	222,00
49,20	114,49	196,00	272,00	284,00	234,00
49,24	106,09	184,00	268,00	314,00	210,00
49,28	125,44	228,00	292,00	304,00	216,00
49,32	118,81	186,00	242,00	328,00	210,00
49,36	110,25	168,00	288,00	284,00	188,00
49,40	96,04	206,00	262,00	306,00	182,00
49,44	104,04	184,00	260,00	332,00	212,00
49,48	121,00	172,00	284,00	306,00	214,00
49,52	110,25	188,00	272,00	290,00	192,00
49,56	102,01	210,00	260,00	280,00	202,00
49,60	114,49	172,00	270,00	278,00	174,00
49,64	114,49	200,00	276,00	278,00	200,00
49,68	116,64	216,00	298,00	254,00	188,00
49,72	129,96	182,00	252,00	286,00	202,00
49,76	96,04	184,00	274,00	282,00	208,00
49,80	108,16	176,00	278,00	284,00	202,00
49,84	96,04	192,00	272,00	304,00	210,00
49,88	112,36	178,00	242,00	274,00	208,00
49,92	118,81	196,00	268,00	304,00	194,00
49,96	90,25	188,00	264,00	306,00	204,00
50,00	121,00	196,00	232,00	300,00	198,00
50,04	118,81	196,00	250,00	318,00	220,00
50,08	86,49	214,00	270,00	278,00	184,00
50,12	108,16	190,00	254,00	280,00	188,00
50,16	121,00	188,00	238,00	260,00	192,00
50,20	100,00	178,00	238,00	258,00	180,00
50,24	100,00	156,00	222,00	286,00	208,00
50,28	98,01	168,00	244,00	288,00	210,00
50,32	125,44	168,00	230,00	272,00	216,00
50,36	121,00	176,00	242,00	280,00	204,00
50,40	100,00	158,00	248,00	278,00	172,00
50,44	110,25	206,00	224,00	262,00	192,00
50,48	114,49	168,00	246,00	256,00	190,00

50,52	104,04	176,00	216,00	300,00	202,00
50,56	88,36	198,00	240,00	272,00	190,00
50,60	106,09	170,00	248,00	270,00	230,00
50,64	118,81	166,00	228,00	272,00	190,00
50,68	110,25	172,00	240,00	244,00	182,00
50,72	106,09	186,00	238,00	272,00	168,00
50,76	100,00	196,00	246,00	256,00	180,00
50,80	94,09	198,00	224,00	246,00	172,00
50,84	112,36	200,00	216,00	268,00	188,00
50,88	104,04	170,00	226,00	252,00	156,00
50,92	112,36	180,00	256,00	232,00	188,00
50,96	108,16	182,00	212,00	246,00	180,00
51,00	106,09	198,00	234,00	238,00	168,00
51,04	121,00	188,00	212,00	274,00	164,00
51,08	84,64	196,00	218,00	234,00	172,00
51,12	116,64	226,00	222,00	242,00	166,00
51,16	102,01	208,00	180,00	278,00	178,00
51,20	118,81	212,00	202,00	222,00	164,00
51,24	108,16	174,00	200,00	262,00	174,00
51,28	110,25	204,00	218,00	234,00	206,00
51,32	112,36	184,00	212,00	260,00	166,00
51,36	114,49	154,00	214,00	258,00	164,00
51,40	92,16	158,00	198,00	278,00	146,00
51,44	114,49	162,00	208,00	250,00	148,00
51,48	98,01	156,00	208,00	264,00	170,00
51,52	127,69	180,00	228,00	244,00	156,00
51,56	98,01	144,00	250,00	262,00	174,00
51,60	106,09	136,00	222,00	242,00	192,00
51,64	114,49	184,00	214,00	232,00	168,00
51,68	84,64	190,00	224,00	222,00	156,00
51,72	98,01	182,00	206,00	224,00	164,00
51,76	114,49	178,00	190,00	220,00	152,00
51,80	94,09	172,00	202,00	216,00	156,00
51,84	112,36	200,00	204,00	230,00	158,00
51,88	104,04	168,00	210,00	228,00	152,00
51,92	94,09	154,00	204,00	242,00	158,00
51,96	98,01	160,00	210,00	210,00	168,00
52,00	88,36	154,00	206,00	236,00	162,00
52,04	88,36	180,00	188,00	238,00	140,00
52,08	94,09	172,00	188,00	230,00	166,00
52,12	86,49	172,00	194,00	242,00	182,00
52,16	106,09	192,00	202,00	216,00	168,00
52,20	104,04	168,00	204,00	222,00	160,00
52,24	96,04	164,00	192,00	232,00	158,00
52,28	102,01	170,00	188,00	222,00	142,00
52,32	110,25	172,00	172,00	232,00	148,00
52,36	102,01	176,00	220,00	226,00	164,00
52,40	118,81	166,00	186,00	254,00	148,00
52,44	102,01	196,00	190,00	200,00	146,00
52,48	92,16	138,00	204,00	244,00	180,00
52,52	88,36	170,00	202,00	206,00	156,00
52,56	82,81	154,00	192,00	190,00	146,00
52,60	104,04	180,00	206,00	212,00	166,00
52,64	98,01	182,00	192,00	202,00	152,00
52,68	106,09	160,00	204,00	186,00	134,00
52,72	100,00	166,00	192,00	234,00	150,00
52,76	86,49	158,00	228,00	208,00	146,00

52,80	94,09	176,00	164,00	214,00	158,00
52,84	81,00	170,00	200,00	190,00	150,00
52,88	84,64	174,00	194,00	214,00	162,00
52,92	92,16	174,00	208,00	198,00	154,00
52,96	82,81	162,00	194,00	194,00	170,00
53,00	94,09	184,00	192,00	198,00	166,00
53,04	102,01	158,00	194,00	198,00	150,00
53,08	75,69	170,00	206,00	184,00	132,00
53,12	86,49	174,00	192,00	200,00	150,00
53,16	90,25	188,00	218,00	188,00	156,00
53,20	90,25	164,00	216,00	194,00	144,00
53,24	92,16	146,00	170,00	190,00	168,00
53,28	98,01	172,00	200,00	238,00	166,00
53,32	94,09	194,00	204,00	184,00	154,00
53,36	79,21	176,00	194,00	164,00	174,00
53,40	79,21	162,00	240,00	220,00	126,00
53,44	94,09	150,00	204,00	176,00	156,00
53,48	79,21	168,00	190,00	222,00	158,00
53,52	82,81	128,00	188,00	200,00	154,00
53,56	86,49	182,00	210,00	178,00	148,00
53,60	116,64	166,00	194,00	198,00	154,00
53,64	98,01	172,00	188,00	160,00	146,00
53,68	100,00	190,00	166,00	202,00	140,00
53,72	88,36	138,00	200,00	176,00	136,00
53,76	94,09	174,00	174,00	178,00	156,00
53,80	73,96	168,00	174,00	194,00	142,00
53,84	79,21	180,00	182,00	196,00	132,00
53,88	90,25	160,00	172,00	182,00	152,00
53,92	90,25	206,00	184,00	192,00	166,00
53,96	98,01	166,00	176,00	170,00	138,00
54,00	77,44	170,00	174,00	174,00	134,00
54,04	96,04	170,00	188,00	174,00	122,00
54,08	86,49	170,00	186,00	182,00	134,00
54,12	106,09	176,00	198,00	186,00	144,00
54,16	90,25	168,00	182,00	190,00	154,00
54,20	84,64	180,00	214,00	202,00	168,00
54,24	82,81	200,00	164,00	196,00	146,00
54,28	112,36	196,00	182,00	214,00	168,00
54,32	86,49	184,00	180,00	216,00	152,00
54,36	79,21	190,00	216,00	164,00	166,00
54,40	88,36	178,00	192,00	204,00	162,00
54,44	72,25	152,00	198,00	208,00	144,00
54,48	82,81	184,00	192,00	188,00	136,00
54,52	82,81	174,00	194,00	164,00	130,00
54,56	77,44	158,00	176,00	198,00	136,00
54,60	96,04	180,00	194,00	162,00	160,00
54,64	88,36	172,00	200,00	186,00	150,00
54,68	72,25	176,00	194,00	198,00	142,00
54,72	82,81	142,00	168,00	186,00	150,00
54,76	82,81	140,00	162,00	210,00	158,00
54,80	102,01	154,00	216,00	198,00	188,00
54,84	100,00	160,00	188,00	168,00	146,00
54,88	96,04	164,00	190,00	170,00	138,00
54,92	82,81	162,00	216,00	200,00	174,00
54,96	72,25	160,00	200,00	206,00	130,00
55,00	102,01	158,00	170,00	170,00	146,00
55,04	81,00	172,00	226,00	188,00	142,00

55,08	94,09	144,00	176,00	180,00	126,00
55,12	79,21	160,00	186,00	180,00	150,00
55,16	82,81	152,00	192,00	184,00	142,00
55,20	90,25	138,00	172,00	192,00	162,00
55,24	75,69	136,00	178,00	182,00	144,00
55,28	86,49	142,00	210,00	172,00	136,00
55,32	81,00	164,00	186,00	180,00	152,00
55,36	77,44	168,00	202,00	166,00	138,00
55,40	88,36	172,00	184,00	200,00	108,00
55,44	72,25	174,00	192,00	200,00	160,00
55,48	90,25	162,00	210,00	168,00	142,00
55,52	79,21	148,00	198,00	210,00	142,00
55,56	77,44	166,00	196,00	190,00	140,00
55,60	75,69	148,00	192,00	192,00	132,00
55,64	72,25	190,00	188,00	188,00	164,00
55,68	81,00	184,00	200,00	194,00	146,00
55,72	90,25	182,00	178,00	186,00	136,00
55,76	75,69	172,00	190,00	206,00	164,00
55,80	67,24	184,00	208,00	190,00	130,00
55,84	77,44	192,00	176,00	156,00	142,00
55,88	82,81	180,00	168,00	176,00	124,00
55,92	75,69	168,00	164,00	198,00	144,00
55,96	75,69	168,00	174,00	176,00	158,00
56,00	82,81	154,00	200,00	176,00	128,00
56,04	60,84	156,00	152,00	178,00	150,00
56,08	81,00	168,00	168,00	198,00	110,00
56,12	60,84	174,00	160,00	198,00	142,00
56,16	81,00	180,00	166,00	162,00	158,00
56,20	68,89	172,00	182,00	190,00	156,00
56,24	82,81	166,00	190,00	194,00	160,00
56,28	84,64	168,00	174,00	192,00	138,00
56,32	72,25	174,00	178,00	158,00	140,00
56,36	56,25	168,00	188,00	192,00	130,00
56,40	75,69	160,00	192,00	194,00	124,00
56,44	67,24	164,00	182,00	182,00	140,00
56,48	77,44	154,00	172,00	182,00	134,00
56,52	86,49	154,00	192,00	188,00	130,00
56,56	77,44	186,00	166,00	180,00	154,00
56,60	65,61	160,00	192,00	202,00	124,00
56,64	70,56	152,00	158,00	186,00	130,00
56,68	65,61	150,00	206,00	192,00	140,00
56,72	62,41	150,00	190,00	194,00	138,00
56,76	73,96	164,00	186,00	174,00	132,00
56,80	77,44	156,00	182,00	186,00	150,00
56,84	77,44	168,00	172,00	186,00	132,00
56,88	79,21	148,00	188,00	170,00	130,00
56,92	81,00	178,00	202,00	176,00	146,00
56,96	73,96	138,00	182,00	154,00	96,00
57,00	70,56	182,00	164,00	170,00	128,00
57,04	64,00	148,00	162,00	162,00	160,00
57,08	82,81	190,00	186,00	168,00	154,00
57,12	88,36	172,00	186,00	198,00	128,00
57,16	65,61	166,00	194,00	144,00	134,00
57,20	75,69	154,00	196,00	144,00	134,00
57,24	72,25	158,00	178,00	198,00	120,00
57,28	84,64	158,00	232,00	166,00	136,00
57,32	79,21	154,00	172,00	196,00	126,00

57,36	67,24	154,00	186,00	162,00	142,00
57,40	88,36	178,00	178,00	168,00	132,00
57,44	84,64	158,00	164,00	172,00	122,00
57,48	72,25	154,00	182,00	162,00	140,00
57,52	84,64	156,00	180,00	158,00	128,00
57,56	65,61	136,00	176,00	180,00	126,00
57,60	94,09	160,00	194,00	182,00	144,00
57,64	96,04	164,00	194,00	178,00	138,00
57,68	72,25	174,00	188,00	174,00	126,00
57,72	82,81	152,00	188,00	194,00	136,00
57,76	86,49	166,00	180,00	192,00	136,00
57,80	73,96	168,00	224,00	168,00	134,00
57,84	77,44	150,00	200,00	170,00	122,00
57,88	65,61	170,00	184,00	172,00	140,00
57,92	72,25	178,00	198,00	146,00	136,00
57,96	62,41	172,00	194,00	164,00	140,00
58,00	47,61	170,00	216,00	178,00	120,00
58,04	82,81	144,00	188,00	162,00	126,00
58,08	56,25	150,00	156,00	182,00	138,00
58,12	59,29	152,00	178,00	186,00	134,00
58,16	70,56	152,00	168,00	158,00	114,00
58,20	59,29	158,00	160,00	170,00	136,00
58,24	65,61	186,00	162,00	174,00	120,00
58,28	62,41	166,00	172,00	164,00	136,00
58,32	88,36	180,00	152,00	158,00	126,00
58,36	72,25	146,00	196,00	196,00	144,00
58,40	64,00	146,00	180,00	160,00	122,00
58,44	62,41	178,00	174,00	160,00	100,00
58,48	53,29	172,00	178,00	156,00	128,00
58,52	62,41	174,00	156,00	168,00	144,00
58,56	72,25	156,00	172,00	168,00	136,00
58,60	75,69	164,00	154,00	180,00	112,00
58,64	67,24	120,00	150,00	134,00	126,00
58,68	65,61	174,00	156,00	160,00	130,00
58,72	65,61	138,00	158,00	154,00	122,00
58,76	64,00	162,00	158,00	160,00	138,00
58,80	62,41	150,00	142,00	174,00	142,00
58,84	77,44	154,00	158,00	184,00	132,00
58,88	77,44	160,00	168,00	186,00	140,00
58,92	67,24	154,00	188,00	180,00	134,00
58,96	67,24	174,00	178,00	188,00	116,00
59,00	46,24	152,00	140,00	174,00	140,00
59,04	67,24	150,00	158,00	198,00	142,00
59,08	75,69	168,00	162,00	160,00	142,00
59,12	59,29	144,00	174,00	160,00	124,00
59,16	59,29	140,00	166,00	180,00	126,00
59,20	70,56	164,00	148,00	174,00	106,00
59,24	65,61	174,00	154,00	172,00	132,00
59,28	64,00	160,00	156,00	152,00	114,00
59,32	67,24	182,00	170,00	186,00	120,00
59,36	54,76	168,00	180,00	180,00	122,00
59,40	81,00	166,00	168,00	166,00	122,00
59,44	59,29	184,00	162,00	192,00	134,00
59,48	62,41	158,00	156,00	174,00	110,00
59,52	68,89	160,00	172,00	154,00	114,00
59,56	70,56	164,00	174,00	160,00	138,00
59,60	57,76	176,00	160,00	170,00	124,00

59,64	72,25	164,00	140,00	182,00	158,00
59,68	57,76	178,00	156,00	168,00	126,00
59,72	49,00	170,00	160,00	162,00	150,00
59,76	62,41	134,00	154,00	152,00	148,00
59,80	59,29	164,00	146,00	180,00	128,00
59,84	64,00	152,00	144,00	158,00	142,00
59,88	43,56	164,00	142,00	166,00	130,00
59,92	50,41	166,00	170,00	172,00	138,00
59,96	75,69	160,00	136,00	150,00	114,00
60,00		162,00	152,00	162,00	126,00

6. Bibliography

1. **Gaade, L. H.** *Koordinationschemie.* Weinheim : Wiley-VCH, 1998.

2. **P. Gütlich, A. Hauser, H. Spiering.** *Angew. Chem.* 1994, 106, pp. 2109 - 2141.

3. **R. Boča, F. Renz, M. Boča, H. Fuess, W. Haase, G. Kickelbick, W. Linert, M. Vrbová-Schikora.** *Inorg. Chem. Commun.* 2005, 8, pp. 227 - 230.

4. **L. Cambi, A. Cagnasso.** *Atti Accad. Naz. Lincei.* 1931, 13, p. 809.

5. **L. Cambi, L. Szegö.** *Ber. Dtsch. Chem. Ges.* 1931, 64, p. 259.

6. **L. Cambi, L. Szegö, A. Cagnasso.** *Atti Accad. Naz. Lincei.* 1932, 15, p. 266.

7. **L. Cambi, L. Malatesta.** *Ber. Dtsch. Chem. Ges.* 1937, 70, p. 2067.

8. **W. A. Baker, H. M. Bobonich.** *Inorg. Chem.* 1964, 3, p. 1184.

9. **König, E.** *Structure and Bonding.* 1991, 76, pp. 53 - 153.

10. **Y. Garcia, P. J. van Koningsbruggen, R. Lapouyade, L. Fournès, L. Rabardel, O. Kahn, V. Ksenofontov, G. Levchenko, P. Gütlich.** *Chem. Mater.* 1998, 10, p. 2426.

11. **Gütlich, P.** *Hyperfine Interactions.* 1987, 33, pp. 105 - 132.

12. **E. Meissner, H. Köppen, H. Spiering, P. Gütlich.** *Chem. Phys. Lett.* 1983, 95 (2), pp. 163 - 166.

13. **J. J. McGarvey, I. Lawthers, K. Heremans, H. Toftlund.** *Inorg. Chem.* 1990, 29, pp. 252 - 256.

14. **S. Decurtins, P. Gütlich, C. P. Köhler, H. Spiering, A. Hauser.** *Chem. Phys. Lett.* 1984, 105, pp. 1 - 4.

15. **S. Decurtins, P. Gütlich, K. M. Hasselbach, H. Spiering, A. Hauser.** *Inorg. Chem.* 1985, 24, pp. 2174 - 2178.

16. **S. Decurtins, P. Gütlich, C. P. Köhler, H. Spiering.** *J. Chem. Soc. Chem. Commun.* 1985, pp. 430 - 432.

17. **B. Richter, A. Kirste, S. Hansel, M. von Ortenberg, A. Absmeier, W. Linert, R. Grössinger.** *J. of Magn. and Mag. Mat.* 2007, 310, pp. 2731 - 2733.

18. **L. Cambi, L. Szegö.** *Chem. Ber. Dtsch. Ges.* 1931, 64, p. 2591.

19. —. *Chem. Ber. Dtsch. Ges.* 1933, 66, p. 656.

20. **A.H. Ewald, R.L. Martin, I. Ross, A.H. White.** *Proc. R. Soc. London, Ser. A.* 1964, 280, p. 235.

21. **A.H. White, R. Roper, E. Kokot, H. Waterman, R.L. Martin.** *Austr. J. Chem.* 1964, 17, p. 294.

22. **R.M. Golding, W.C. Tennant, C.R. Kanekar, R.L. Martin, A.H. White.** *J. Chem. Phys.* 1966, 45, p. 2688.

23. **A.H. Ewald, R.L. Martin, E. Sinn, A.H. White.** *Inorg. Chem.* 1969, 8, p. 1837.

24. **K.A. Reeder, E.V. Dose, L.J. Wilson.** *Inorg. Chem.* 1978, 17, p. 1071.

25. **M.S. Haddad, W.D. Federer, M.W. Lynch, D.N. Hendrickson.** *Inorg. Chem.* 1981, 20, p. 131.

26. **H. Oshio, K. Kitazaki. J. Mishiro, N. Kato, Y. Maeda, Y. Takashima.** *J. Chem. (Dalton Trans).* 1987, p. 1341.

27. **S. Schenker, A.R.M. Dyson.** *Inorg. Chem.* 1996, 35, p. 4676.

28. **D.M. Halepoto, D.G.L. Holt, L.F. Larkworthy, G.J. Leigh, D.C. Povey, W. Smith.** *J. Chem. Soc. Chem. Comm.* 1989, 18, p. 1322.

29. **M. Sorai, Y. Yumoto, D.M. Halepoto, L.F. Larkworthy.** *J. Phys. Chem. Solids.* 1993, 54 (4), p. 421.

30. **J.H. Ammeter, R. Bucher, N. Oswald.** *J. Am. Chem. Soc.* 1974, 96, p. 7883.

31. **M.E. Switzer, R. Wang, M.F. Rettig, A.H. Maki.** *J. Am. Chem. Soc.* 1974, 96, p. 7669.

32. **D. Cozak, F. Gauvin.** *Organometallics.* 1987, 6, p. 1912.

33. **R.C. Stoufer, D.H. Bush, W.B. Hardley.** *J. Am. Chem. Soc.* 1961, 83, p. 3732.

34. **R.C. Stouter, D.W. Smith, E.A. Cleavenger, T.E. Norris.** *Inorg. Chem.* 1966, 5, p. 1167.

35. **J. Zarembowitch, O. Kahn.** *Inorg. Chem.* 1984, 23, p. 589.

36. **Zarembowitch, J.** *New. J. Chem.* 1992, 16, p. 255.

37. **J. Faus, M. Julve, F. Lloret, J.A. Real, J. Sletten.** *Inorg. Chem.* 1994, 33, p. 5535.

38. **K. Heinze, G. Huttner, L. Zsolnai, P. Schober.** *Inorg. Chem.* 1997, 36, p. 5457.

39. **P.G. Sim, E. Sinn.** *J. Am. Chem. Soc.* 1981, 103, p. 241.

40. **L. Kaustov, M.E. Tal, A.I. Shames, Z. Gross.** *Inorg. Chem.* 1997, 36, p. 3503.

41. **Kläui, W.** *J. Chem. Soc. Chem. Comm.* 1979, p. 700.

42. **P. Gütlich, B.R. McGarvey, W. Kläui.** *Inorg. Chem.* 1980, 19, p. 3704.

43. **W. Eberspach, N. El Murr, W. Kläui.** *Angew. Chem. Int. Ed. Engl.* 1982, 21, p. 915.

44. **G. Navon, W. Kläui.** *Inorg. Chem.* 1984, 23, p. 2722.

45. **W. Kläui, W. Eberspach, P. Gütlich.** *Inorg. Chem.* 1987, 26, p. 3977.

46. **Griffith, J.S.** *Proc. Roy. Soc.* 1959, 23, p. 23.

47. **C.J. Ballahausen, A.D. Liehr.** *J. Am. Chem. Soc.* 1959, 81, p. 538.

48. **Goodwin, H.A.** *Coord. Chem. Rev.* 1976, 18, p. 293.

49. **König, E.** *Prog. Inorg. Chem.* 1987, 35, p. 527.

50. **E. König, G. Ritter, S. K. Kulshreshta.** *Chem. Rev.* 1985, 85, p. 219.

51. **L. Wiehl, G. Kiel, C. P. Köhler, H. Spiering, P. Gütlich.** *Inorg. Chem.* 1986, 25, p. 1565.

52. **B. Gallois, J.-A. Real, C. Hauw, J. Zarembowitch.** *Inorg. Chem.* 1990, 29, S. 1152.

53. **I. Sanner, E. Meißner, H. Köppen, H. Spiering.** *Chem. Phys.* 1984, 86, p. 227.

54. **N. Willenbacher, H. Spiering.** *J. Phys. C.: Solid State Phys.* 1988, 21, p. 1423.

55. **H. Spiering, N. Willenbacher.** *J. Phys.: Condens. Matter.* 1989, 1, p. 10089.

56. **J. Jung, G. Schmitt, L. Wiehl, A. Hauser, K. Knorr, H. Spiering, P. Gütlich.** *Z. Phys. B.* 1996, 100, p. 523.

57. **M. Sorai, J. Ensling, K. M. Hasselbach, P. Gütlich.** *Chem. Phys.* 1977, 20, p. 197.

58. **T. Buchen, P. Gütlich, K. H. Sugiyarto, H. A. Goodwin.** *Chem. Eur. J.* 1996, 2, p. 1134.

59. **K. H. Sugiyarto, K. Weitner, D. C. Craig, H. A. Goodwin.** *Aust. J. Chem.* 1997, 50, p. 869.

60. **J. F. Letard, P. Guionneau, E. Codjovi, O. Lavastre, G. Bravic, D. Chasseau, O. Kahn.** *J. Am. Chem. Soc.* 1997, 119, p. 10861.

61. **J. F. Letard, P. Guionneau, L. Rabardel, J. A. K. Howard, A. E. Goeta, D. Chasseau, O. Kahn.** *Inorg. Chem.* 1998, 37, p. 4432.

62. **Z. J. Zhong, J. Q. Tao, Z. Yu, C. Y. Dun, Y. J. Liu, X. Z. You.** *J. Chem. Soc. Dalton Trans.* 1998, p. 327.

63. **E. König, G. Ritter, W. Irler, S. M. Nelson.** *Inorg. Chim. Acta.* 1979, 37, p. 169.

64. **E. W. Müller, H. Spiering, P. Gütlich.** *J. Chem. Phys.* 1983, 79, p. 1439.

65. **D. H. Everett, W. I. Whitton.** *Trans. Fraraday Soc.* 1952, 48, p. 749.

66. **D. H. Everett, F. W. Smith.** *Trans. Faraday Soc.* 1954, 50, p. 187.

67. **Everett, D. H.** *Trans. Faraday Soc.* 1954, 50, p. 1077.

68. **H. B. Jonassen, J. O. Terry, A. D. Harris.** *Inorg. Nucl. Chem.* 1963, pp. 1239 - 1243.

69. **Y. Garcia, O. Kahn, L. Rabardel, B. Chansou, L. Salmon, J.-P. Tuchagues.** *Inorg. Chem.* 1999, 38, p. 4663.

70. **A. B. Kudryavtsev, R. F. Jameson, W. Linert.** *The Law of Mass Action.* s.l. : Springer, 2001.

71. **P. Gütlich, H.A. Goodwin, [ed.].** *Spin Crossover in Transition Metal Compounds I - III.* Berlin : Springer Verlag, 2004.

72. **G. Agusti, A.B. Gaspar, M.C. Munoz, J.A. Real.** *Inorg. Chem.* 2007: doi: 10.1021/ic70099s.

73. **P. Gütlich, V. Ksenofontov, A.B. Gaspar.** *Coord. Chem. Rev.* 2005, 249, p. 1811.

74. **A. Galet, A.B. Gaspar, G. Agusti, M.C. Munoz, G. Levchenko, J.A. Real.** *Eur. J. Inorg. Chem.* 2006, p. 3571.

75. **G. Molnar, T. Guillon, N.O. Moussa, L. Rechignat, T. Kitazawa, M. Nardone, A. Bousseksou.** *Chem. Phys. Lett.* 2006, 432, p. 152.

76. **P. Gütlich, A. Hauser, H. Spiering.** *Angew. Chem. Int. Ed. Engl.* 1994, 33, p. 2024.

77. **D.C. Fisher, H.G. Drickamer.** *J. Chem. Phys.* 1971, 54, p. 4825.

78. **J.-P. Rueff, C.C. Kao, V.V. Struzhkin, J. Badro, J. Shu, R.J. Hemely, H.K. Mao.** *Phys. Rev. Lett.* 1999, 82, p. 3284.

79. **J. J. McGarvey, I. Lawthers.** *J. Chem. Soc, Chem. Commun.* 1982, p. 906.

80. **Hauser, A.** *Chem. Phys. Lett.* 1986, 124, p. 543.

81. —. *J. Chem. Phys.* 1991, 94, p. 2741.

82. **P. Gütlich, Y. Garcia, H. A. Goodwin.** *Chem. Soc. Rev.* 2000, 29, p. 419.

83. **Hauser, A.** *Coord. Chem. Rev.* 1991, 111, p. 275.

84. —. *Comments Inorg. Chem.* 1995, 17, p. 17.

85. **E. Buhks, G. Navon, M. Bixon, J. Jortner.** *J. Am. Chem. Soc.* 1980, 102, p. 2918.

86. **J.-F. Létard, P. Guionneau, O. Nguyen, J. S. Costa, S. Marcén, G. Chastanet, M. Marchivie, L. Capes.** *Chem. Eur. J.* 2005, 11, p. 4582.

87. **Létard, J.-F.** *J. Mater. Chem.* 2006, 16, p. 2550.

88. **N. Sasaki, T. Kambara.** *J. Phys. Chem.* 1982, 15, p. 1035.

89. **Y. Qi, E.W. Müller, H. Spiering, P. Gütlich.** *Chem. Phys. Lett.* 1983, 101, p. 503.

90. **A. Bousseksou, N. Negre, M. Goiran, L. Salmon, J.-P. Tuchauges, M.-L. Boillot, K. Boukheddaden, F. Varret.** *Eur. Phys. J.* 2000, B13, pp. 451 - 456.

91. **F. Palacio, E. Ressouche, J. Schweizer.** *Introduction to Physical Techniques in Molecular Magnetism: Structural and Macroscopic Techniques.* Spain : Servicio de Publicaciones de la Universidad de Zaragoza, 1999.

92. **J. H. Takemoto, B. Hutchinson.** *Inorg. Chem.* 1973, 12, p. 705.

93. **J. H. Takemoto, B. Streusand, B. Hutchinson.** *Spectrochim. Acta Part A.* 1974, 30, p. 827.

94. **M. Valtiner, H. Paulsen, P. Weinberger, W. Linert.** *MATCH.* 2007, 57 (3), pp. 749 - 761.

95. **M. Enamullah, F. Renz, U. El-Ayaan, G. Wiesinger, W. Linert.** *Vibrational Spectroscopy.* 1997, 14(1), p. 95.

96. **M. Enamullah, M. N. Uddin, D. Hossain, M. Kabir, A. Awwal, W. Linert.** *J. Coord. Chem.* 2000, 49, p. 171.

97. **M. Enamullah, V. Gutmann, W. Linert.** *Vibr. Spectr.* 1995, 9, p. 265.

98. **M. Enamullah, W. Linert.** *J. Coord. Chem.* 1995, 35, p. 325.

99. —. *J. Coord. Chem.* 1996, 40(3), p. 193.

100. —. *J. Coord. Chem.* 1996, 38(4), p. 337.

101. —. *Thermichim. Acta.* 2002, 338, pp. 401 - 406.

102. **M. Enamullah, W. Linert, V. Gutmann, R. F. Jameson.** *Monatsh. Chem.* 1994, 125, p. 1301.

103. **M. Hasegawa, F. Renz, T. Hara, Y. Kikuchi, Y. Fukuda, J. Okubo, T. Hoshi, W. Linert.** *Chem. Physics.* 2002, 277, pp. 21 - 30.

104. **F. Renz, M. Hasegawa, T. Hoshi, U. El-Ayaan, W. Linert, Y. Fukuda.** *Mol. Cryst. Liq. Cryst.* 1999, 335, pp. 531 - 540.

105. **F. Renz, U. El-Ayaan, W. Linert, Y. Fukuda.** *Mol. Cryst. Liq. Cryst.* 1999, 335, pp. 521 - 530.

106. **Konecny, M.** *Diploma Thesis and PhD Thesis - TU Vienna.* Vienna : s.n., 1992/1997.

107. **M. Boča, D. Valigura, I. Svoboda, H. Fuess, W. Linert.** *Acta Cryst.* 2000, C56, p. 838.

108. **M. Vrbová, P. Baran, R. Boča, I. Svoboda, W. Linert, U. Schubert, P. Wiede.** *Polyhedron.* 2000, 19, p. 2195.

109. **R. Boča, M. Boča, H. Ehrenberg, H. Fuess, W. Linert, F. Renz, I. Svoboda.** *Chem. Physics.* 2003, 293, pp. 375 - 395.

110. **R. Boča, P. Baran, L. Dlhán, J. Shima, G. Wiesinger, F. Renz, U. El-Ayaan, W. Linert.** *Polyhedron.* 1997, 35, p. 47.

111. **R. Boča, P. Baran, M. Boča, L. Dlhán, H. Fuess, W. Haase, W. Linert, G. Wltschek, B. Papánková, R. Werner.** *Inorg. Chim. Acta.* 1998, 278, p. 190.

112. **M. Boča, R. Boča, D. Valigura, G. Kickelbick, W. Linert, I. Svoboda, H. Fuess.** *Inorg. Chim. Acta.* 2002, 338, pp. 36 - 50.

113. **W. Linert, F. Renz, R. Boča.** *J. Coord. Chem.* 1996, 40, p. 293.

114. **W. Linert, M. Enamullah, R. F. Jameson, V. Gutmann.** *Monatsh. Chem.* 1994, 125, p. 661.

115. **A. W. Addison, P. J. Burke.** *J. Heterocyclic Chem.* 1981, 18, p. 803.

116. **Konecny, M.** *Research Report.* Kitagawa Laboratories. 2006.

117. **L. Slyper, K. Kloc, J. Mlochowski.** *Tetrahedron Letters.* 1980, 36, pp. 123 - 129.

118. **Light, R. J.** *J. Org. Chem.* 1961, 26, pp. 1296 - 1299.

119. **Asao, T.** *Bulletin of the Chem. Soc. of Japan.* 1961, V34, pp. 151 - 153.

120. **C. Piguet, B. Bocquet, E. Müller, A. F. Williams.** *Helv. Chim. Acta.* 1989, 72, p. 323.

121. **L. L. Wang, M. M. Joullié.** *J. Am. Soc.* 1957, 79, pp. 5706 - 5708.

122. **K. H. Taffs, L. V. Prosser, F. B. Wigton, M. M. Joullié.** *J. Org. Chem.* 1961, 26, pp. 462 - 467.

123. **K. Isele, V. Broughton, C. J. Matthews, A. F. Williams, G. Bernardinelli, P. Franz, S. Decurtins.** *J. Chem. Soc., Dalton Trans.* 2002, pp. 3899 - 3905.

124. **Tavman, A.** *Zhurnal Neorganicheskoi Khimii.* 2005, V50 (9), pp. 1445 - 1449.

125. **D. Davidson, M. Weiss, M. Jelling.** *J. Org. Chem.* 1937, 2, pp. 328 - 334.

126. **Schütze, W.** *J. f. prakt. Chemie.* 4, 1964, Vol. 24, pp. 164 - 182.

127. **Halcrow, M. A.** *Polyhedron.* 2007, 26, pp. 3523 - 3576.

128. *3rd European Workshop on Magnetic Molecular Materials.* **J. Kolnaar, J.G. Haasnoot, J. Reedijk.** Aussois : s.n., 1996. p. 26.

129. **Gütlich, P.** *Struct. Bonding.* 1981, 44, p. 83.

130. **I. M. Kolthoff, P. J. Elving.** *Treatise on Analytical Chemistry.* New York : s.n., 1963. Vol. 4.